Volcano Infrasound

Jeffrey Johnson
Dept. of Geosciences
Boise State University



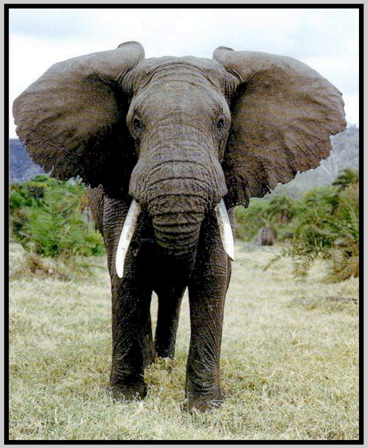

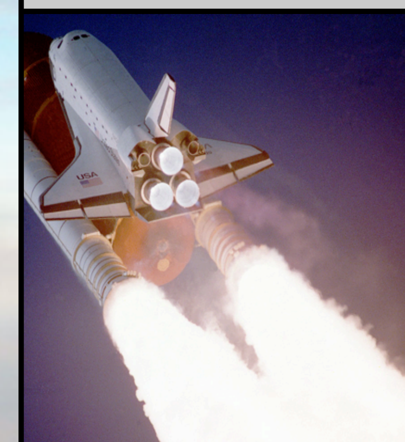



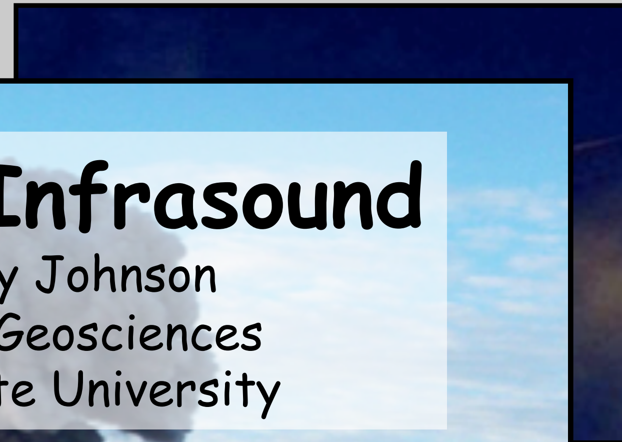

Some interesting facts about infrasound:

Infrasound is sound between ~2mHz (acoustic gravity waves) and 20 Hz (threshold of hearing).

Elephants, whales, hippos, rhinos, giraffes, and aligators use infrasound to communicate! Elephants can "yell" with 15-35 Hz sounds as loud as 117 dB, which can be "heard" tens of kilometers away!

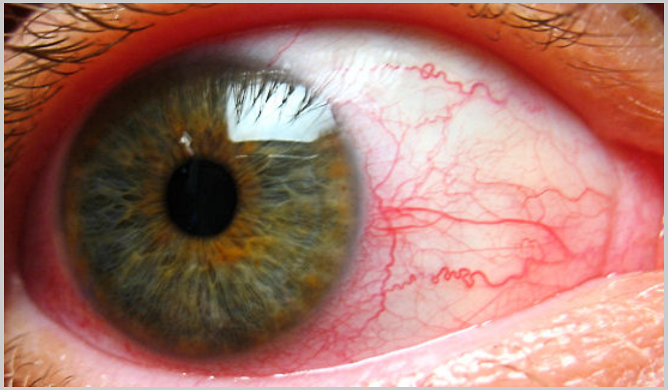

A resonant frequency of the eyeball is at 18 Hz and some ghost sightings have been attributed to excitation of the eye by sounds!

Military has explored infrasound "weapons". Nazi rallies played infrasound to stir up agitation amongst the crowds. Dr. Gavreau during the cold war developed infrasonic "whistles" that were capable of inducing nausea.

Volcanoes produce prodigious infrasound, often peaked at about 1 Hz.

Infrasound: The Good News

- Sound waves in atmosphere come in only one elastic flavor (compressional waves)
- Intrinsic attenuation of infrasound is very low; infrasound propagates far
- Structure of the atmosphere is relatively homogeneous giving rise to (relatively) predictable propagation paths at distances
- Infrasound is typically measured in Pa and can be adequately recorded with low-cost low-frequency sensitive microphones.

Electret condenser elements (ECMs)

Microelectromechanical (MEMS)

Microbarometer

And now the bad news:

- Structure of atmosphere changes and is dependant upon winds and temperatures.

Solution: ***Put microphones local to the source***

- Infrasound recordings are often contaminated by wind noise (atmospheric turbulence) and microbaroms (i.e., low frequency ocean wave sounds)

Solutions: Filter out microbaroms and deploy sensors in low noise environments. Also, put microphones local to the source

Proximal versus Distal Infrasound

•**Local infrasound**: on flanks of (strato)volcano: < ~10 km (excess pressure decay as 1/r). Most active volcanoes emanate infrasounds to local distances.

•**Regional infrasound**: out to first stratospheric and thermospheric refraction: < ~500 km. Generally recorded for relatively "large" eruptions.

•**Global infrasound**: worldwide (pressure decay as $1/r^{1/2}$). Only the very largest eruptions, e.g., Krakatau.

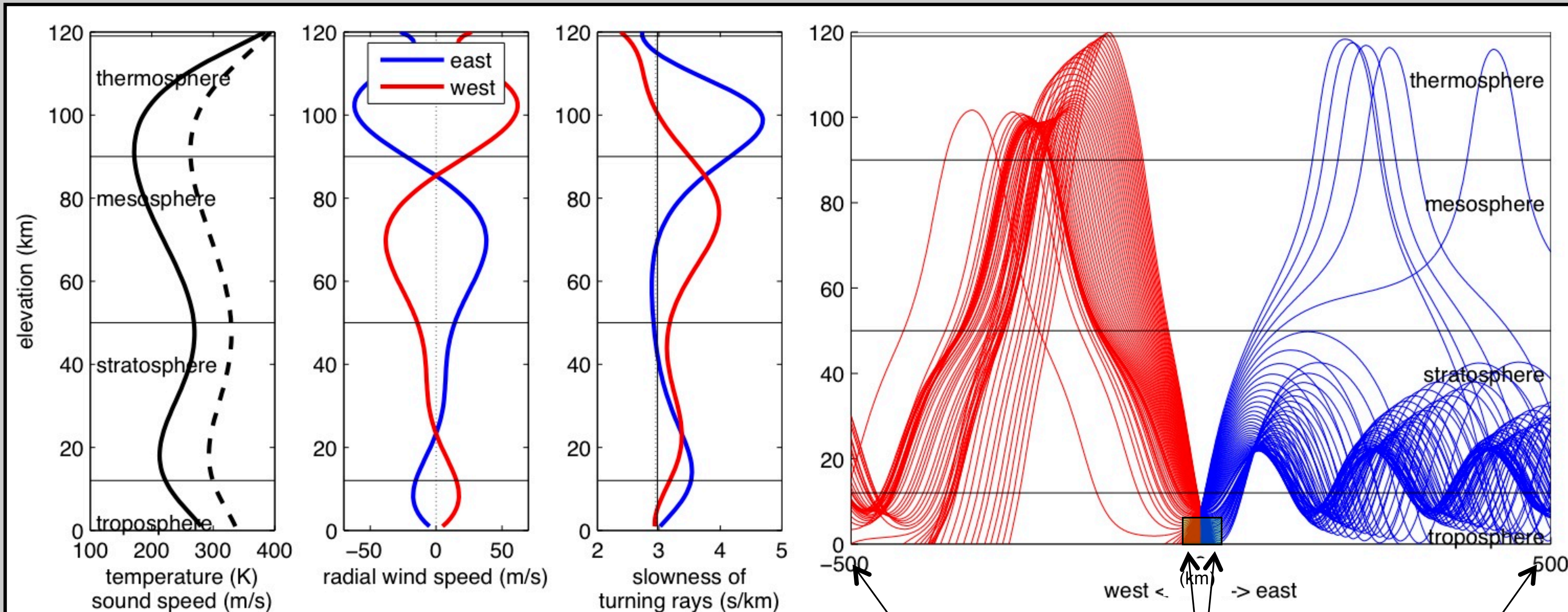

Sample atmospheric profiles

Local distances

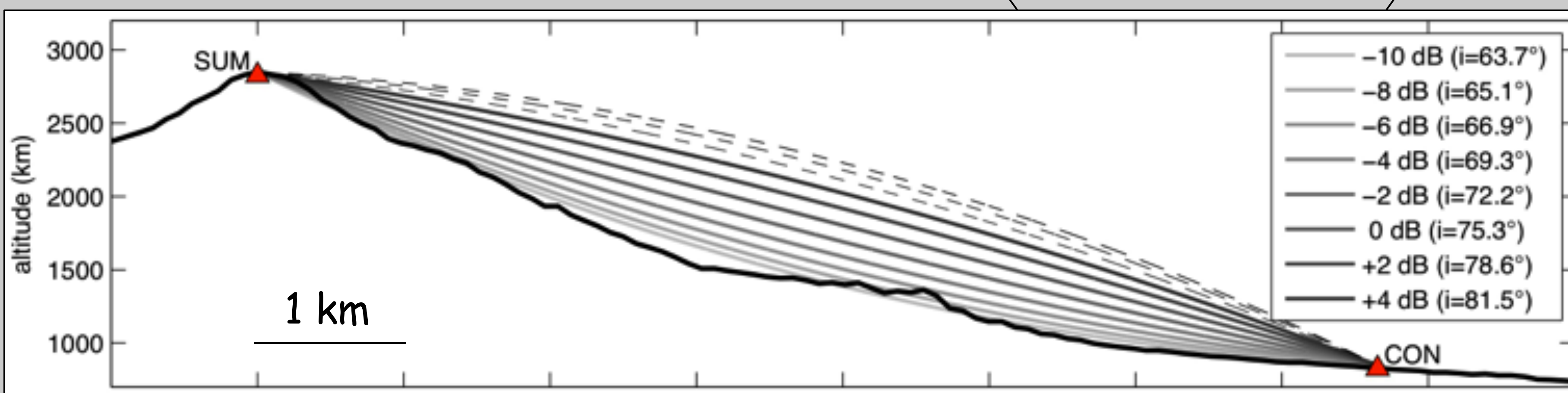

Infrasonic observations of the June 2009 Sarychev Peak eruption, Kuril Islands: Implications for infrasonic monitoring of remote explosive volcanism

Robin S. Matoza [a,*], Alexis Le Pichon [a], Julien Vergoz [a], Pascal Herry [a], Jean-Marie Lalande [a], Hee-il Lee [b], Il-Young Che [b], Alexander Rybin [c]

Journal of Volcanology and Geothermal Research 200 (2011) 35–48

[a] *CEA/DAM/DIF, F-91297 Arpajon, France*
[b] *Earthquake Research Center, Korea Institute of Geoscience and Mineral Resources, Korea*
[c] *Sakhalin Volcanic Eruptions Response Team, Institute of Marine Geology and Geophysics, Yuzhno-Sakhalinsk, Russia*

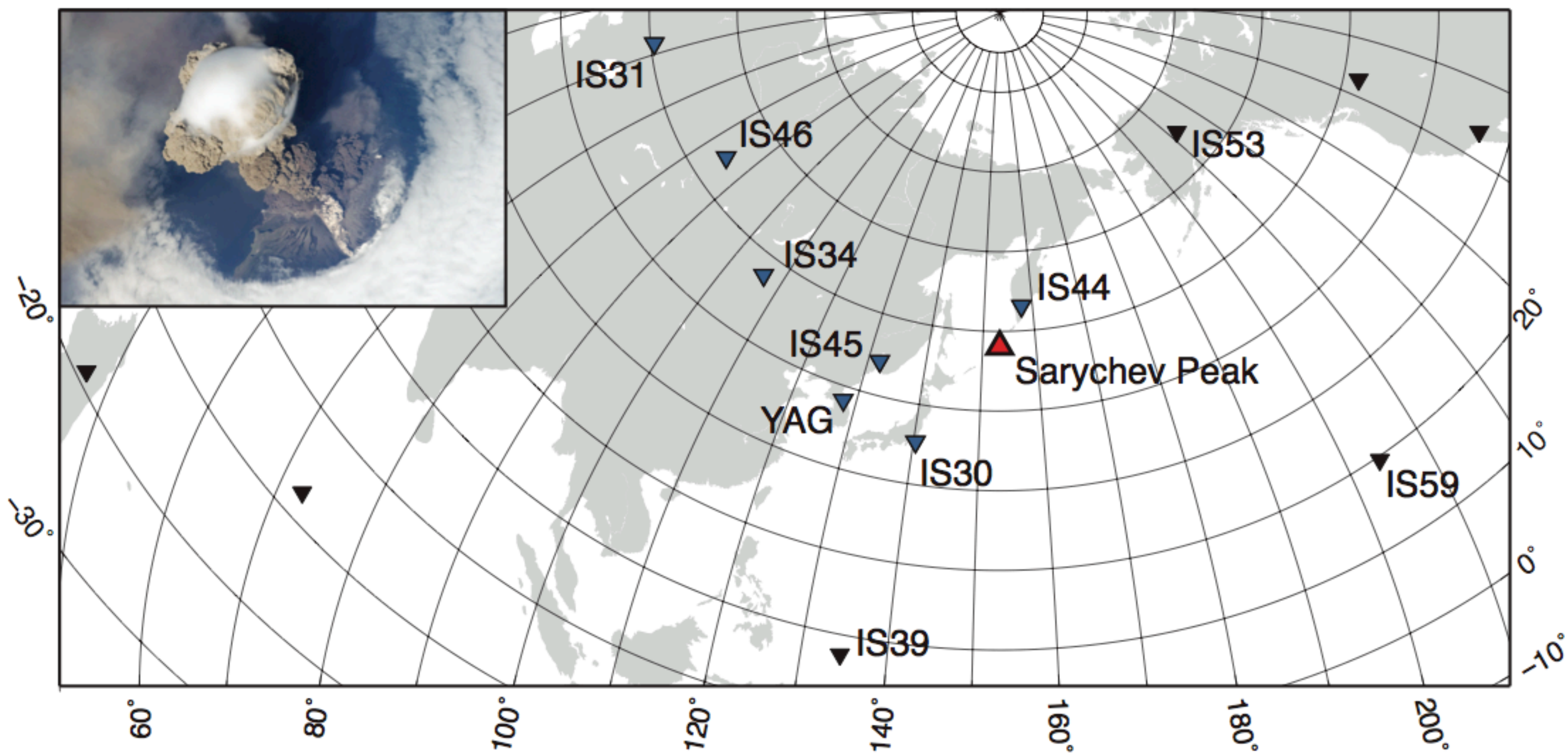

Detections of Sarychev Peak Eruptions in 2009

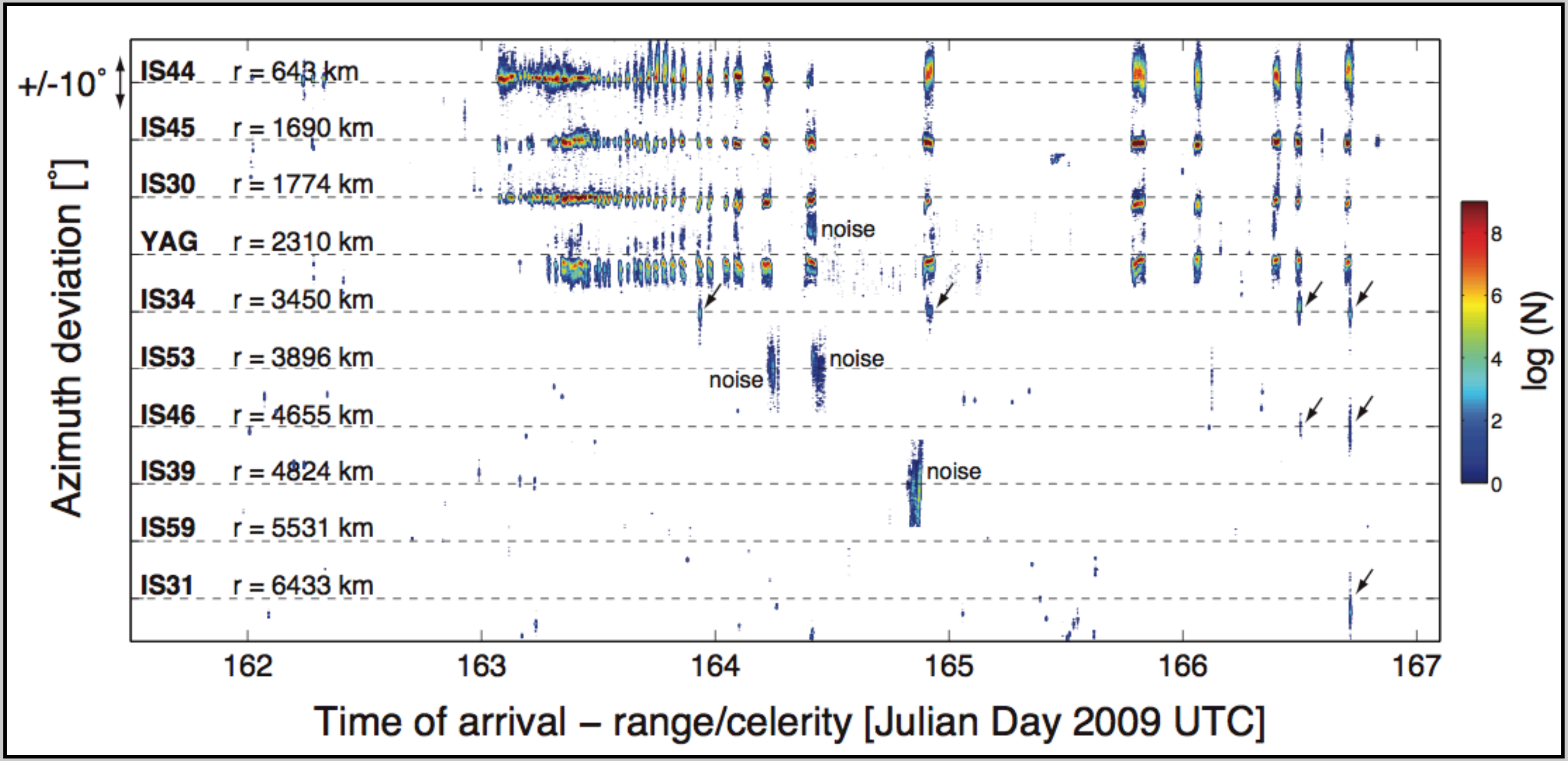

Detections of Sarychev Peak Eruptions in 2009

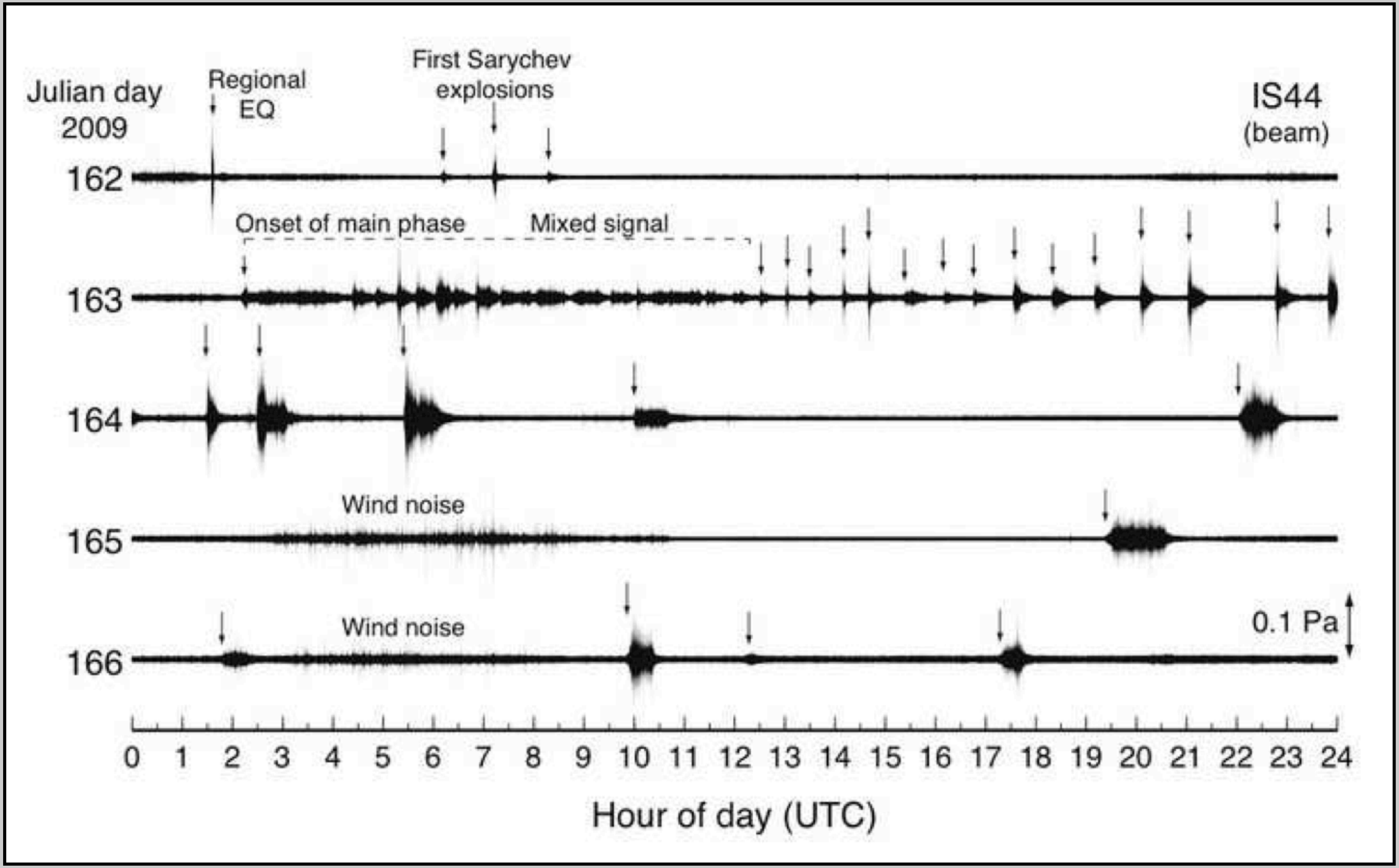

Some regional and global observations of volcano infrasound

Antier, K., Le Pichon, A., Vergniolle, S., Zielinski, C. and Lardy, M., 2007. Multiyear validation of the NRL-G2S wind fields using infrasound from **Yasur**. Journal of Geophysical Research-Atmospheres, 112(D23).

Banister, J.R., 1984. Pressure wave generated by the **Mount St. Helens eruption**. J Geophys. Res., 89(D3): 4895-4904.

Evers, L.G. and Haak, H.W., 2005. The detectability of infrasound in the Netherlands from the Italian volcano Mt. **Etna**. Journal of Atmospheric and Solar-Terrestrial Physics, 67(3): 259-268.

Fee, D., Garces, M. and Steffke, A., 2010. Infrasound from **Tungurahua** Volcano 2006-2008: strombolian to plinian eruptive activity. J. Volc. Geotherm. Res., 193: 67-81.

Fee, D., Steffke, A. and Garces, M., 2010. Characterization of the 2008 **Kasatochi** and Okmok eruptions using remote infrasound arrays. J Geophys. Res., 115(D00L10).

Gorshkov, G.S., 1959. Gigantic eruption of the Volcano **Bezymianny**. Bull. Volcan., 20: 77-109.

Liszka, L. and Garces, M.A., 2002. Infrasonic observations of the **Hekla** eruption of February 26, 2000. J. Low Frequency Noise Vibration and Active Control, 21(1): 1-8.

Matoza, R. et al., 2010. Infrasonic observations of the June 2009 **Sarychev** Peak eruption, Kuril Islands: implications for infrasonic monitoring of explosive volcanism. J. Volc. Geotherm. Res.

Tahira, M., Nomura, M., Sawada, Y. and Kamo, K., 1996. Infrasonic and acoustic-gravity waves generated by the Mount **Pinatubo** eruption of June 15, 1991. In: C.G. Newhall and R.S. PUNONGBAYAN (Editors), Fire and Mud. University of Washington Press, Seattle, pp. 601-614.

Wilson, C.R. and Olson, J.V., 2005. I53US and I55US signals from **Manam** Volcano. Inframatics, 9: 31-35.

Wilson, C.R., Olson, J.V., Oborne, D.L. and Le Pichon, A., 2003. Infrasound from **Erebus** Volcano at I55US in Antarctica. Inframatics, 4: 1-8.

Wilson, C.R. et al., 2006 Infrasonic array observations at I53US of the 2006 **Augustine** Volcano eruptions. Inframatics, 13: 11-25.

Quantifying infrasound "loudness":

Reduced pressure (radial spreading):

$$p_{red} = p \times \frac{r}{r_{red}}$$

p = recorded excess pressure
r = source-receiver propagation distance
r_{red} = reduced distance (1000 m, or 1 km, is often used)

By power (radial spreading):

$$P(t) = \Omega \frac{\overline{p^2(t + r/c)}}{\rho c}$$

ρc = acoustic impedance (density x sound speed = ~380 m kg s^{-1} at STP)
Ω = solid angle area ($2\pi r^2$ for halfspace).

By energy:
Time-integrated acoustic power gives total acoustic energy. Energy is also easily calculated in the frequency domain.

Which volcano is "loudest"?

Santiaguito (Guatemala)

Tungurahua (Ecuador)

Fuego (Guatemala)

Kilauea (Hawaii)

Reventador (Ecuador)

Villarrica (Chile)

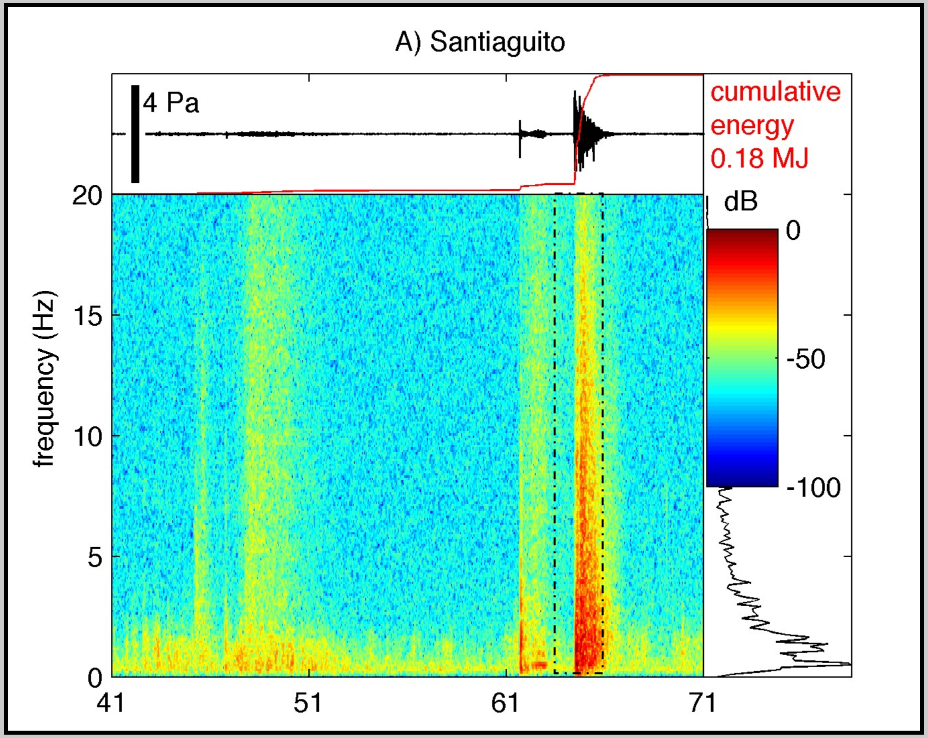

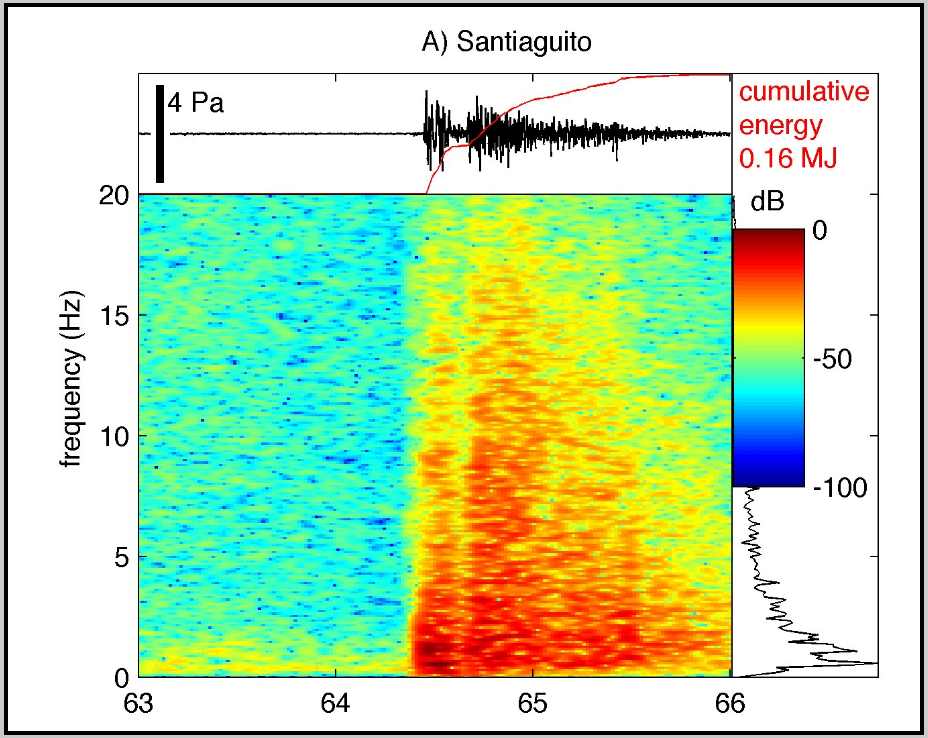

Santiaguito (Guatemala) - pyroclastic-laden eruptions with buoyant plumes up to ~1.2 km. Only about **100 Watts** of acoustic power is associated with time averaged Santiaguito eruptive behavior and is dominated by explosive events. Up to 3000 Watts is generated during eruption.

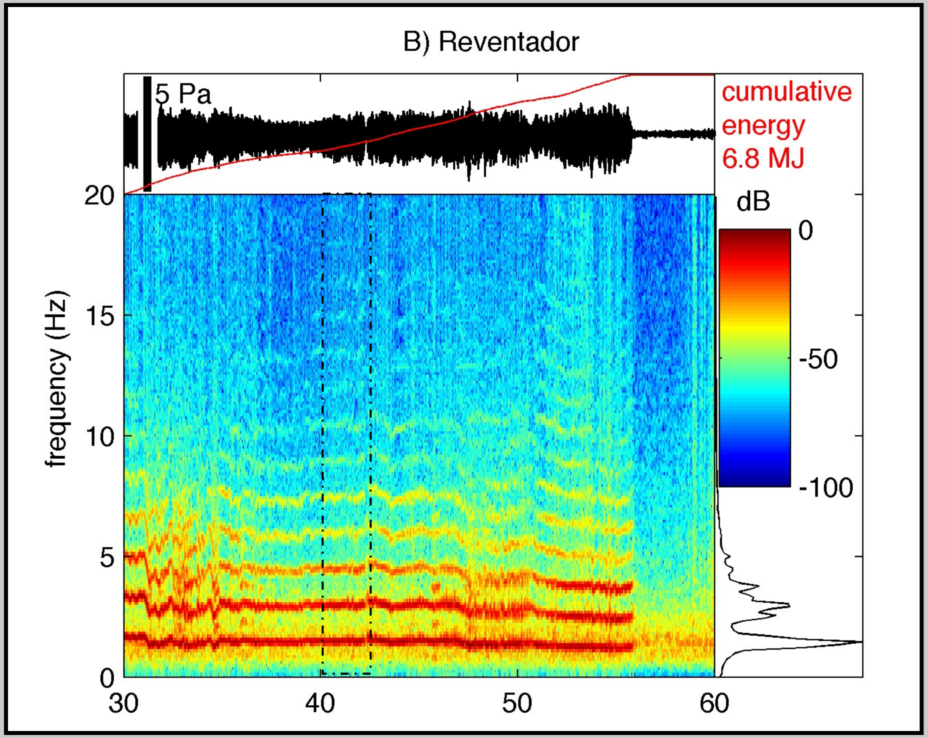

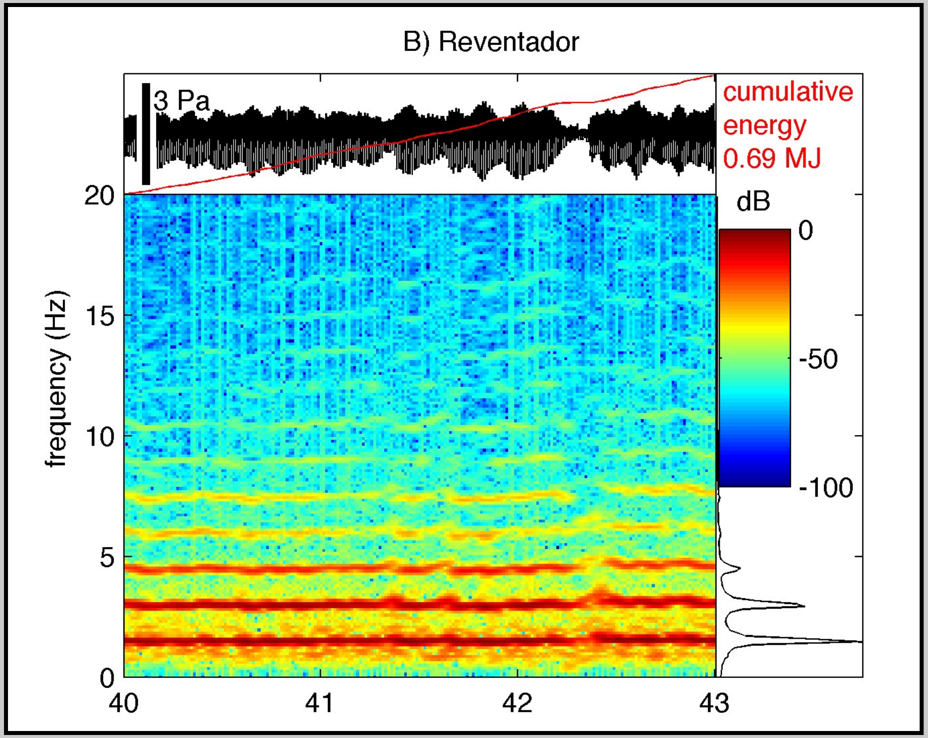

Reventador (Ecuador) - continuous degassing giving rise to ~500-m-high vapor plume. Infrasound is dominated by harmonic tremor ('chugging'), which produces consistent levels of sound and sound power (**~4000 Watts**) until shutting off.

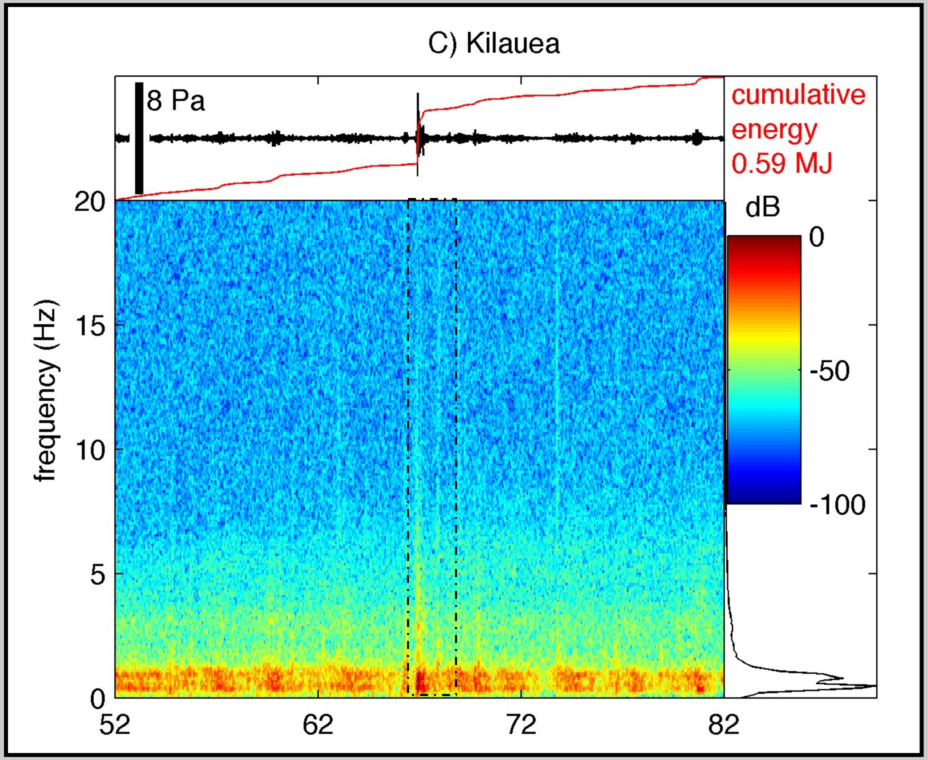

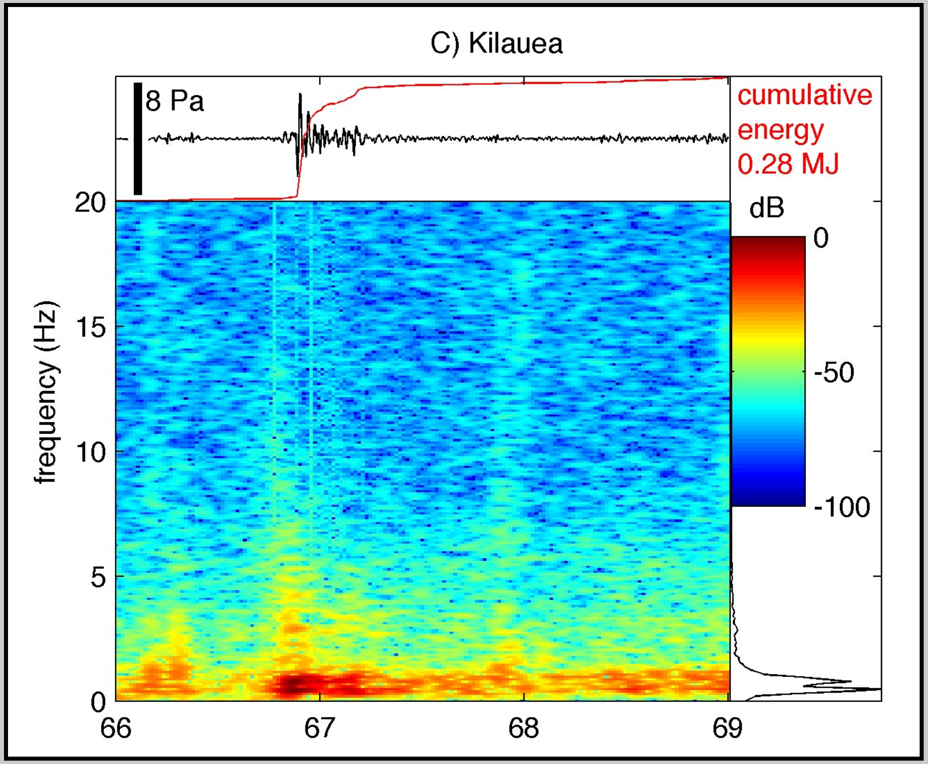

Halemaumau, Kilauea (Hawaii) - striking and long-lived monotonic tremor is continuous for months and associated with open-vent lava lake degassing. Transient infrasound pulses are thought to represent explosions instigated by pit crater collapse during which ash and blocks are expelled several hundred meters. Long term averaged acoustic power is **~300 W**.

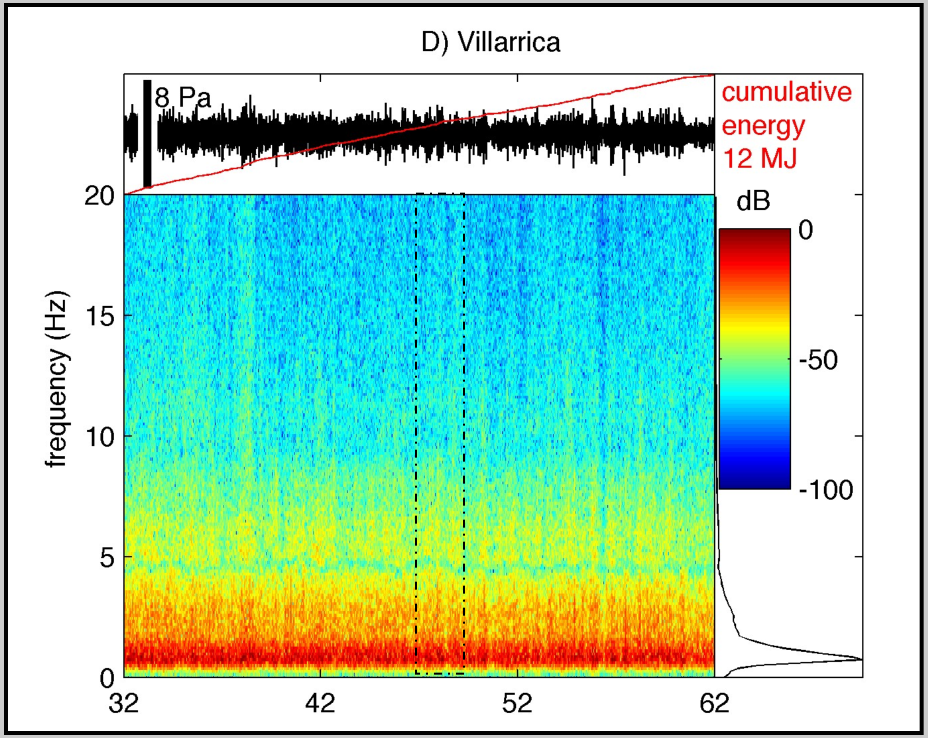

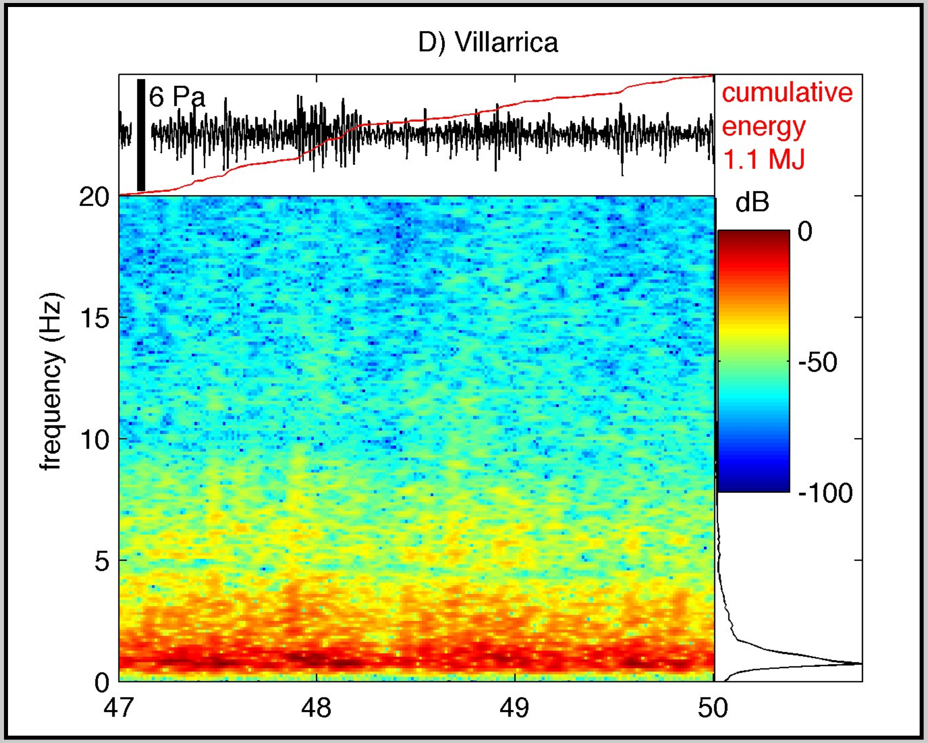

Villarrica (Chile) - like Kilauea, another monotonic tremor system associated with open-vent lava lake activity. Energy is sharply peaked at 0.77 Hz. Small Strombolian explosions at bottom of crater are not associated with infrasound transients. Sustained acoustic power is **~6500 W**.

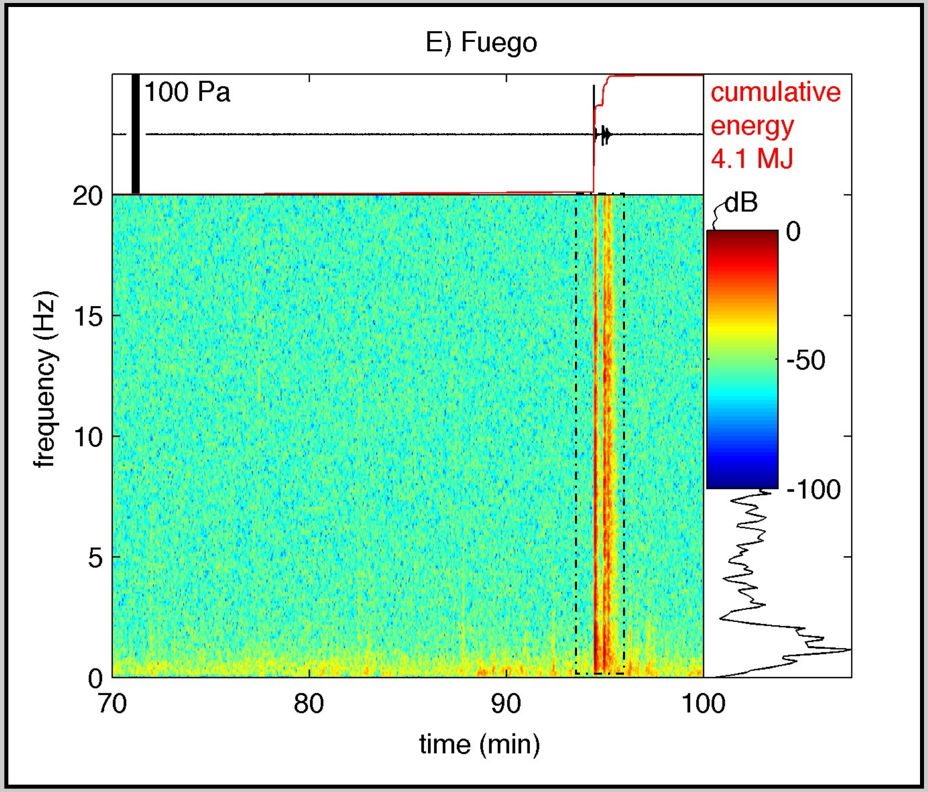

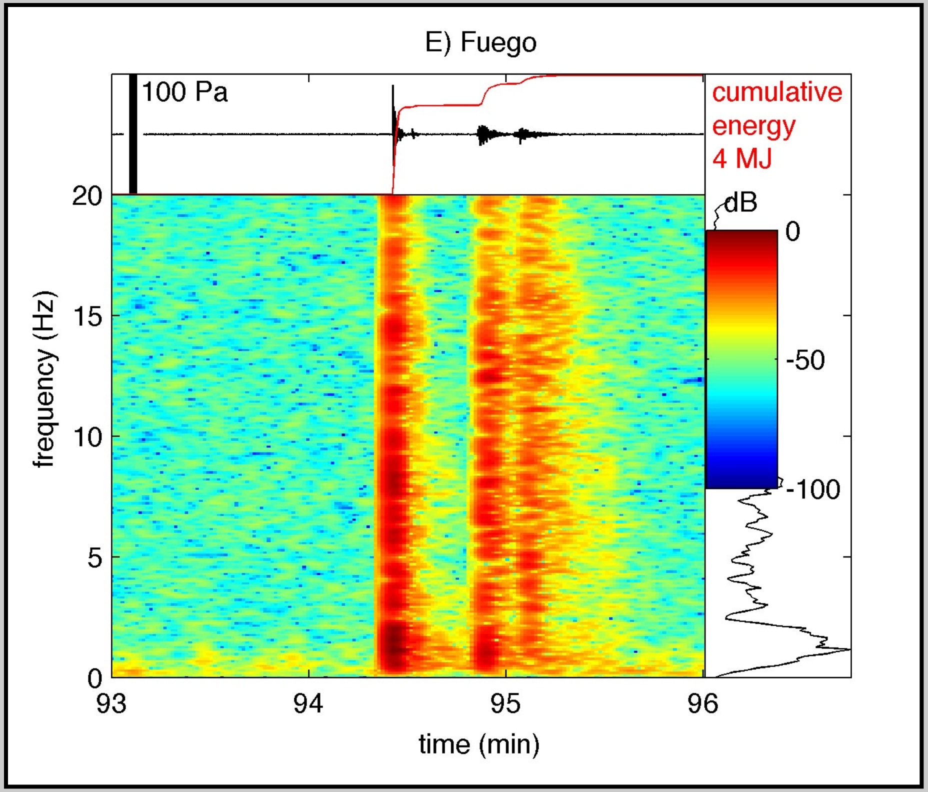

Fuego (Guatemala) - short-duration Strombolian/Vulcanian explosions generate intense, short-lived infrasound transients, which are relatively broad band in character. Almost all acoustic energy is released during these short events when acoustic power reaches ~100,000 W. Long-term averaged acoustic power is **~2200 W**.

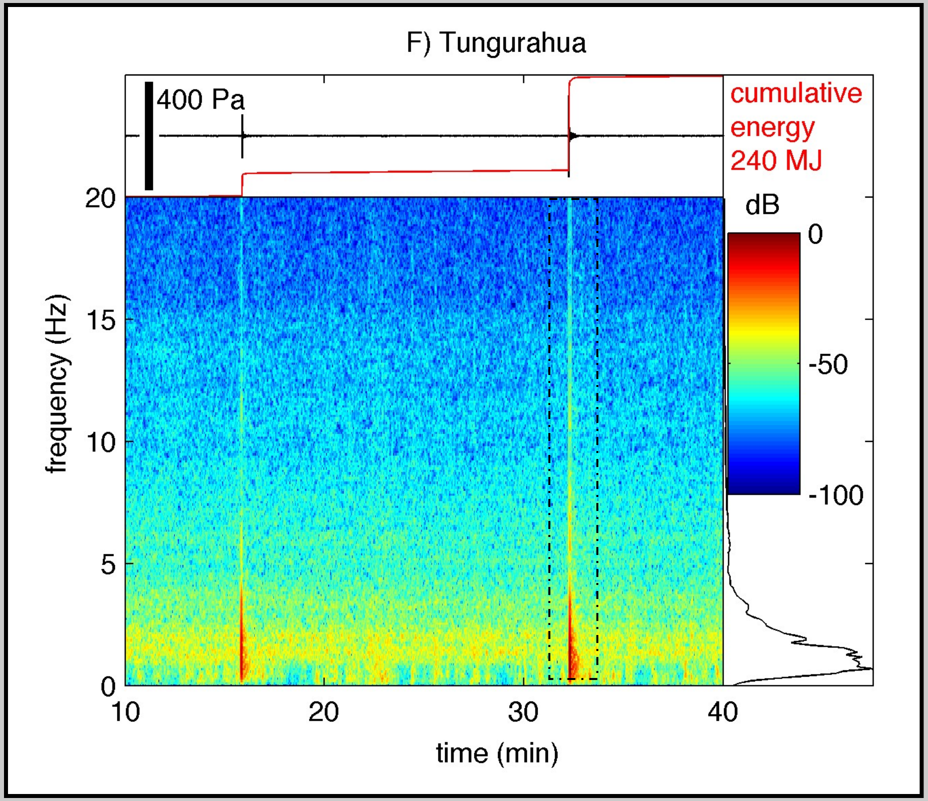

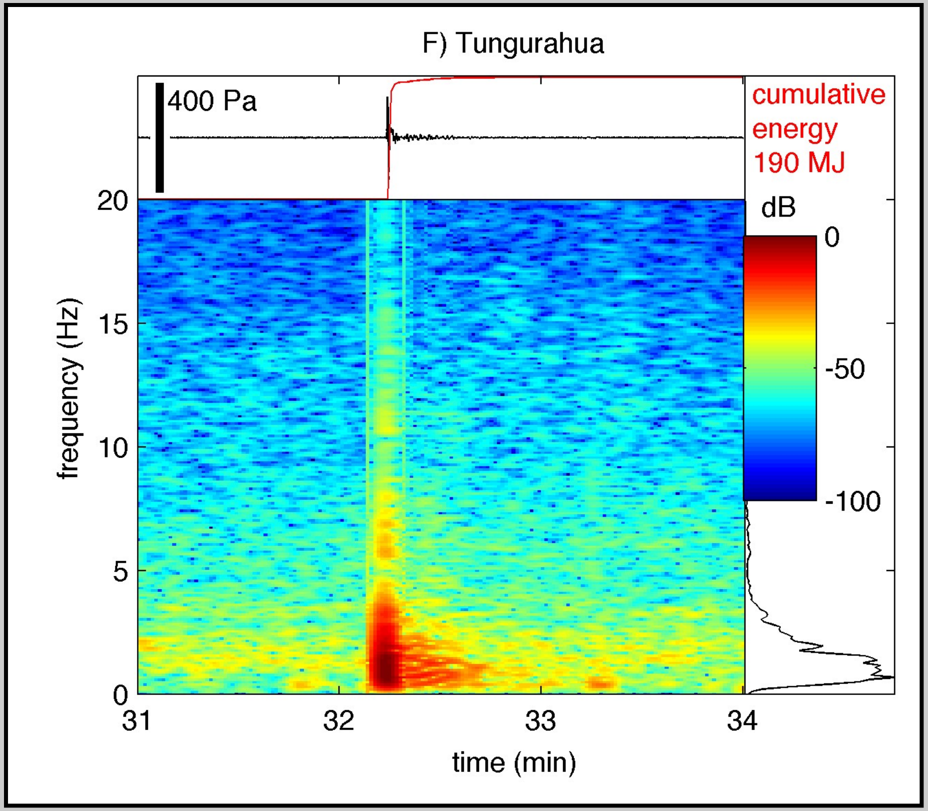

Tungurahua (Ecuador) - short-duration Vulcanian explosions ejecting ballistics to ~2 km generate intense, short-lived infrasound transients, which are confined to frequencies below about 5 Hz. Peak acoustic power is as great as 10 MWatts (10,000,000 Watts) and time-averaged power is more than **100,000 W**.

Amplitudes and energies of some volcanic eruptions






	Trace reference start time (yyyy:ddd:hh)	Station distance (km)	max pressure (Pa)	Reduced pressure at 1 km (Pa)	30-minute total energy (MJ) from Figure 1
a) Santiaguito	2009:001:11	0.4	4.4	1.8	0.18
b) Reventador	2005:236:16	1.7	0.9	1.5	6.8
c) Kilauea	2008:190:09	2.4	1.3	3.2	0.59
d) Villarrica	2010:22:12	0.1	58	2.9	12
e) Fuego	2007:117:13	7.0	5.9	41	4.1
f) Tungurahua	2009:165:15	5.5	27	150	240

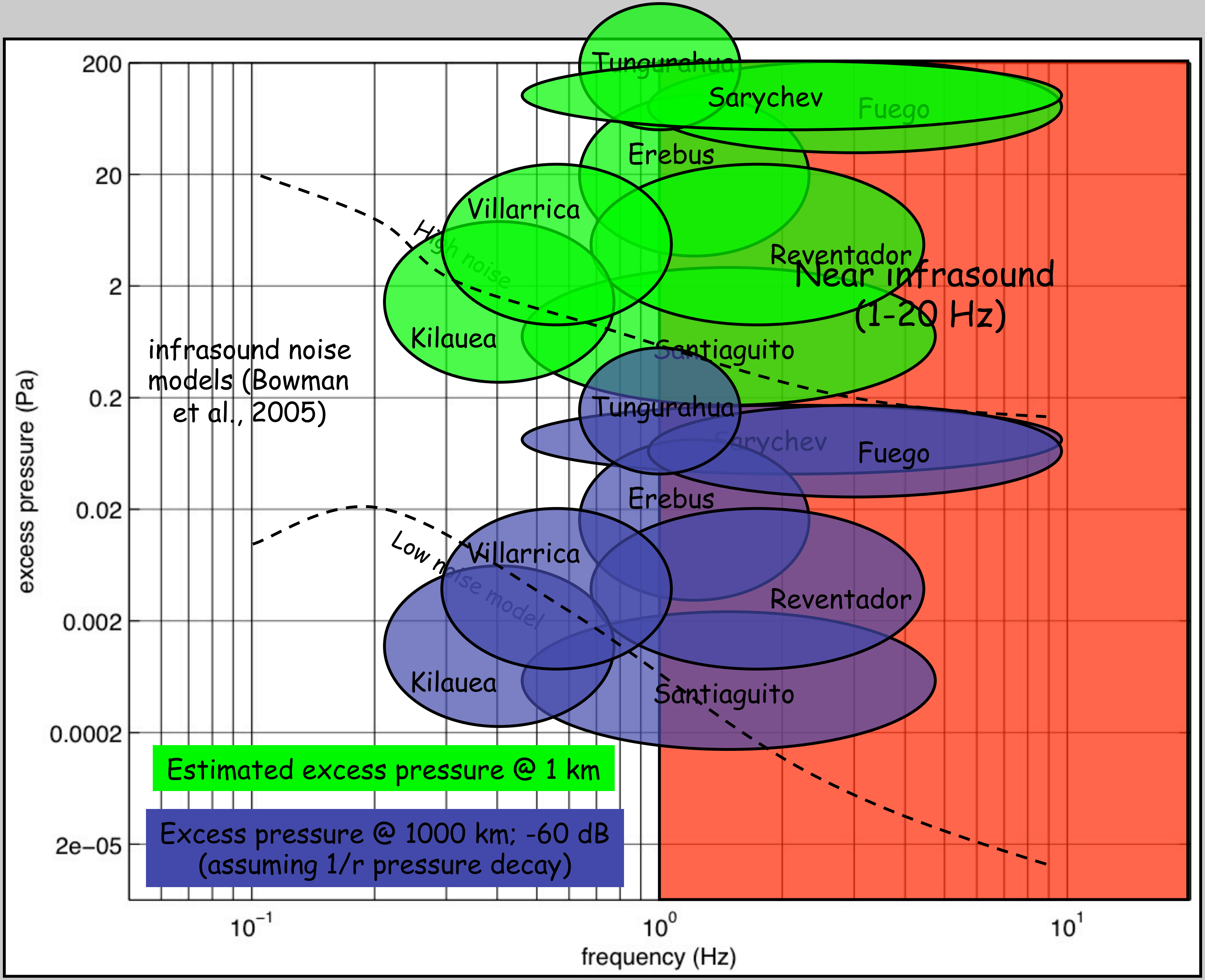

Tungurahua
Sarychev
Fuego
Erebus
Villarrica
Reventador
Near infrasound
(1-20 Hz)
Kilauea
Santiaguito
infrasound noise
models (Bowman
et al., 2005)
High noise
Low noise model
Estimated excess pressure @ 1 km
Excess pressure @ 1000 km; -60 dB
(assuming 1/r pressure decay)
excess pressure (Pa)
frequency (Hz)
200
20
2
0.2
0.02
0.002
0.0002
2e−05
10^{-1}
10^{0}
10^{1}

Sound Pressure Level and (Infra)sounds

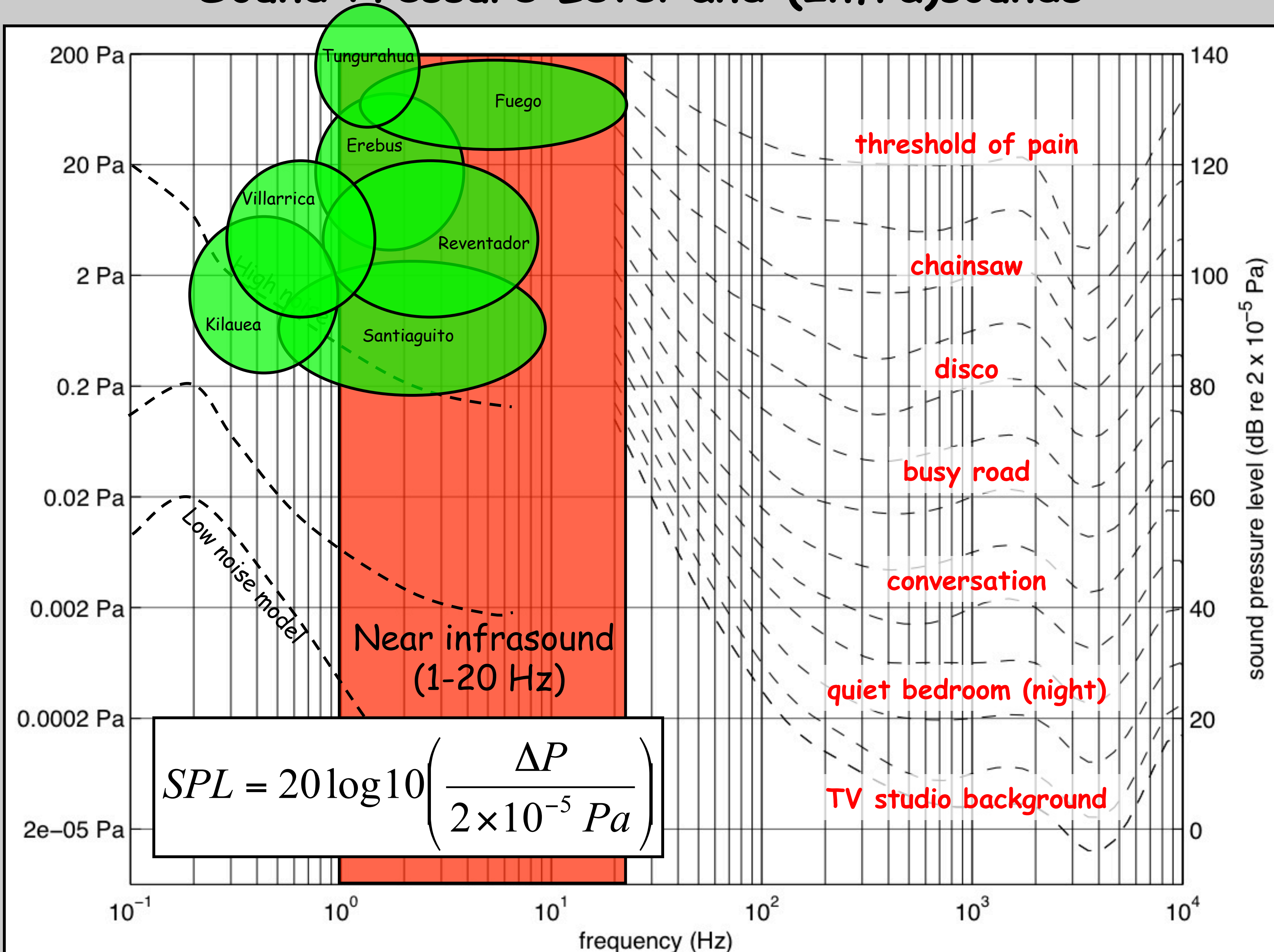

$$SPL = 20\log 10\left(\frac{\Delta P}{2\times 10^{-5}\ Pa}\right)$$


Erebus

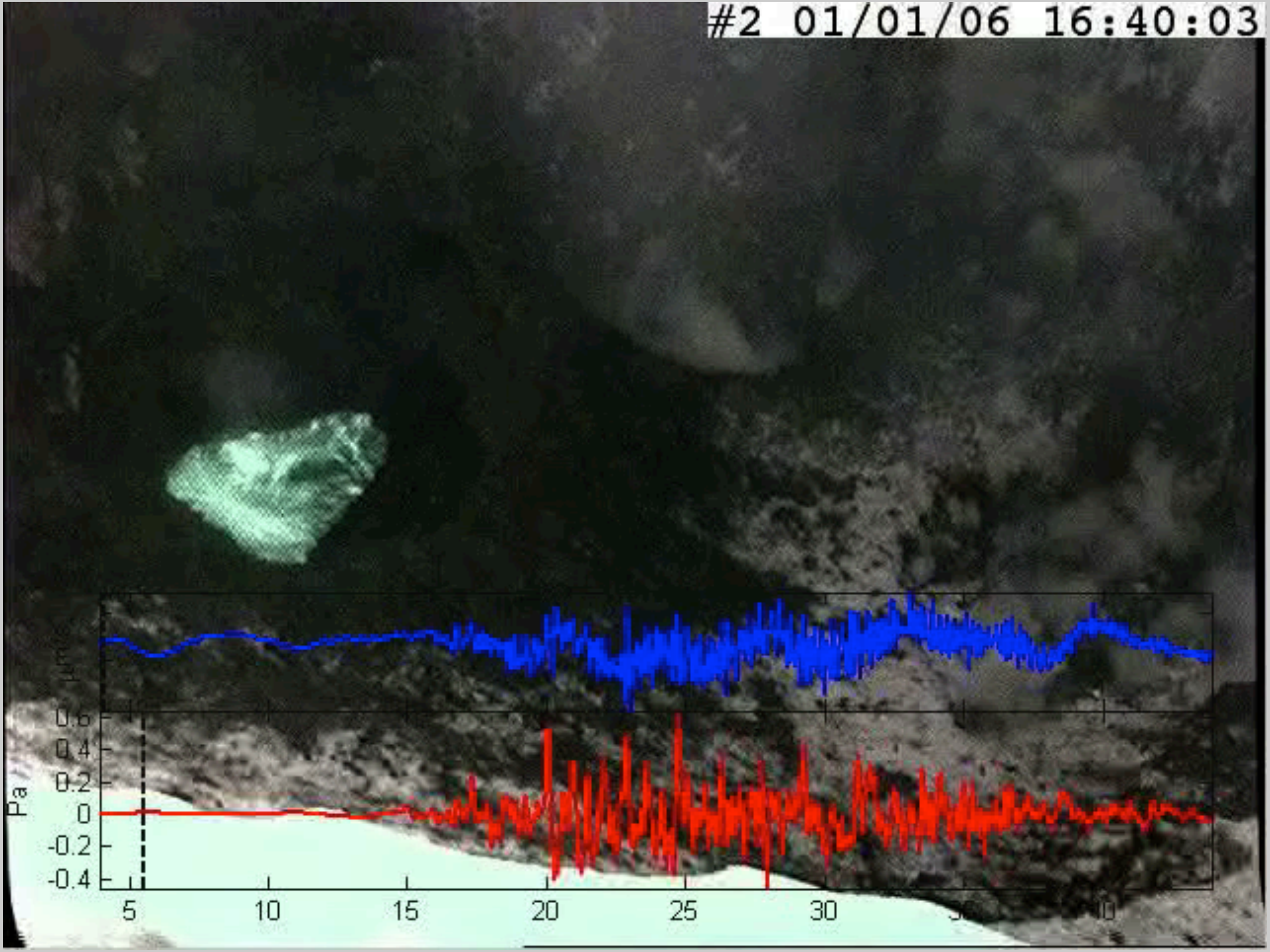
#2 01/01/06 16:40:03
Pa
0.6
0.4
0.2
0
-0.2
-0.4
5
10
15
20
25
30


#2 12/31/05 04:32:20
pressure (Pa)
6
4
2
0
-2
-4
25
30
50
55


#2 12/31/05 10:53:37
40
45
50
55
60
65
70
75


#2 12/31/05 11:44:29
pressure (Pa)
20
0
-20
-40
-60
-80
30
35
40
45
50
55
60
65

FRAGMENTATION
V1
V2
V3
LAVA LAKE

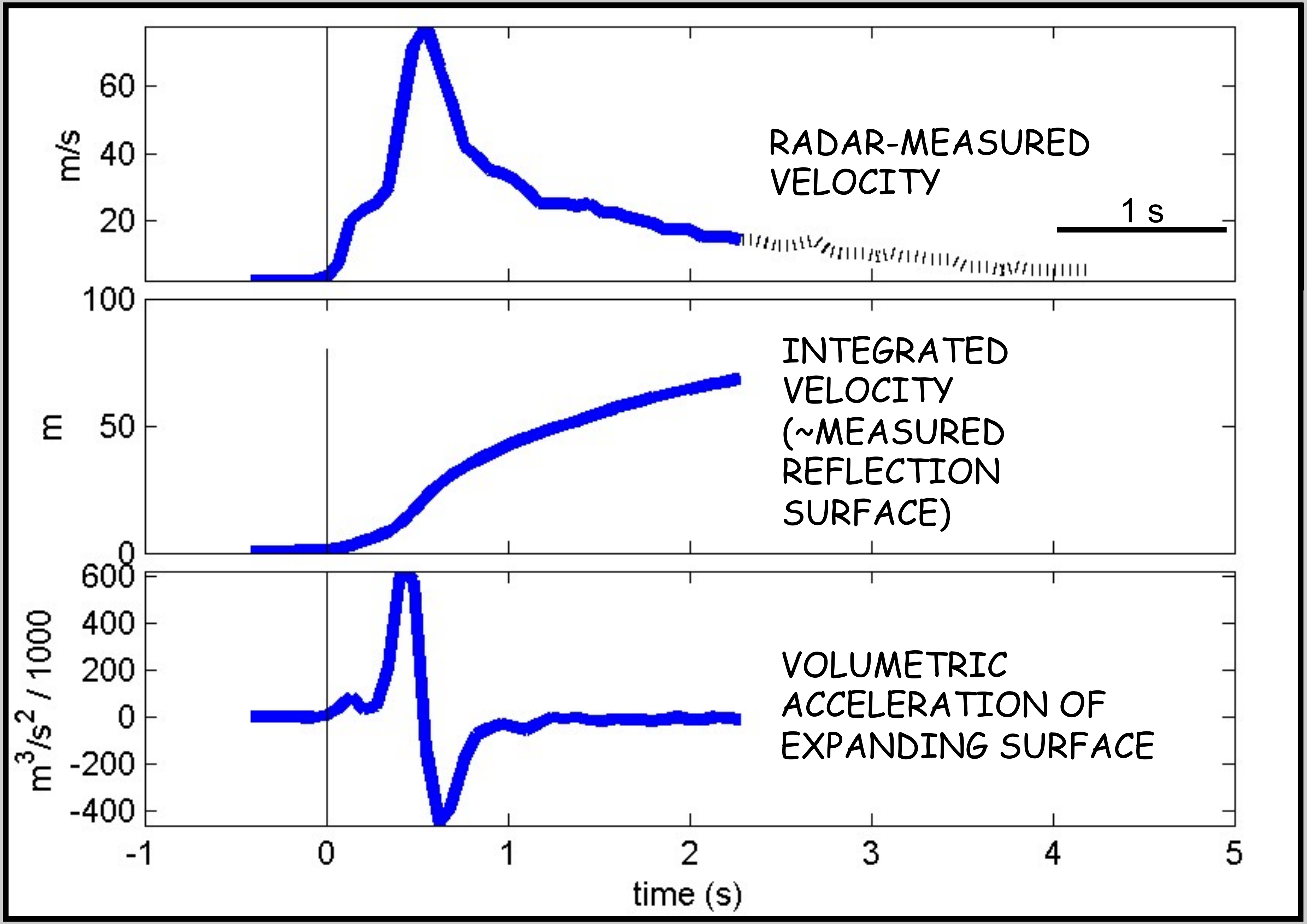

RADAR-MEASURED VELOCITY
1 s
INTEGRATED VELOCITY (~MEASURED REFLECTION SURFACE)
VOLUMETRIC ACCELERATION OF EXPANDING SURFACE
m/s
m
m3/s2 / 1000
time (s)

Lighthill's Acoustic Monopole Source (assuming compact source and linear wave propagation)

$$p(r,t) = \frac{Q(t - r/c)}{2\pi r}$$

Where *p(r,t)* is the excess pressure (in Pa) and *Q* is the source strength, or density x "volumetric acceleration" (in kg/s^2) of the atmosphere

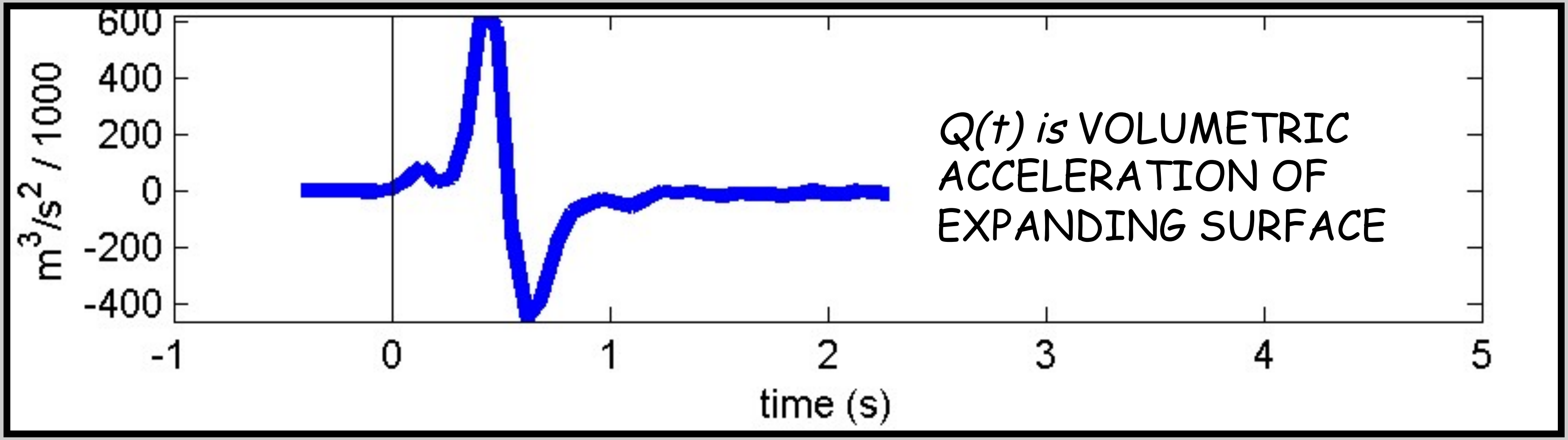

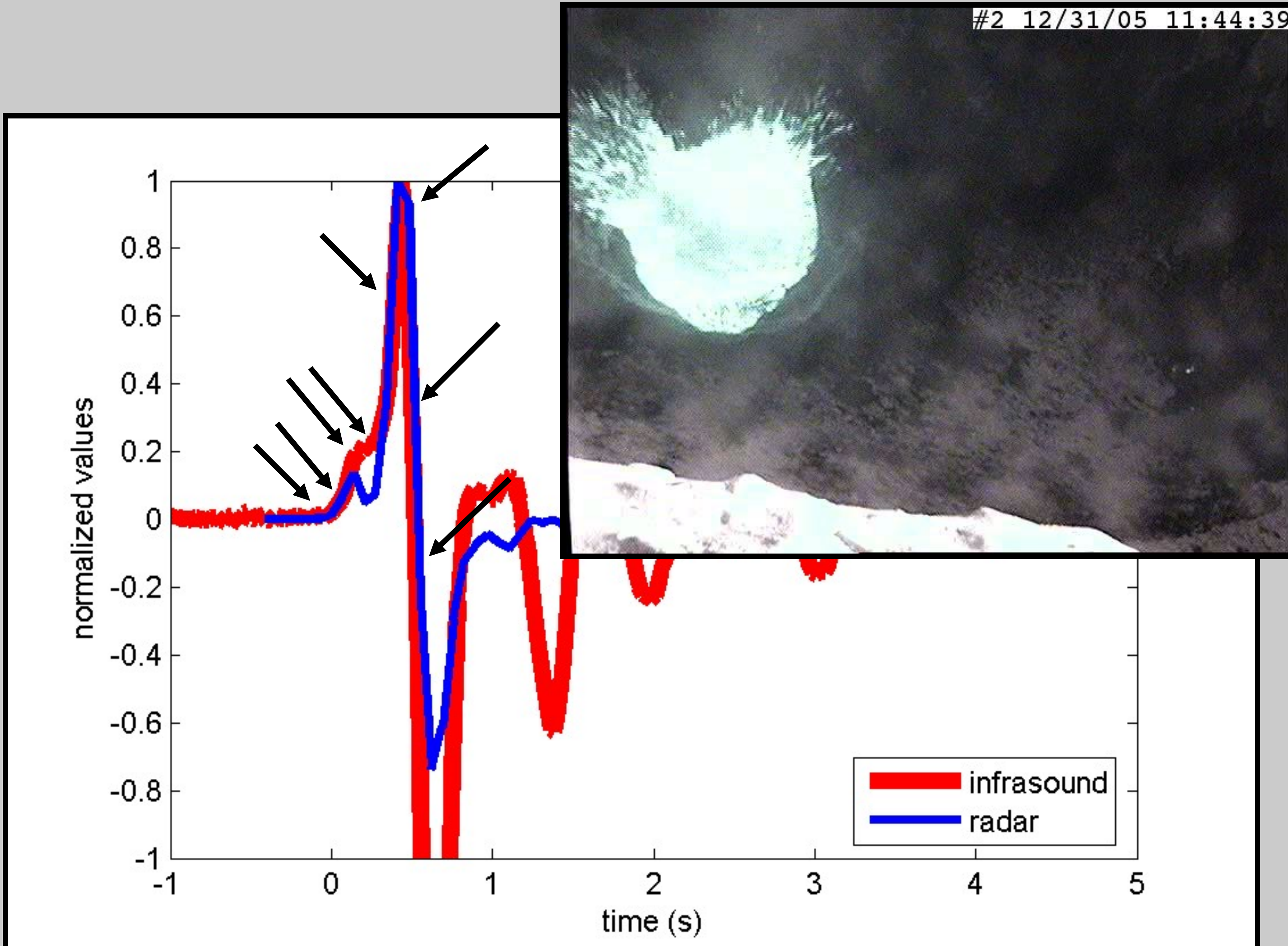

#2 12/31/05 11:44:39
normalized values
time (s)
infrasound
radar
1
0.8
0.6
0.4
0.2
0
-0.2
-0.4
-0.6
-0.8
-1
-1
0
1
2
3
4
5

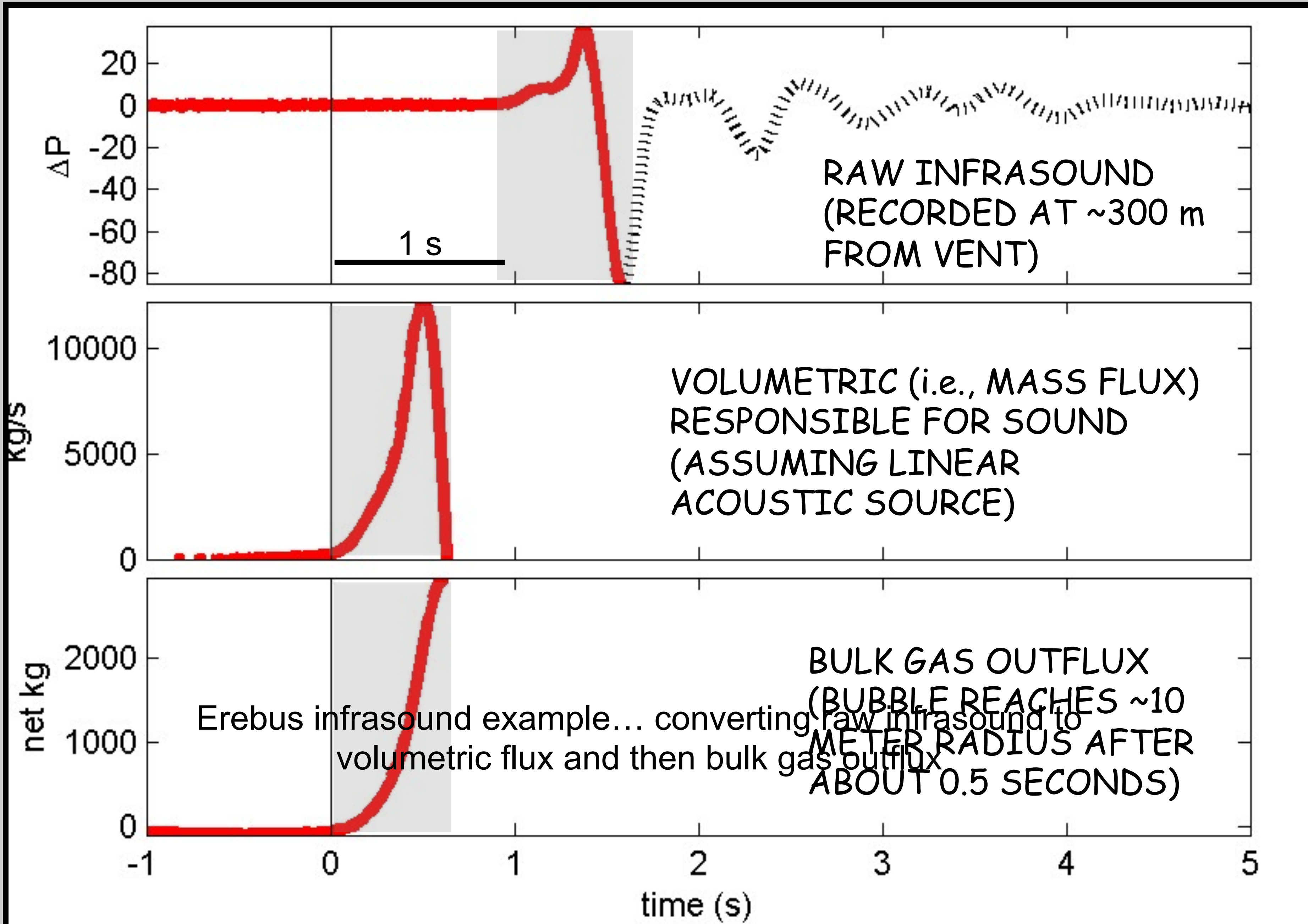

Erebus infrasound example… converting raw infrasound to volumetric flux and then bulk gas outflux


Tungurahua

Erebus

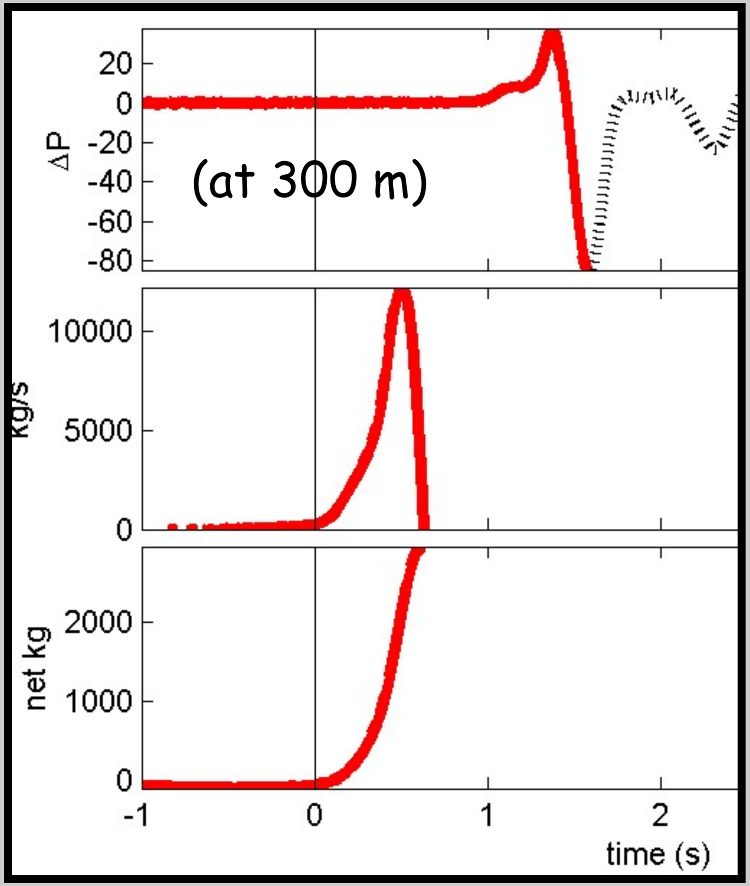

Tungurahua

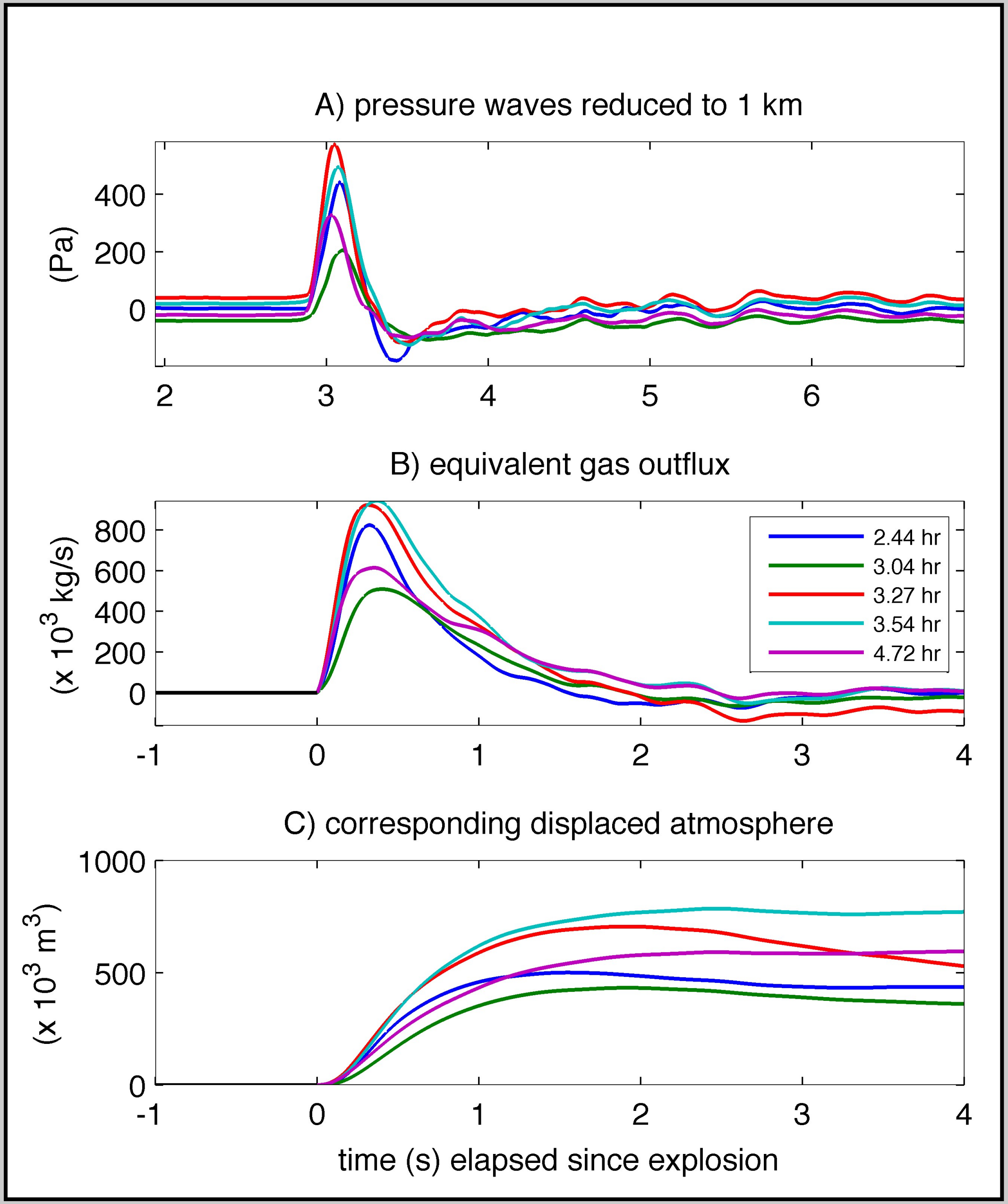


Santiaguito


SGC
01/01/09 12:57 PM

Event #1: occurring Jan 002 at 14:16:46

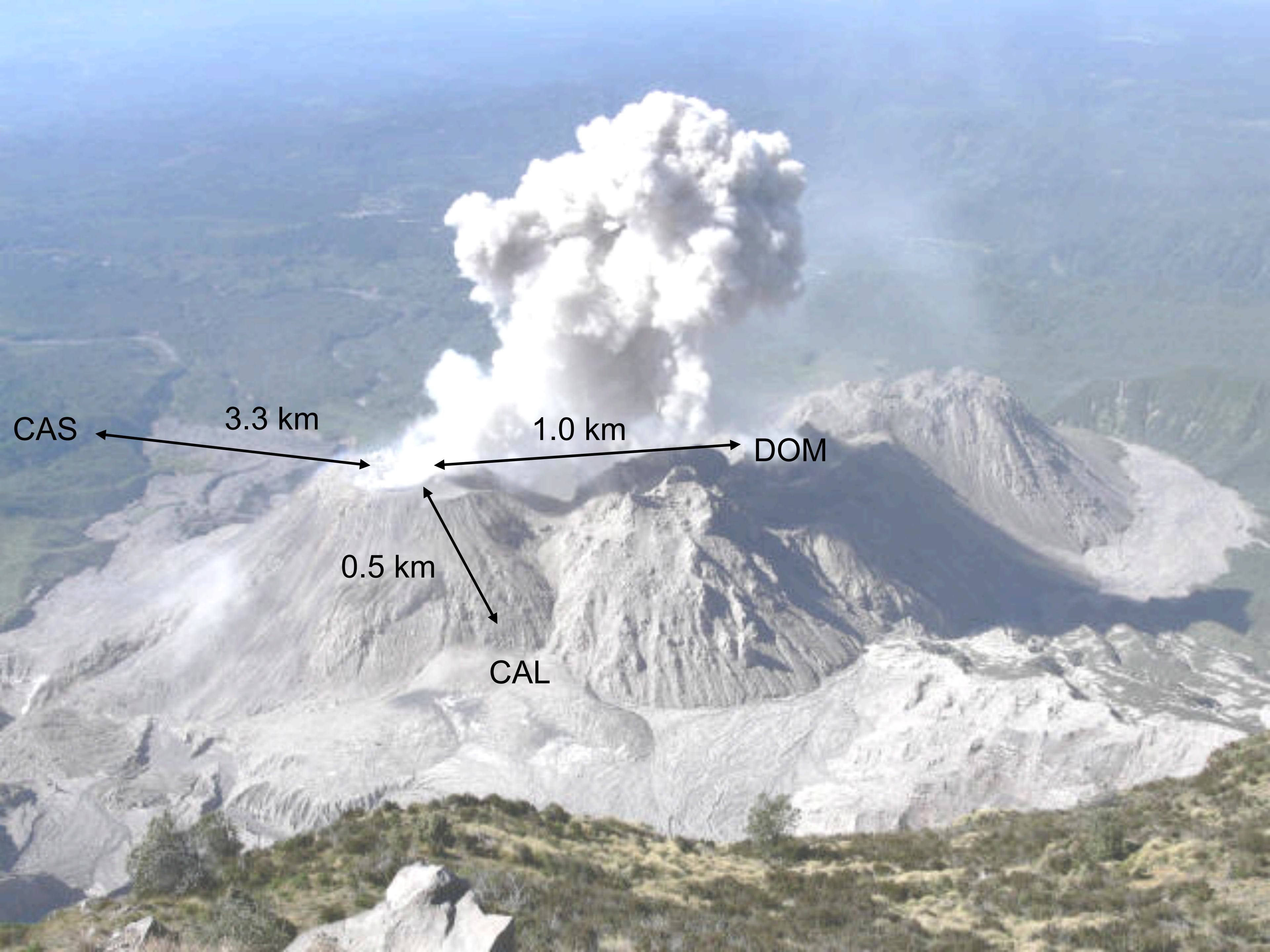
CAS
3.3 km
1.0 km
DOM
0.5 km
CAL

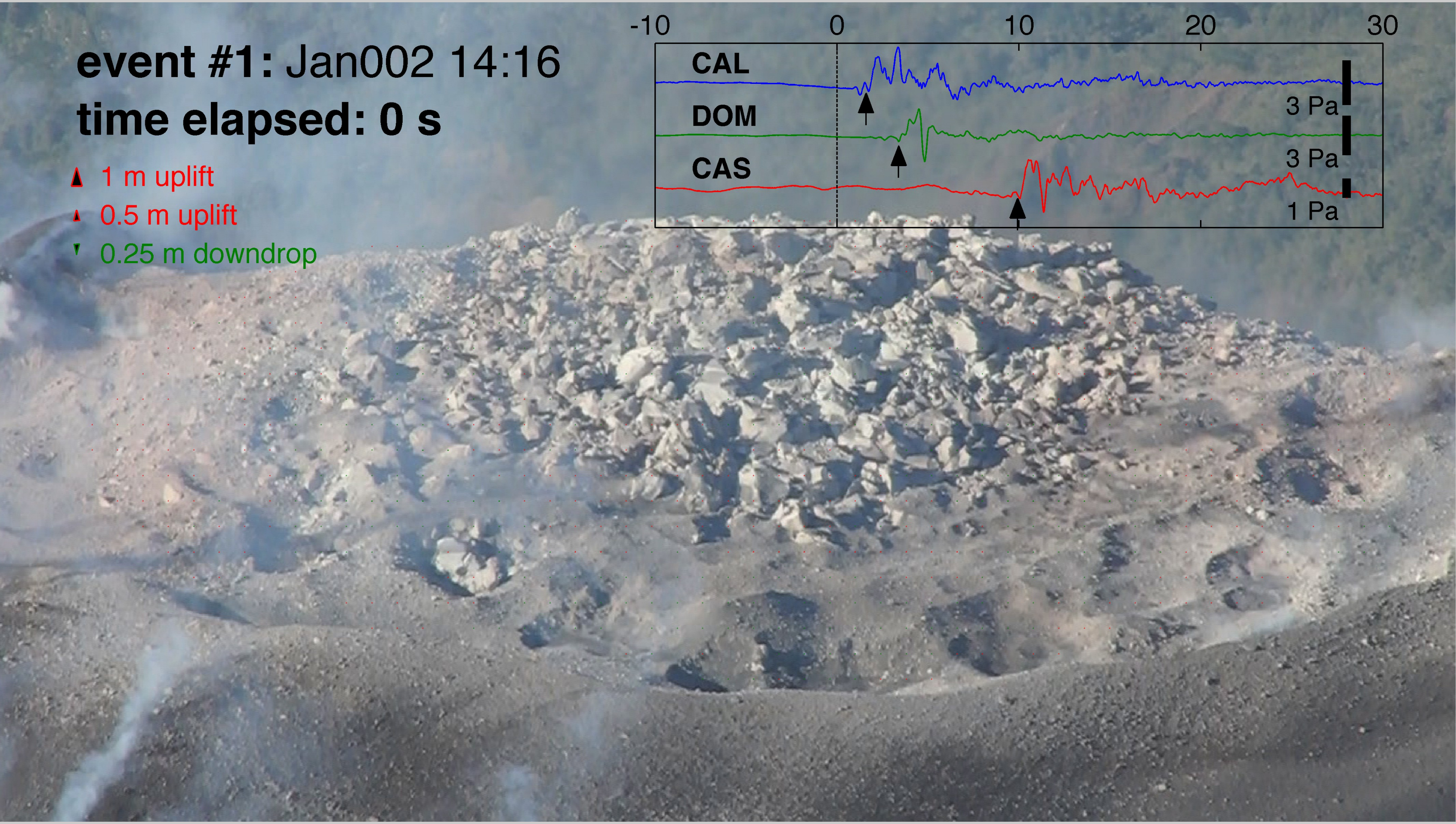

event #1: Jan002 14:16
time elapsed: 0 s
1 m uplift
0.5 m uplift
0.25 m downdrop
-10
0
10
20
30
CAL
DOM
CAS
3 Pa
3 Pa
1 Pa

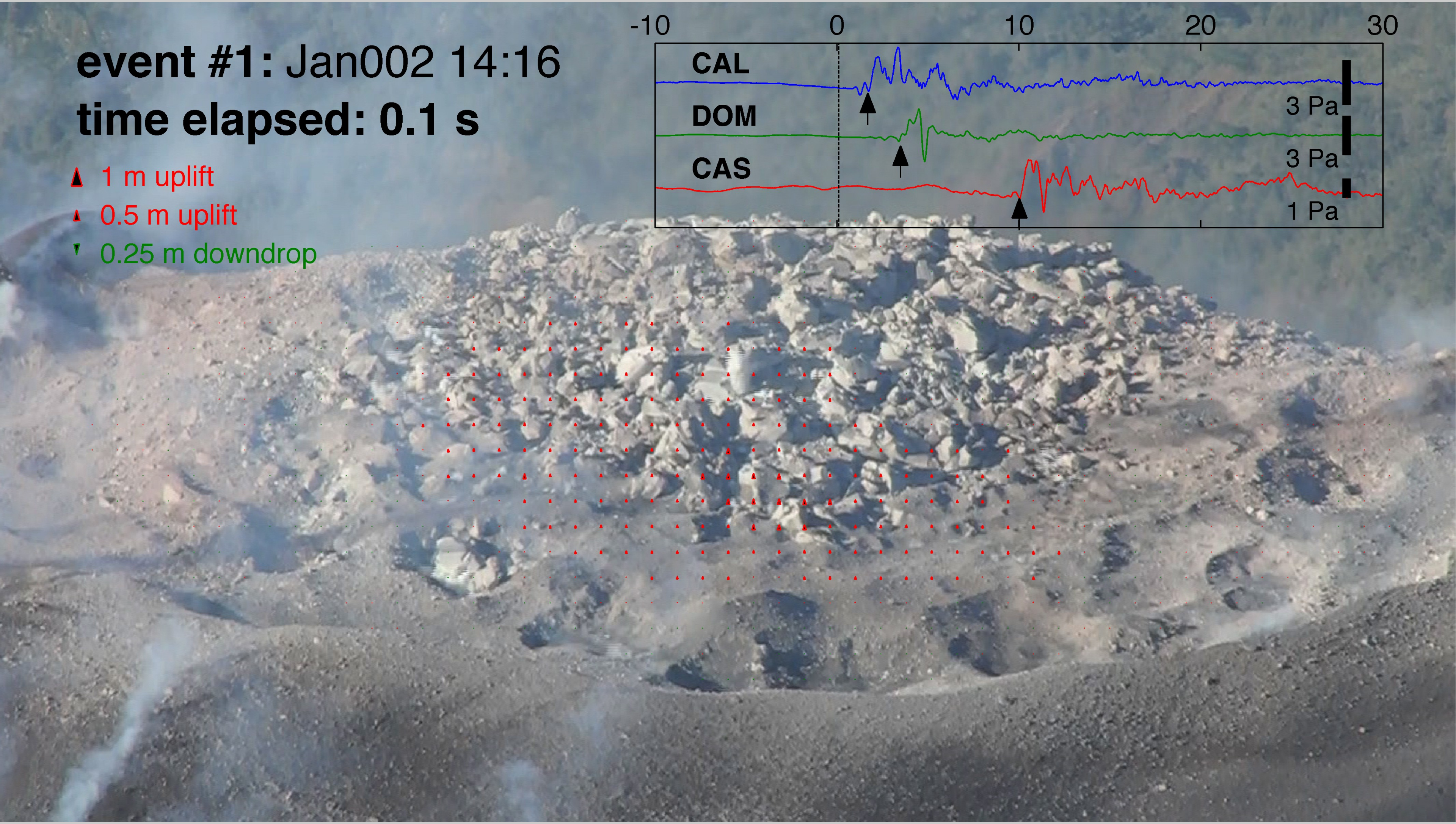

event #1: Jan002 14:16
time elapsed: 0.1 s
1 m uplift
0.5 m uplift
0.25 m downdrop
-10
0
10
20
30
CAL
DOM
CAS
3 Pa
3 Pa
1 Pa

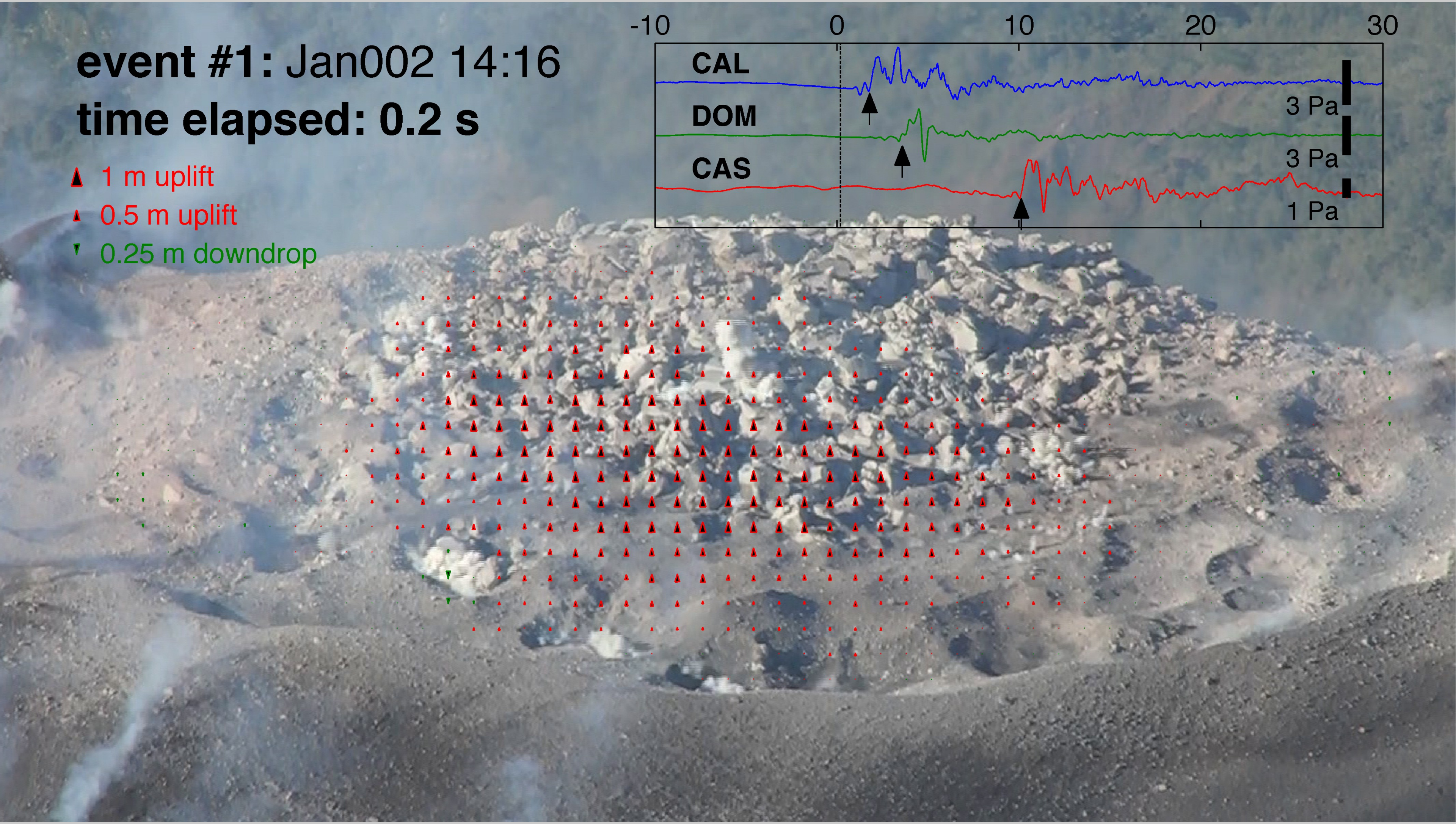

event #1: Jan002 14:16
time elapsed: 0.2 s
1 m uplift
0.5 m uplift
0.25 m downdrop
-10
0
10
20
30
CAL
DOM
CAS
3 Pa
3 Pa
1 Pa

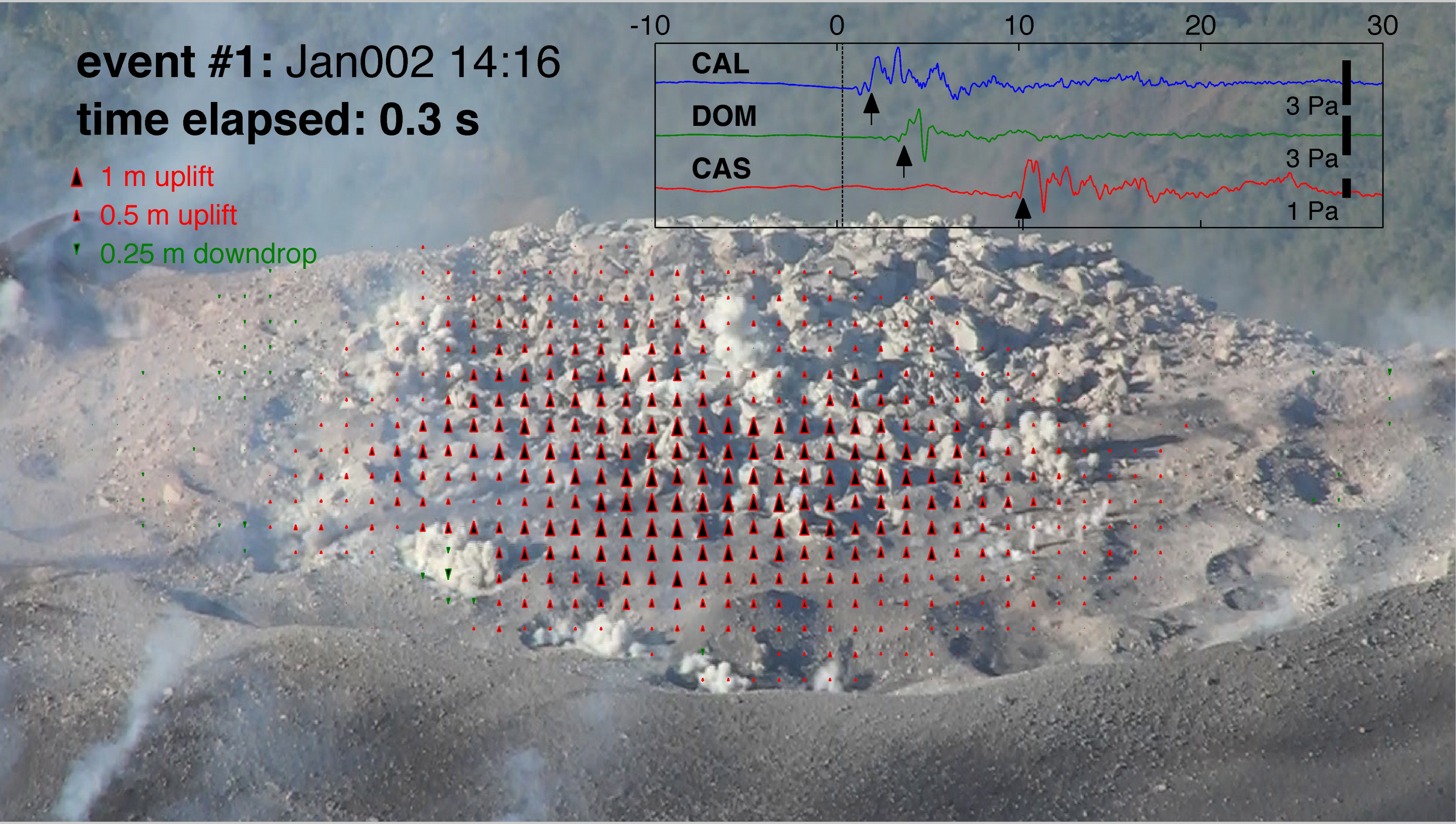
event #1: Jan002 14:16
time elapsed: 0.3 s
1 m uplift
0.5 m uplift
0.25 m downdrop
-10
0
10
20
30
CAL
DOM
CAS
3 Pa
3 Pa
1 Pa

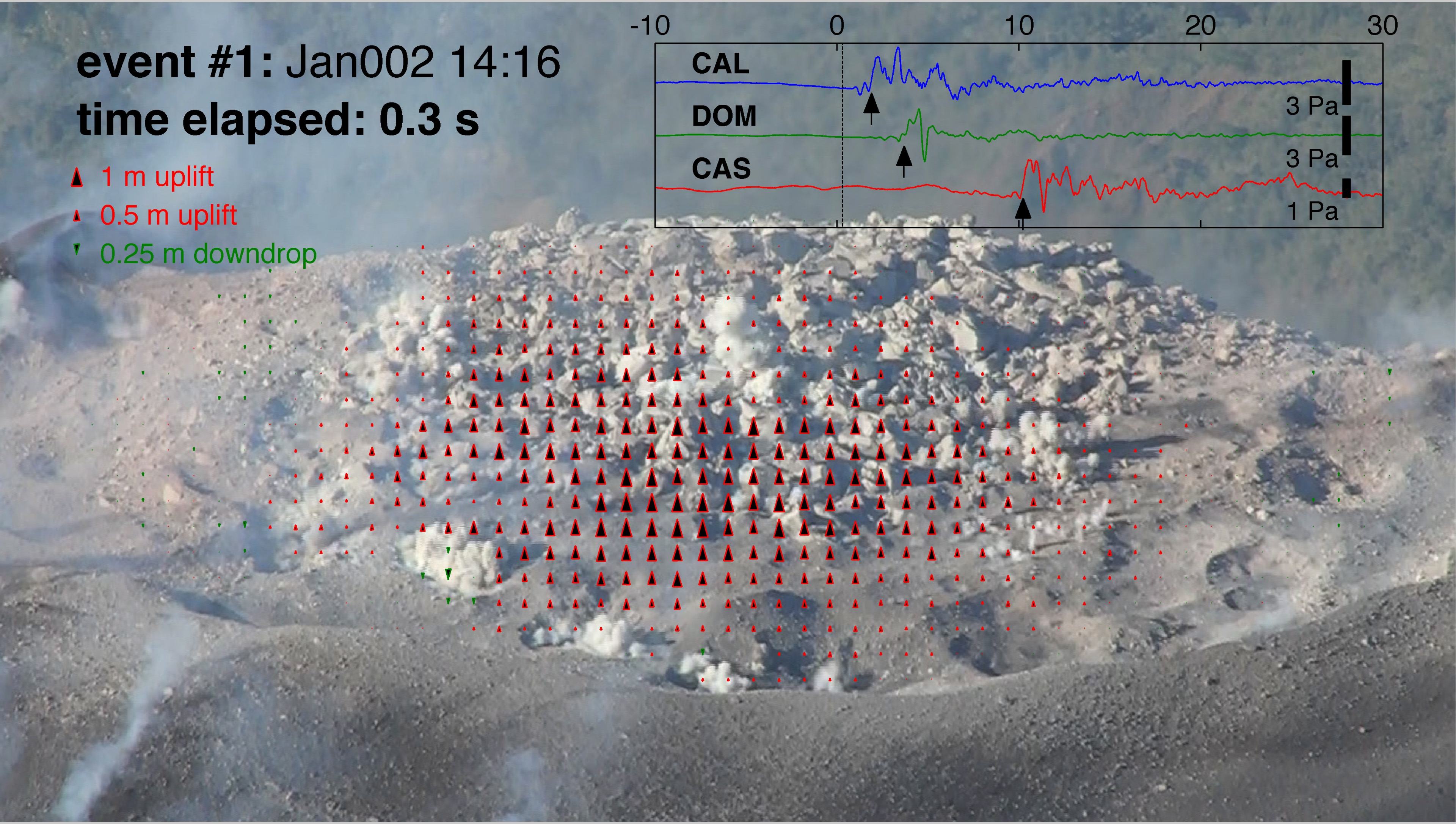

event #1: Jan002 14:16
time elapsed: 0.3 s
1 m uplift
0.5 m uplift
0.25 m downdrop
-10
0
10
20
30
CAL
DOM
CAS
3 Pa
3 Pa
1 Pa

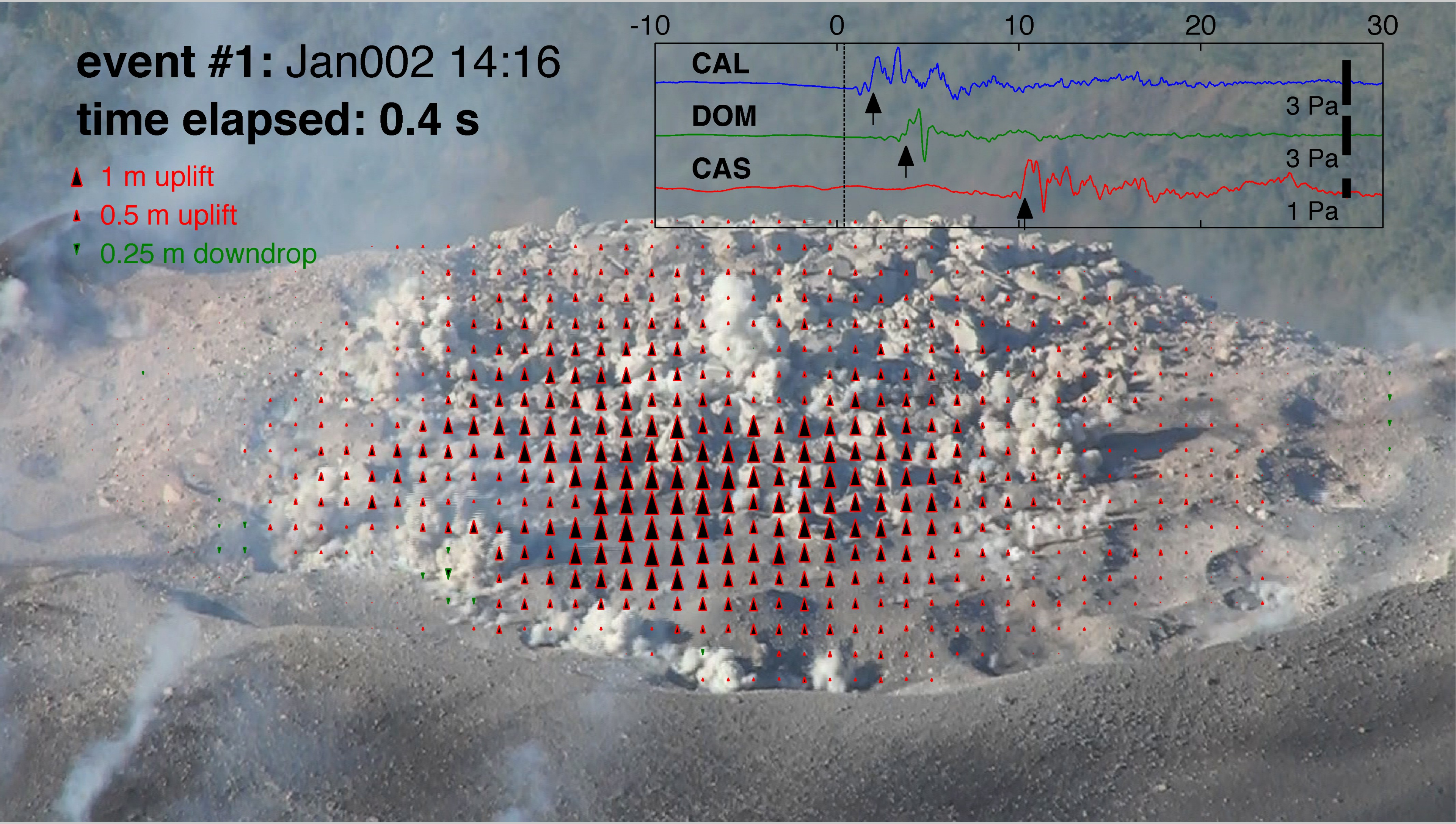

event #1: Jan002 14:16
time elapsed: 0.4 s
1 m uplift
0.5 m uplift
0.25 m downdrop
-10
0
10
20
30
CAL
DOM
CAS
3 Pa
3 Pa
1 Pa

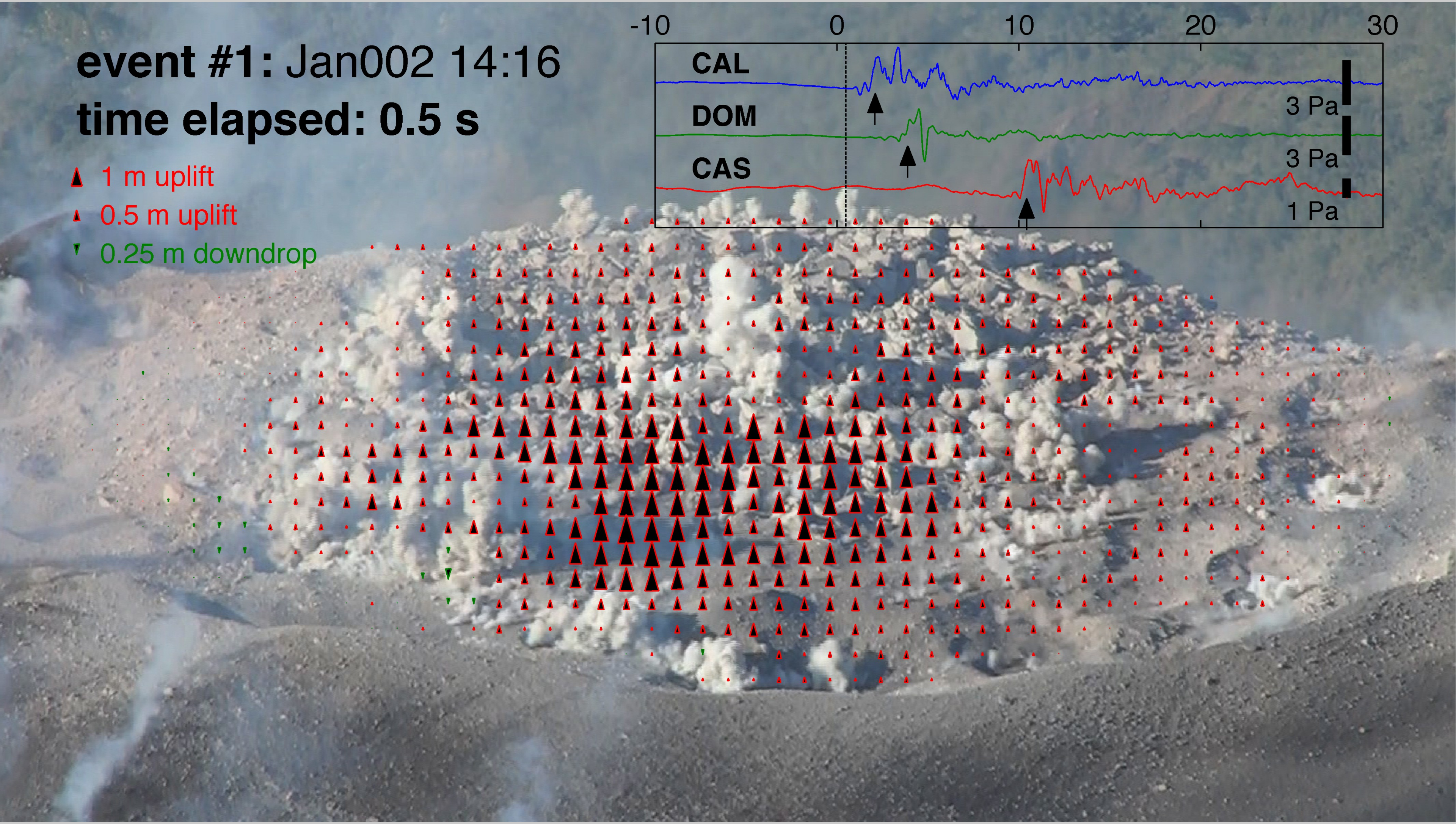

event #1: Jan002 14:16
time elapsed: 0.5 s
1 m uplift
0.5 m uplift
0.25 m downdrop
-10
0
10
20
30
CAL
DOM
CAS
3 Pa
3 Pa
1 Pa

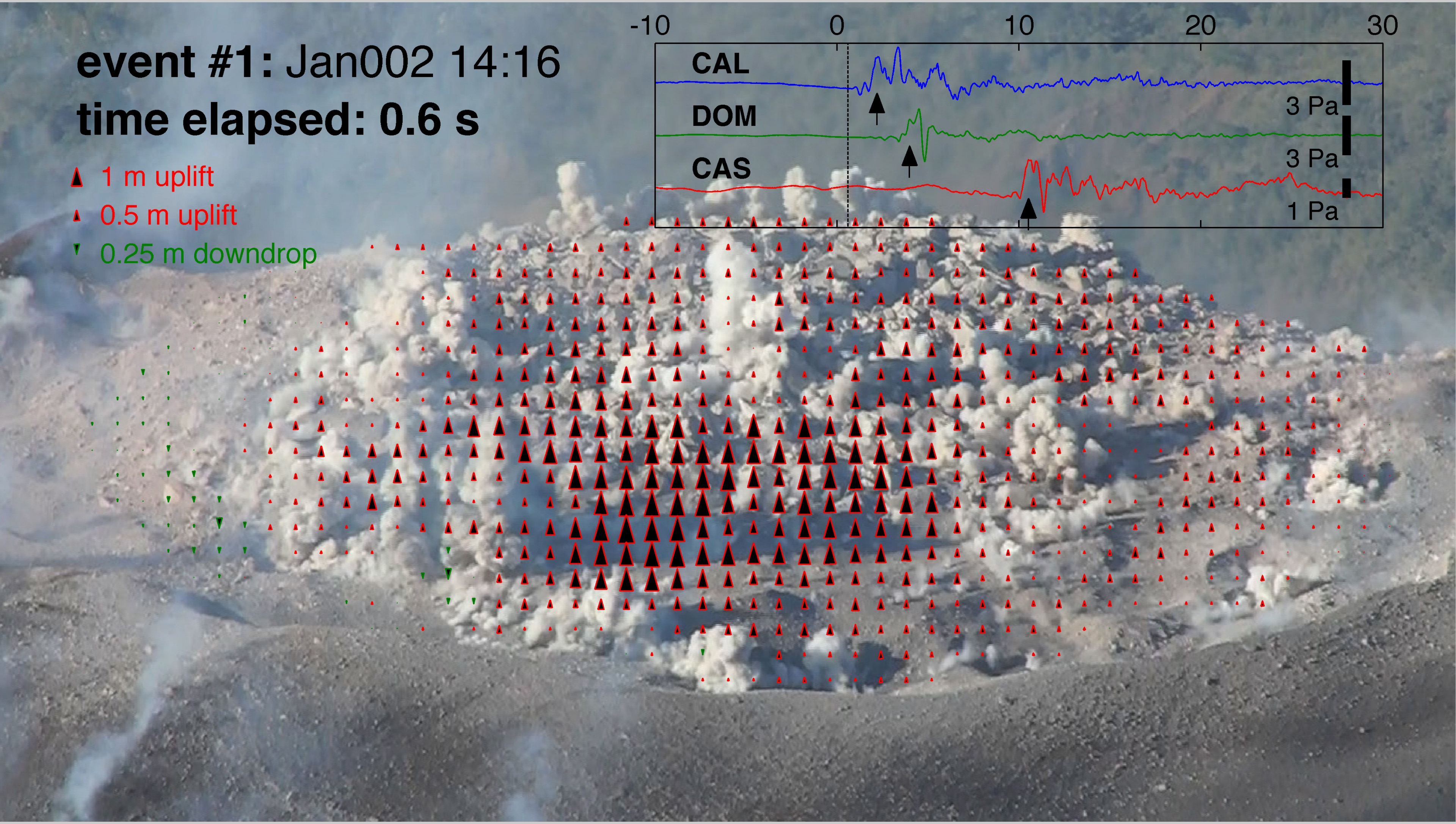

event #1: Jan002 14:16
time elapsed: 0.6 s
1 m uplift
0.5 m uplift
0.25 m downdrop
-10
0
10
20
30
CAL
DOM
CAS
3 Pa
3 Pa
1 Pa

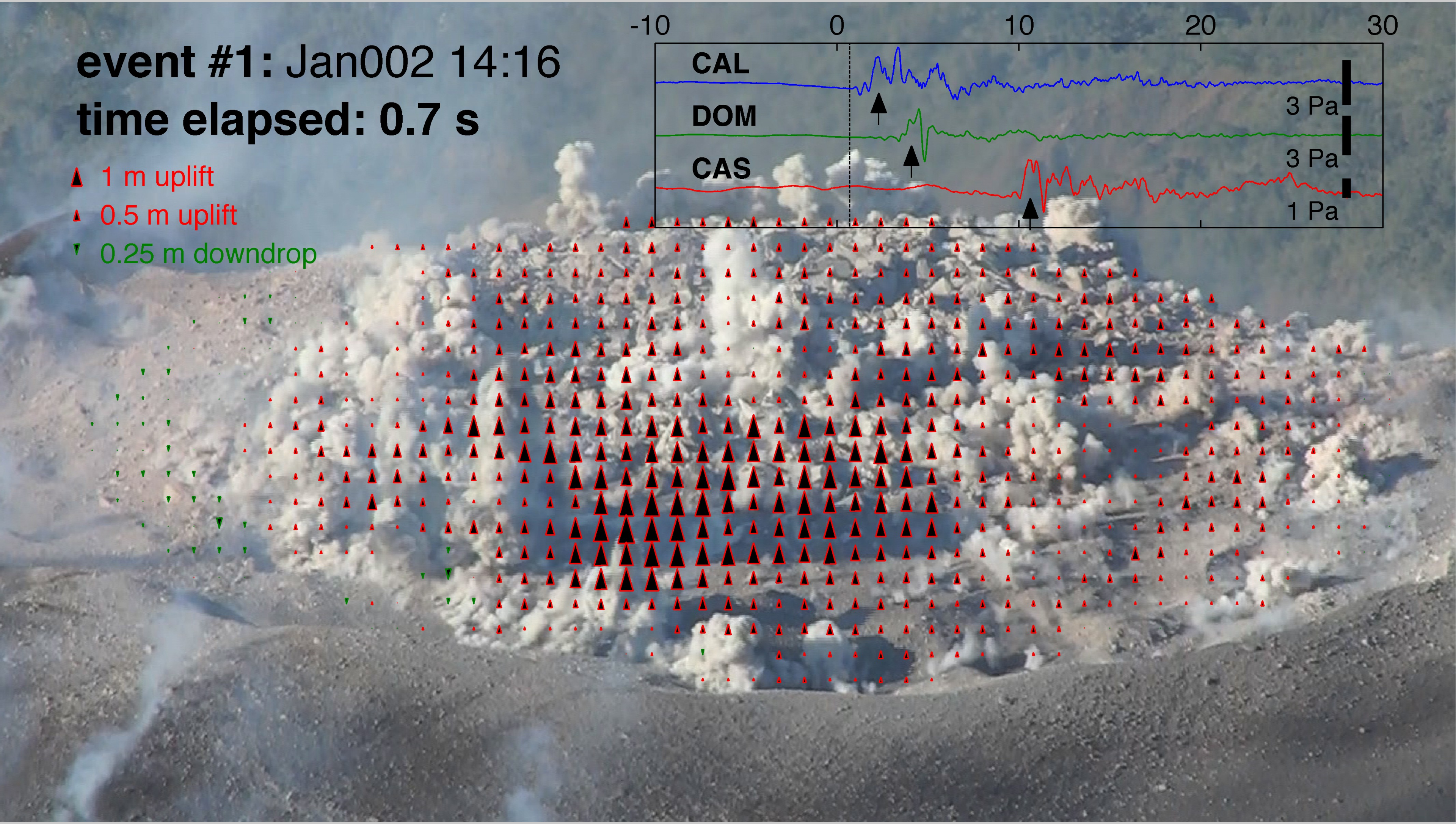

event #1: Jan002 14:16
time elapsed: 0.7 s
1 m uplift
0.5 m uplift
0.25 m downdrop
-10
0
10
20
30
CAL
DOM
CAS
3 Pa
3 Pa
1 Pa

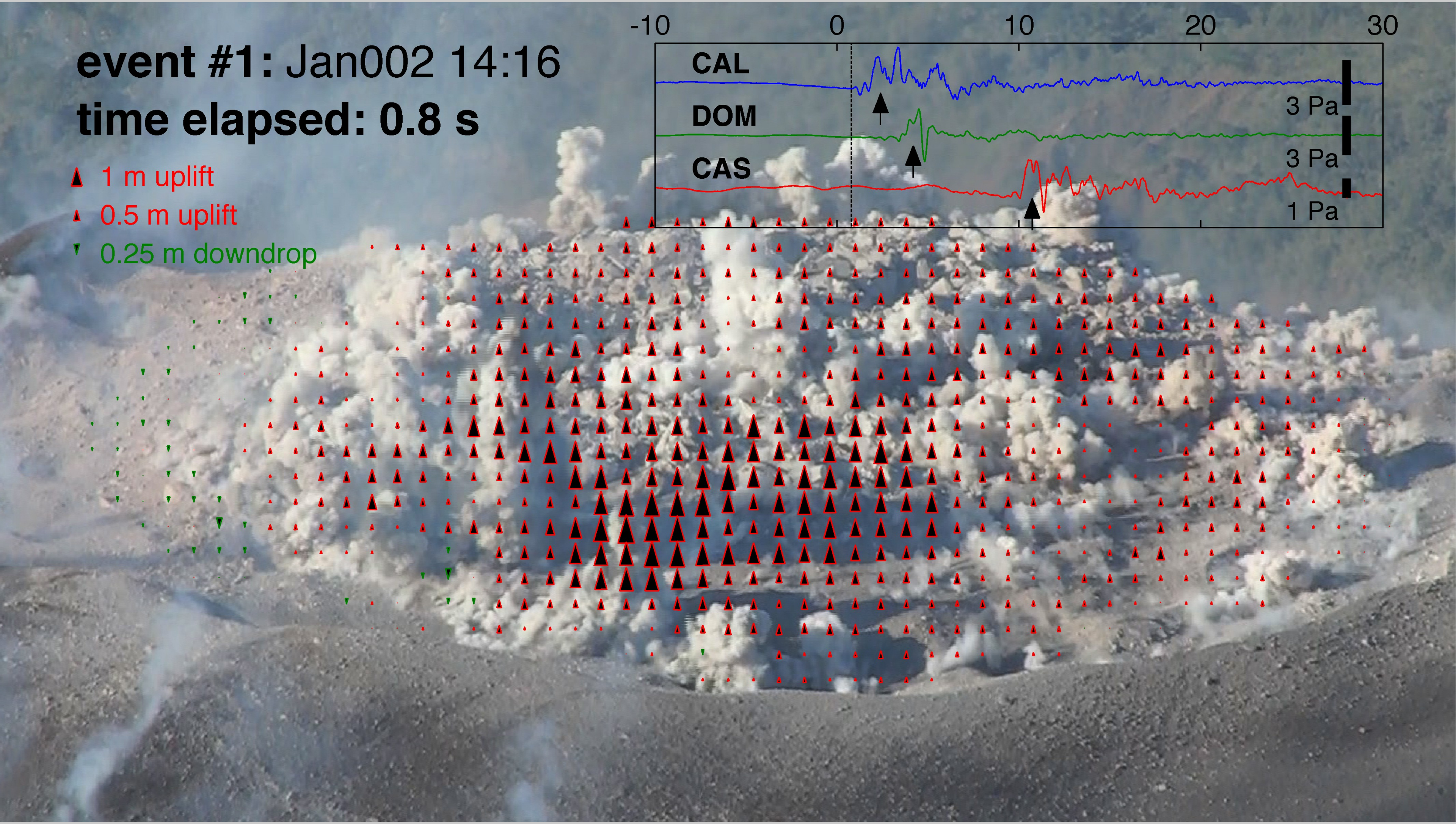
event #1: Jan002 14:16
time elapsed: 0.8 s
1 m uplift
0.5 m uplift
0.25 m downdrop
-10
0
10
20
30
CAL
DOM
CAS
3 Pa
3 Pa
1 Pa

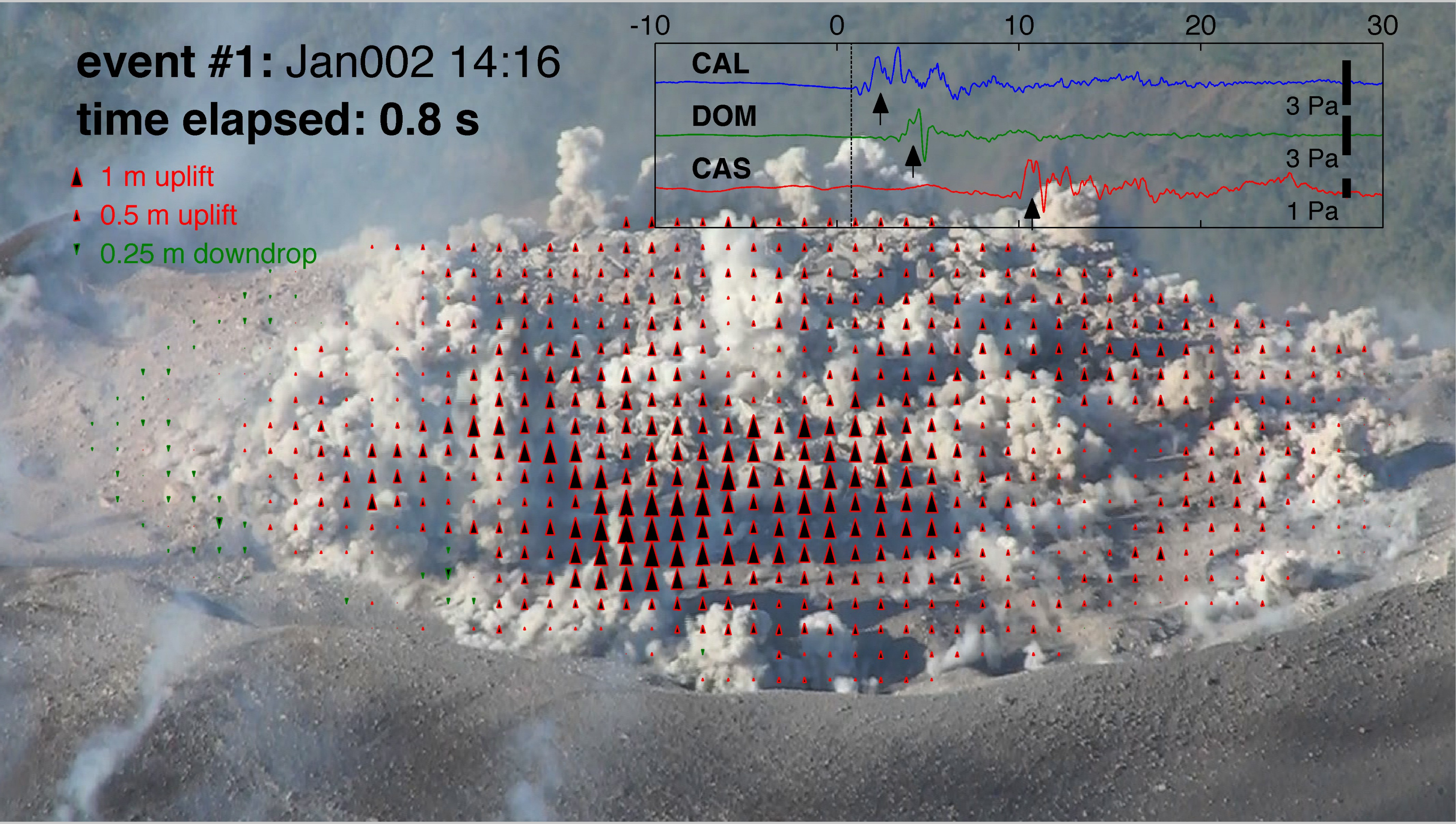

event #1: Jan002 14:16
time elapsed: 0.8 s
1 m uplift
0.5 m uplift
0.25 m downdrop
-10
0
10
20
30
CAL
DOM
CAS
3 Pa
3 Pa
1 Pa

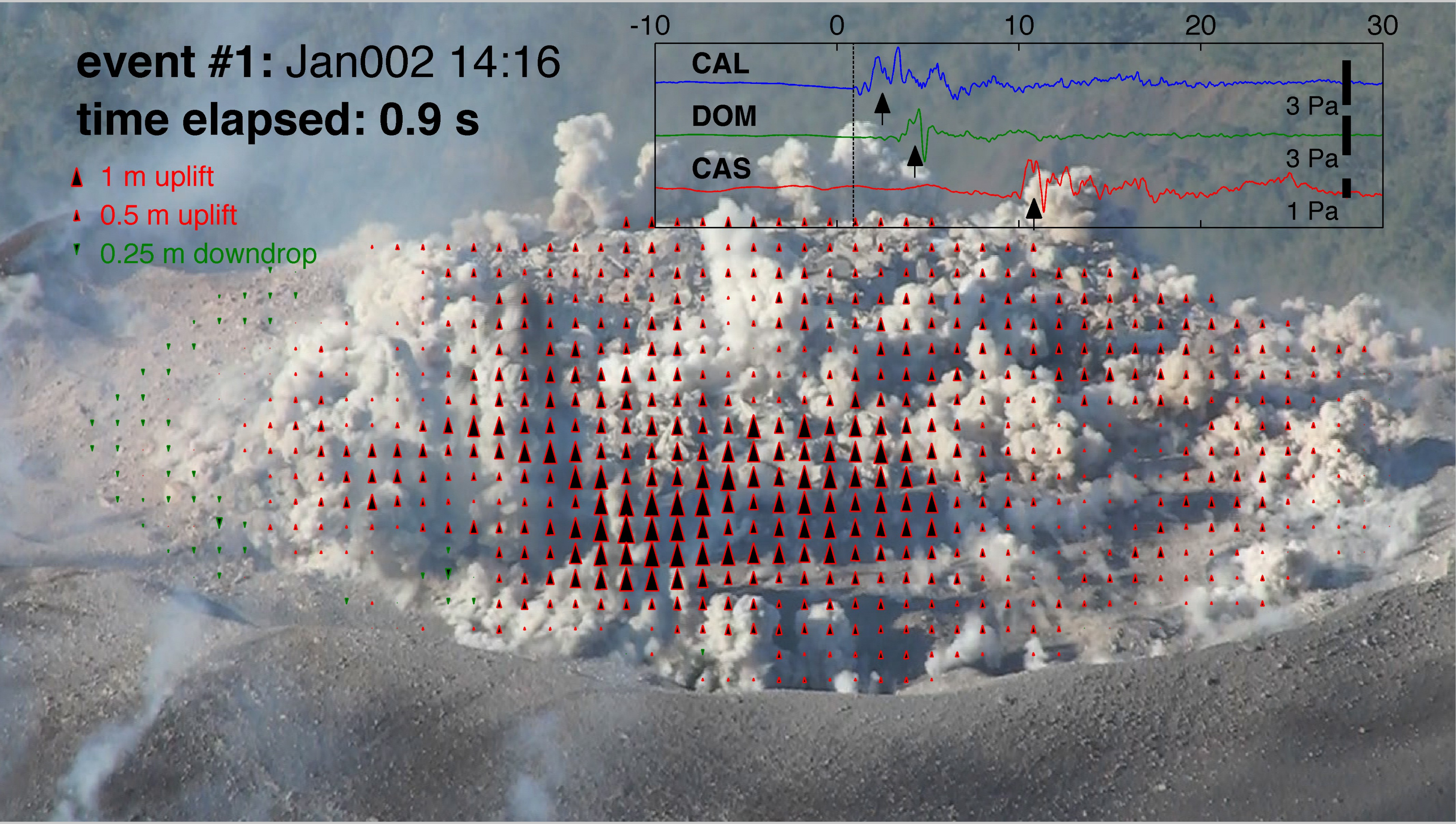

event #1: Jan002 14:16
time elapsed: 0.9 s
1 m uplift
0.5 m uplift
0.25 m downdrop
-10
0
10
20
30
CAL
DOM
CAS
3 Pa
3 Pa
1 Pa

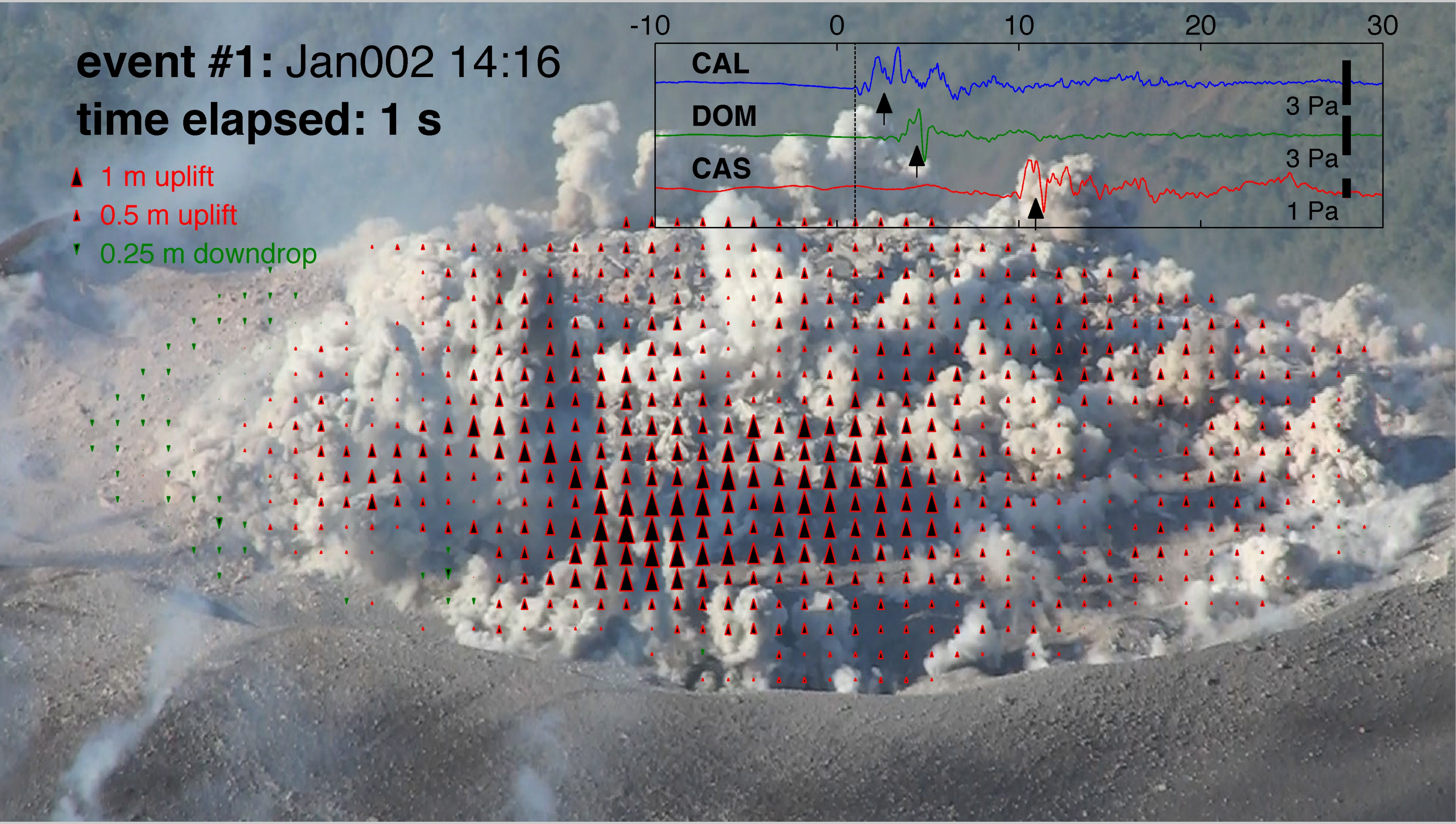

event #1: Jan002 14:16
time elapsed: 1 s
1 m uplift
0.5 m uplift
0.25 m downdrop
-10
0
10
20
30
CAL
DOM
CAS
3 Pa
3 Pa
1 Pa

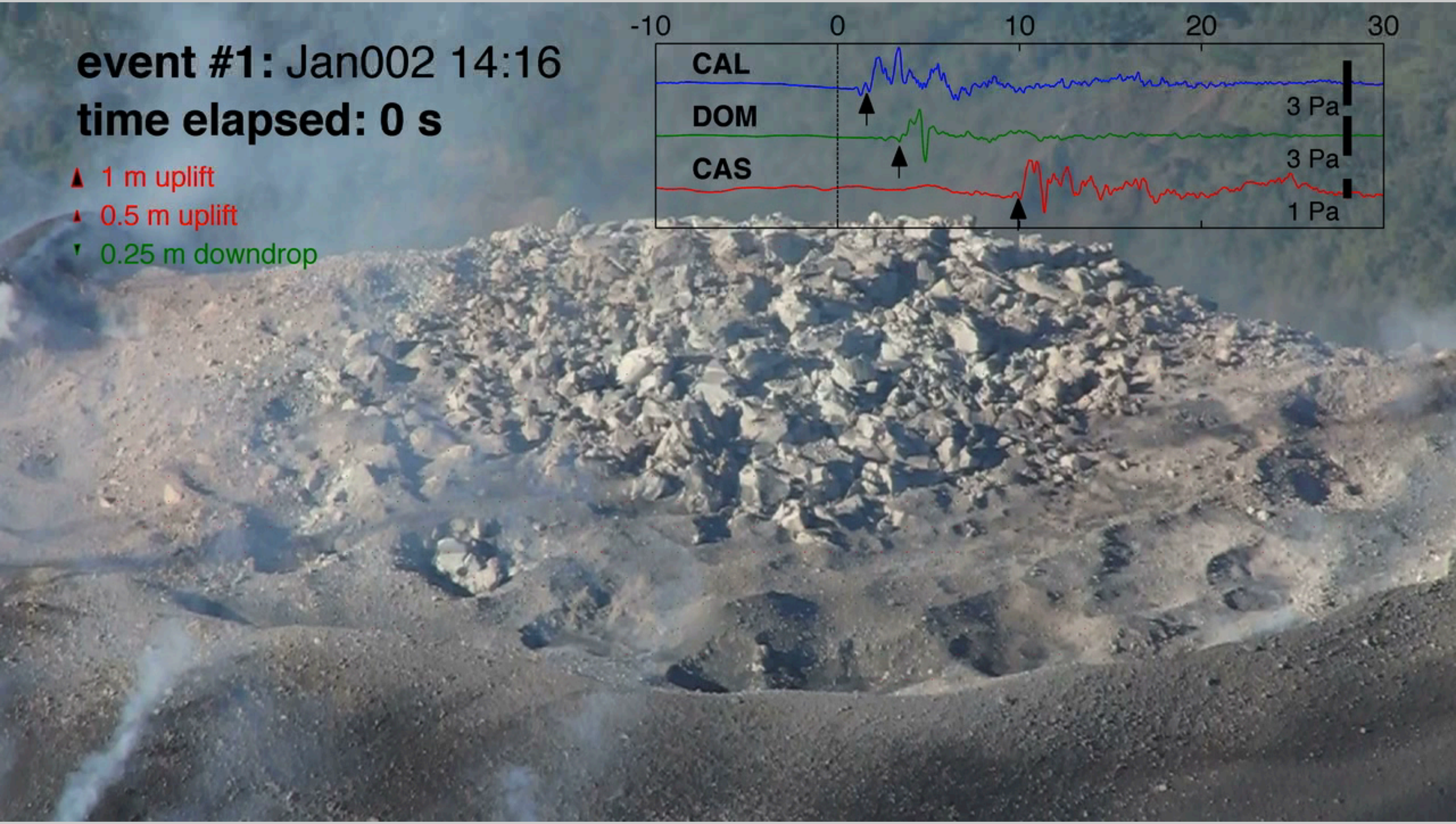

event #1: Jan002 14:16
time elapsed: 0 s
1 m uplift
0.5 m uplift
0.25 m downdrop
-10
0
10
20
30
CAL
DOM
CAS
3 Pa
3 Pa
1 Pa


Villarrica

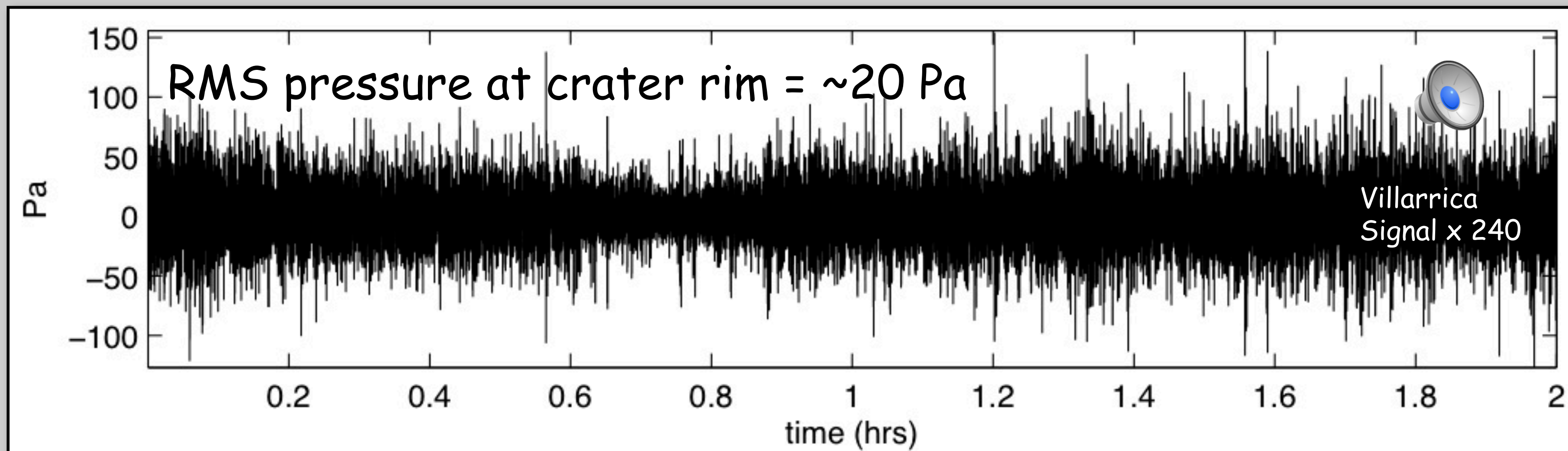

1) Villarrica infrasound is "loud"
- 20 Pa rms (120 dB) at crater rim
- 0.2 Pa rms (80 dB) at 8 km
- detectable out to at least 50 km [Barrientos et al., 2009]

2) Is continuous

Similar observations of infrasonic tremor made during campaigns in 2002, 2004, 2009, 2010 [Johnson et al., 2004; Ripepe et al., 2010; Goto and Johnson, 2011].

3) Has peaked spectral character
- Monotonic varies between 0.6 and 0.8 Hz
- Tremor is NOT harmonic

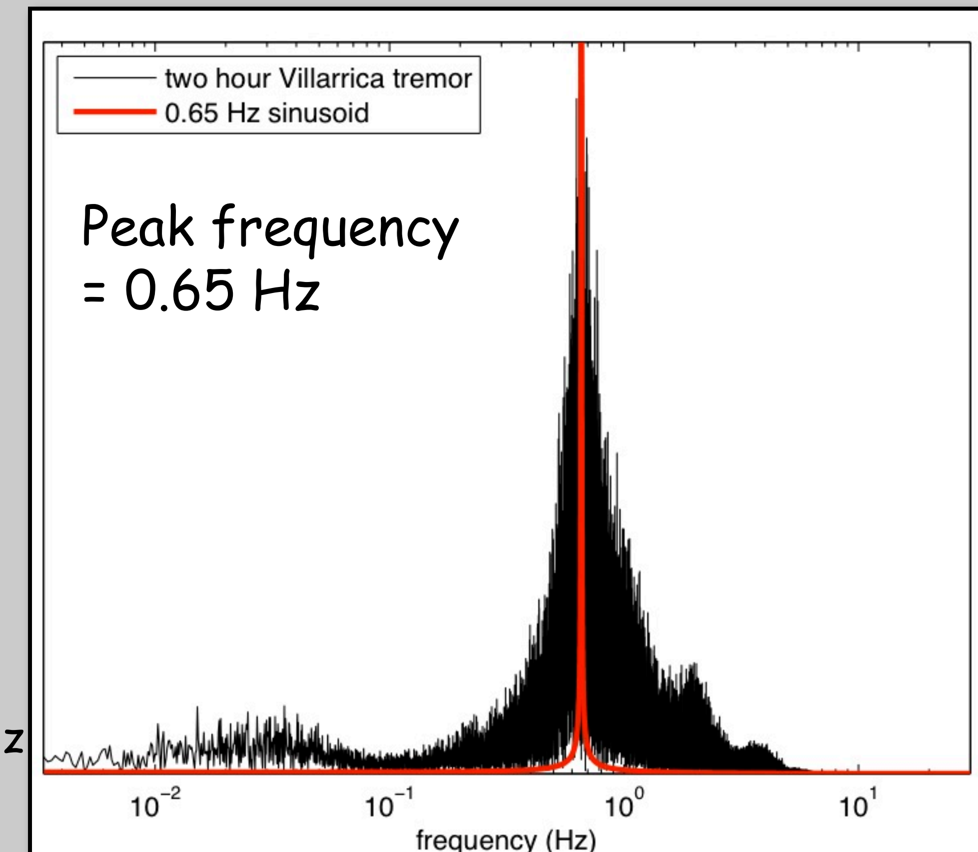

CONAF
7,919 m; 23.23 s;
340.9 m/s
Summit

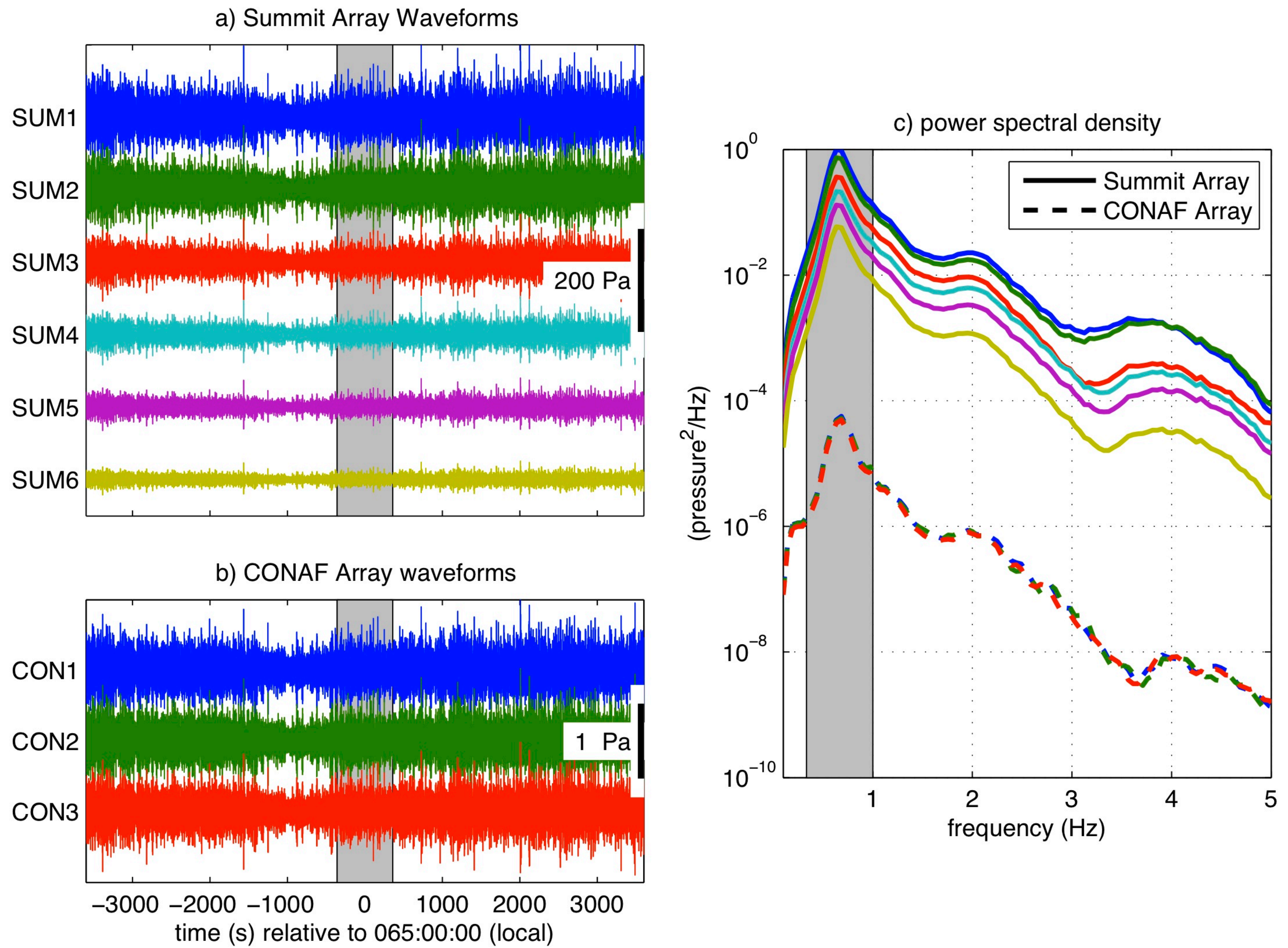

a) Summit Array Waveforms
SUM1
SUM2
SUM3
SUM4
SUM5
SUM6
200 Pa
b) CONAF Array waveforms
CON1
CON2
CON3
1 Pa
−3000 −2000 −1000 0 1000 2000 3000
time (s) relative to 065:00:00 (local)
c) power spectral density
Summit Array
CONAF Array
(pressure^2/Hz)
10^0
10^{-2}
10^{-4}
10^{-6}
10^{-8}
10^{-10}
1 2 3 4 5
frequency (Hz)

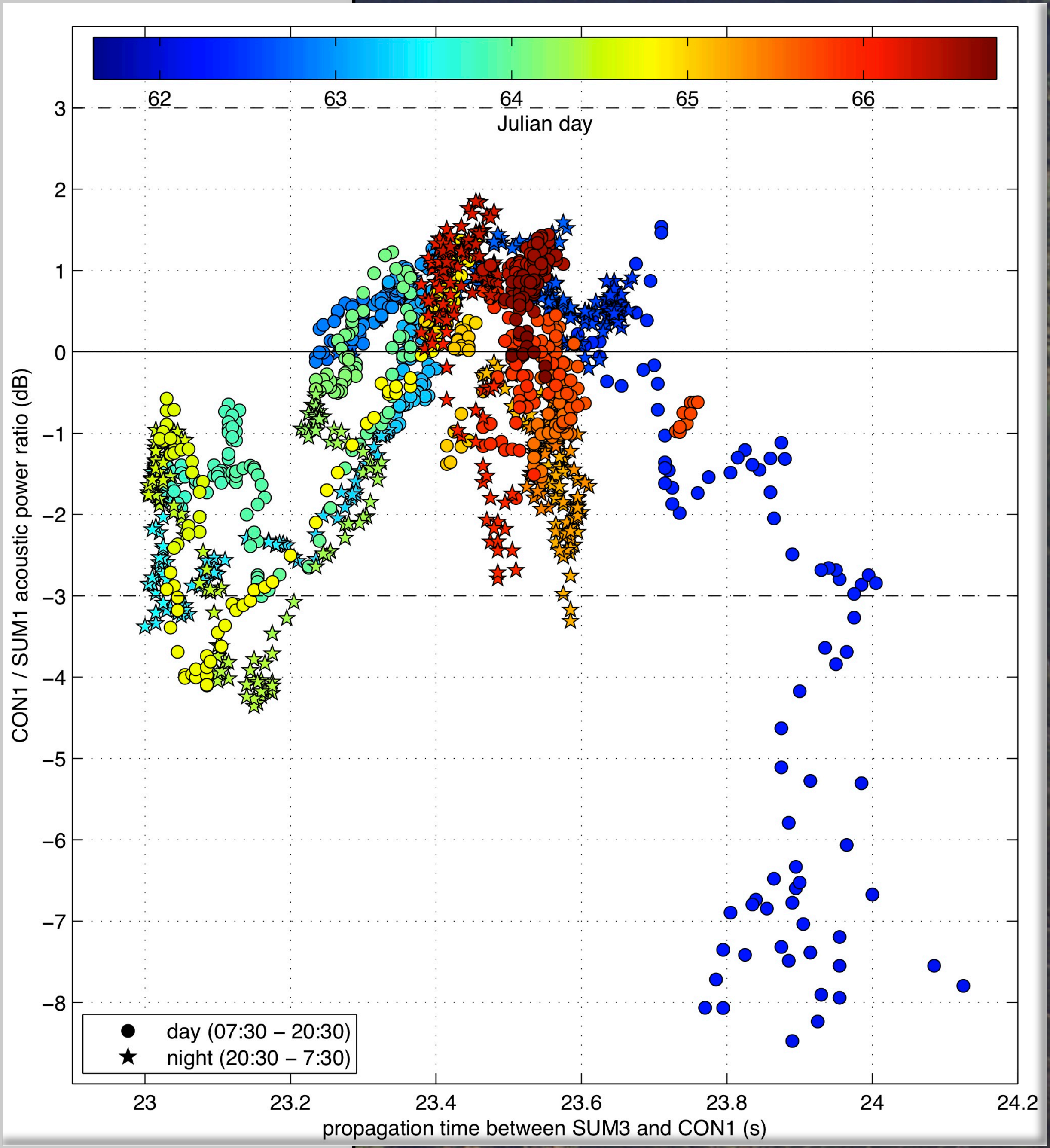
62
63
64
65
66
Julian day
CON1 / SUM1 acoustic power ratio (dB)
propagation time between SUM3 and CON1 (s)
day (07:30 – 20:30)
night (20:30 – 7:30)

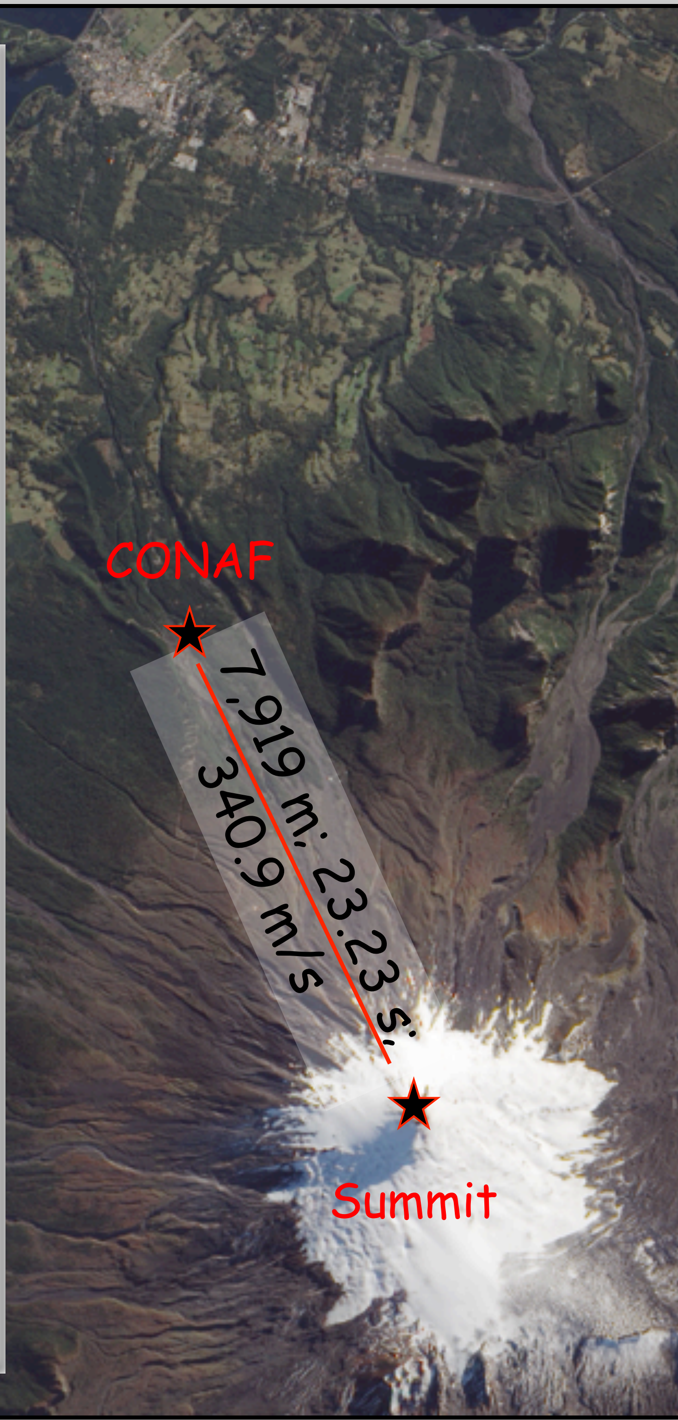
CONAF
7,919 m; 23.23 s;
340.9 m/s
Summit

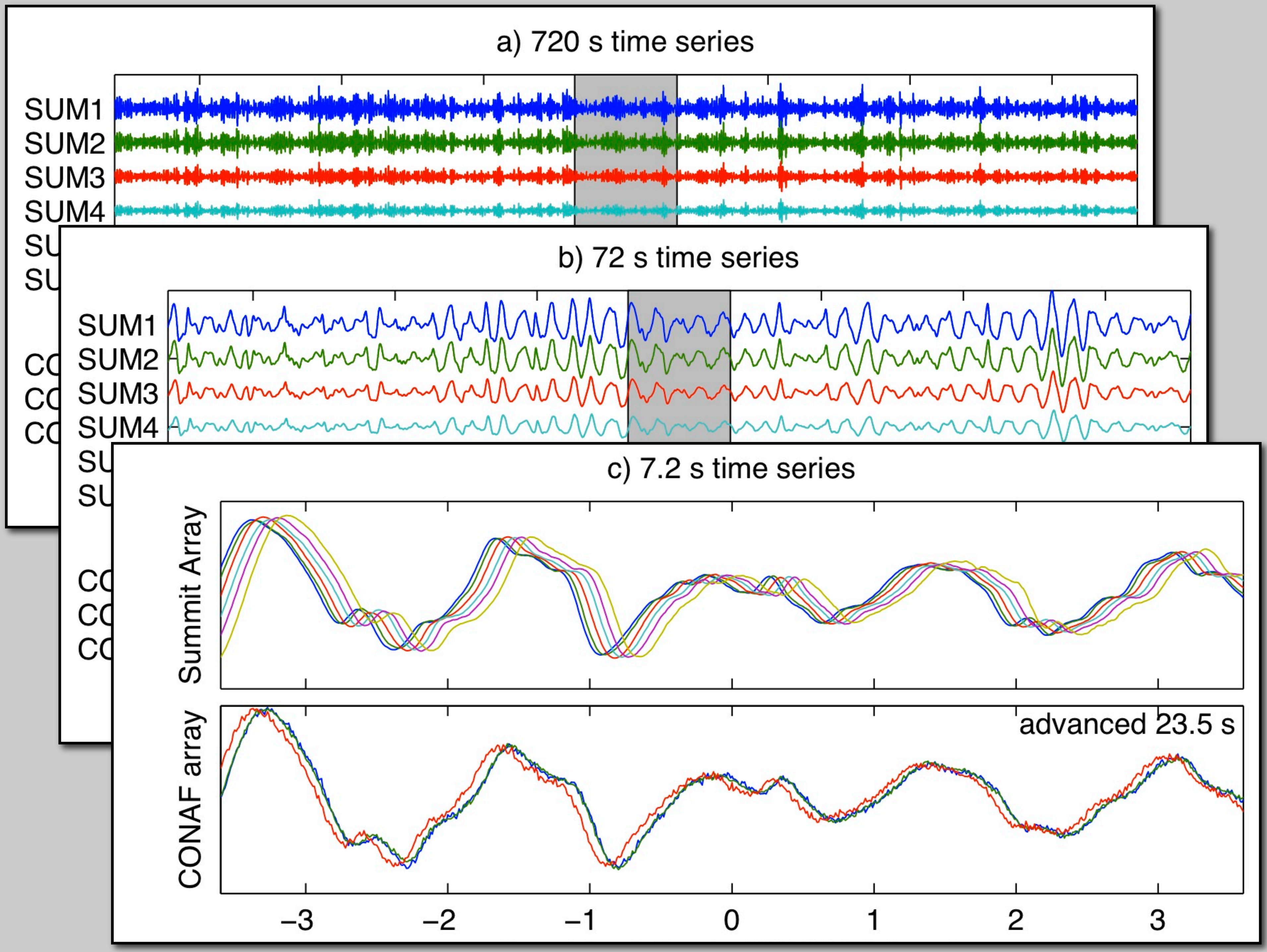
a) 720 s time series
SUM1
SUM2
SUM3
SUM4
b) 72 s time series
SUM1
SUM2
SUM3
SUM4
c) 7.2 s time series
Summit Array
CONAF array
advanced 23.5 s
–3
–2
–1
0
1
2
3

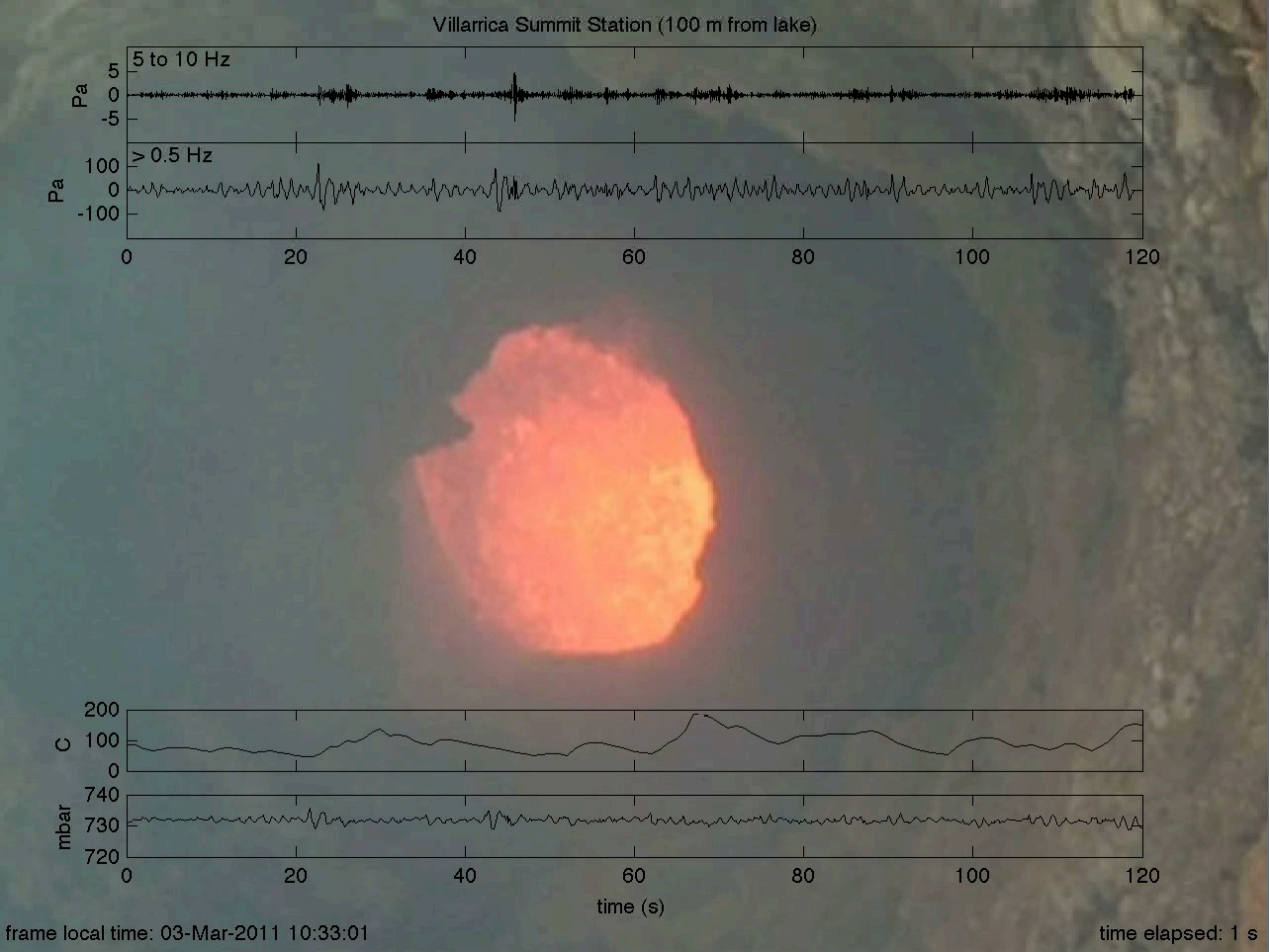
Villarrica Summit Station (100 m from lake)
5 to 10 Hz
Pa
5
0
-5
> 0.5 Hz
Pa
100
0
-100
0
20
40
60
80
100
120
200
C
100
0
740
mbar
730
720
time (s)
frame local time: 03-Mar-2011 10:33:01
time elapsed: 1 s

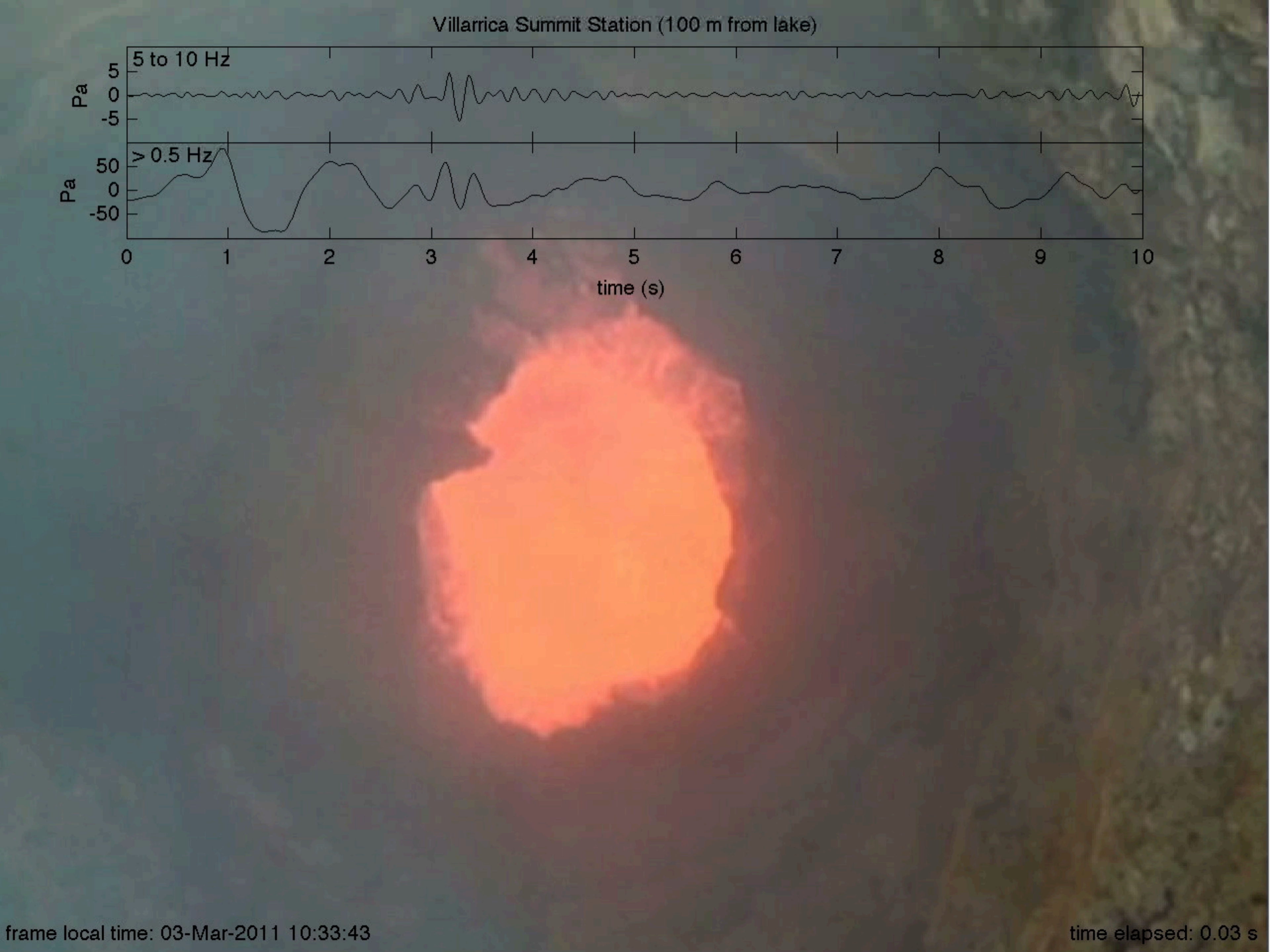
Villarrica Summit Station (100 m from lake)
5 to 10 Hz
Pa
5
0
-5
> 0.5 Hz
50
0
-50
0
1
2
3
4
5
6
7
8
9
10
time (s)
frame local time: 03-Mar-2011 10:33:43
time elapsed: 0.03 s

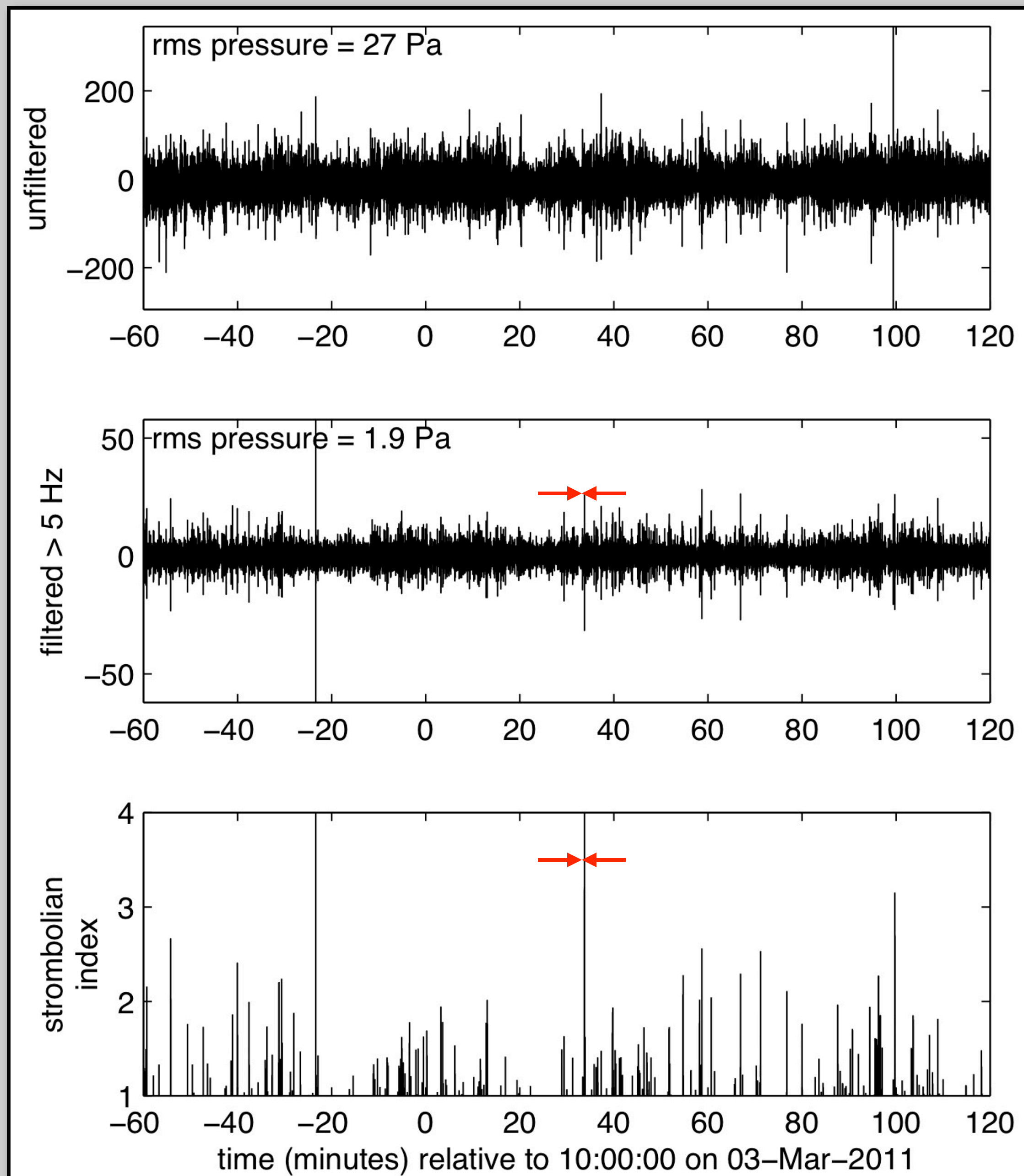
rms pressure = 27 Pa
unfiltered
200
0
−200
−60 −40 −20 0 20 40 60 80 100 120
rms pressure = 1.9 Pa
filtered > 5 Hz
50
0
−50
−60 −40 −20 0 20 40 60 80 100 120
strombolian index
4
3
2
1
−60 −40 −20 0 20 40 60 80 100 120
time (minutes) relative to 10:00:00 on 03−Mar−2011

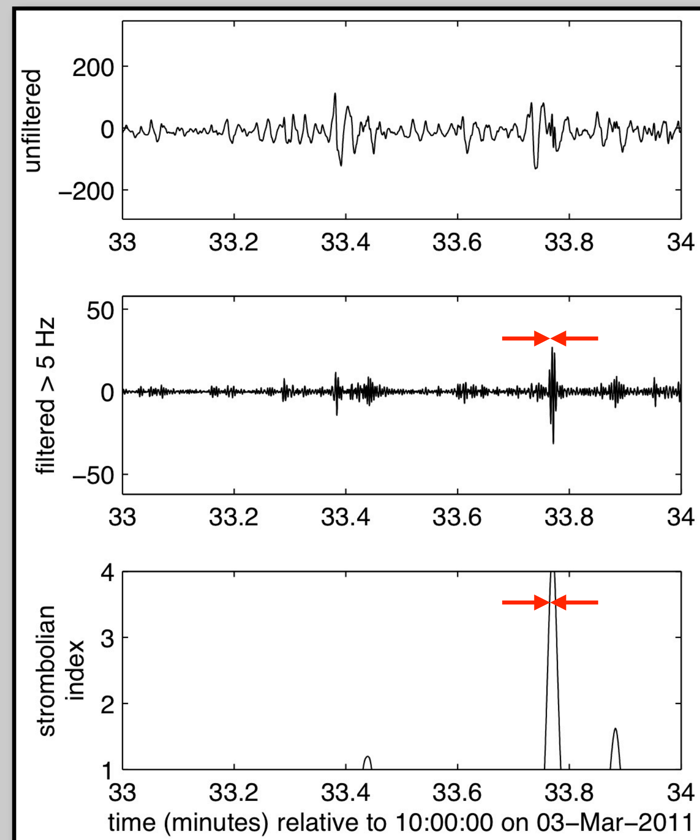
unfiltered
200
0
−200
33 33.2 33.4 33.6 33.8 34
filtered > 5 Hz
50
0
−50
33 33.2 33.4 33.6 33.8 34
strombolian index
4
3
2
1
33 33.2 33.4 33.6 33.8 34
time (minutes) relative to 10:00:00 on 03−Mar−2011

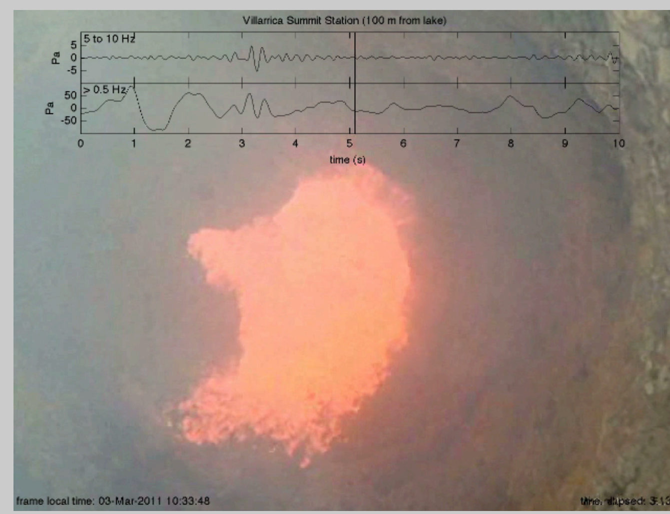
Villarrica Summit Station (100 m from lake)
5 to 10 Hz
> 0.5 Hz
Pa
time (s)
frame local time: 03-Mar-2011 10:33:48

Villarrica as a Helmholtz Resonator
(short pipe frequency approximation)

$$f = \frac{c}{2\pi}\sqrt{\frac{\pi r}{1.7V}}$$

freq (f) = 0.65 Hz

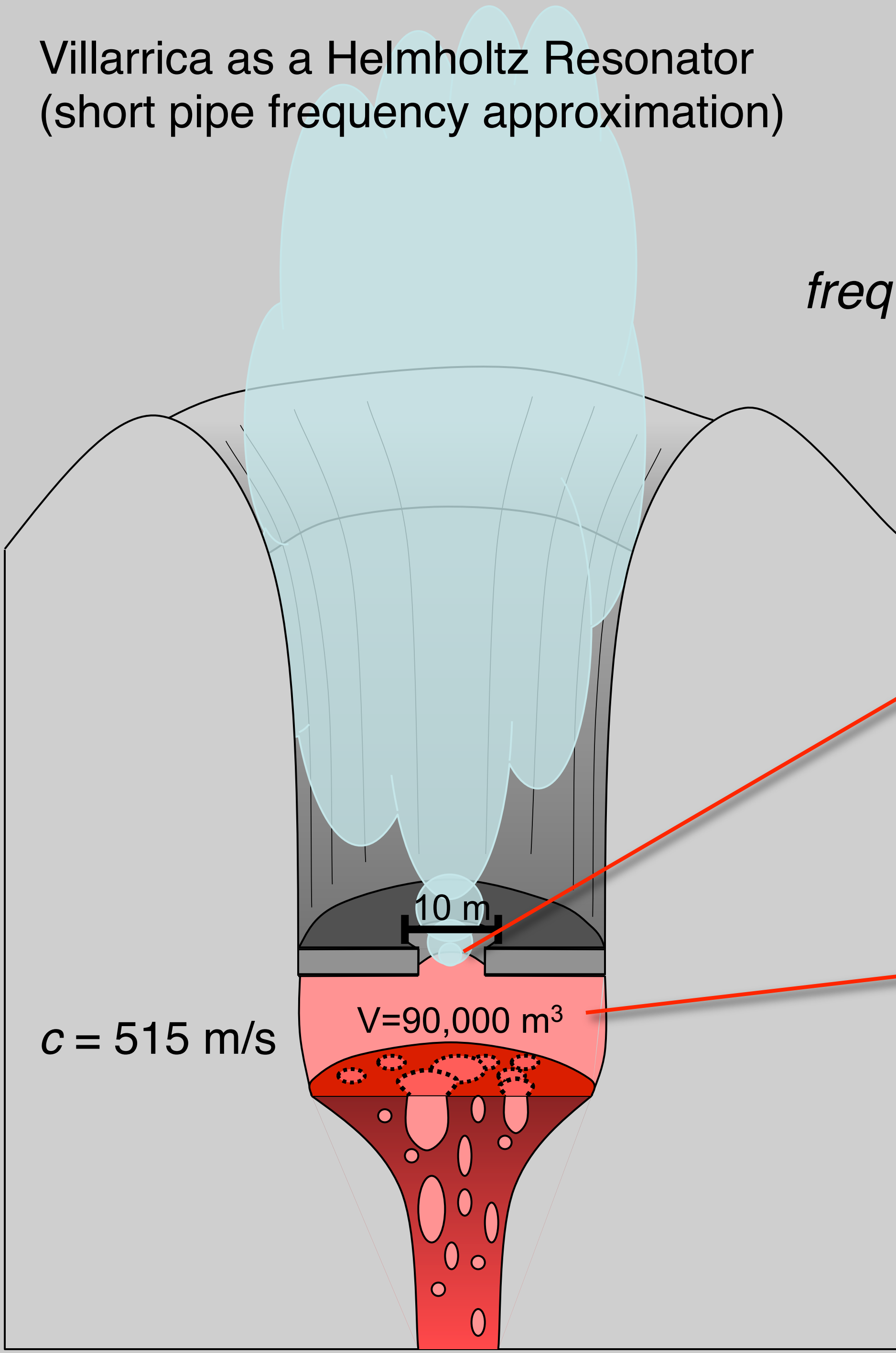

Goto, A., and J. B. Johnson (2011), Monotonic infrasound and Helmholtz resonance at Volcan Villarrica (Chile), *Geophys. Res. Lett.*, *38*(L06301).

Villarrica as a Helmholtz Resonator
(short pipe frequency approximation)

$$f = \frac{c}{2\pi}\sqrt{\frac{\pi r}{1.7V}}$$

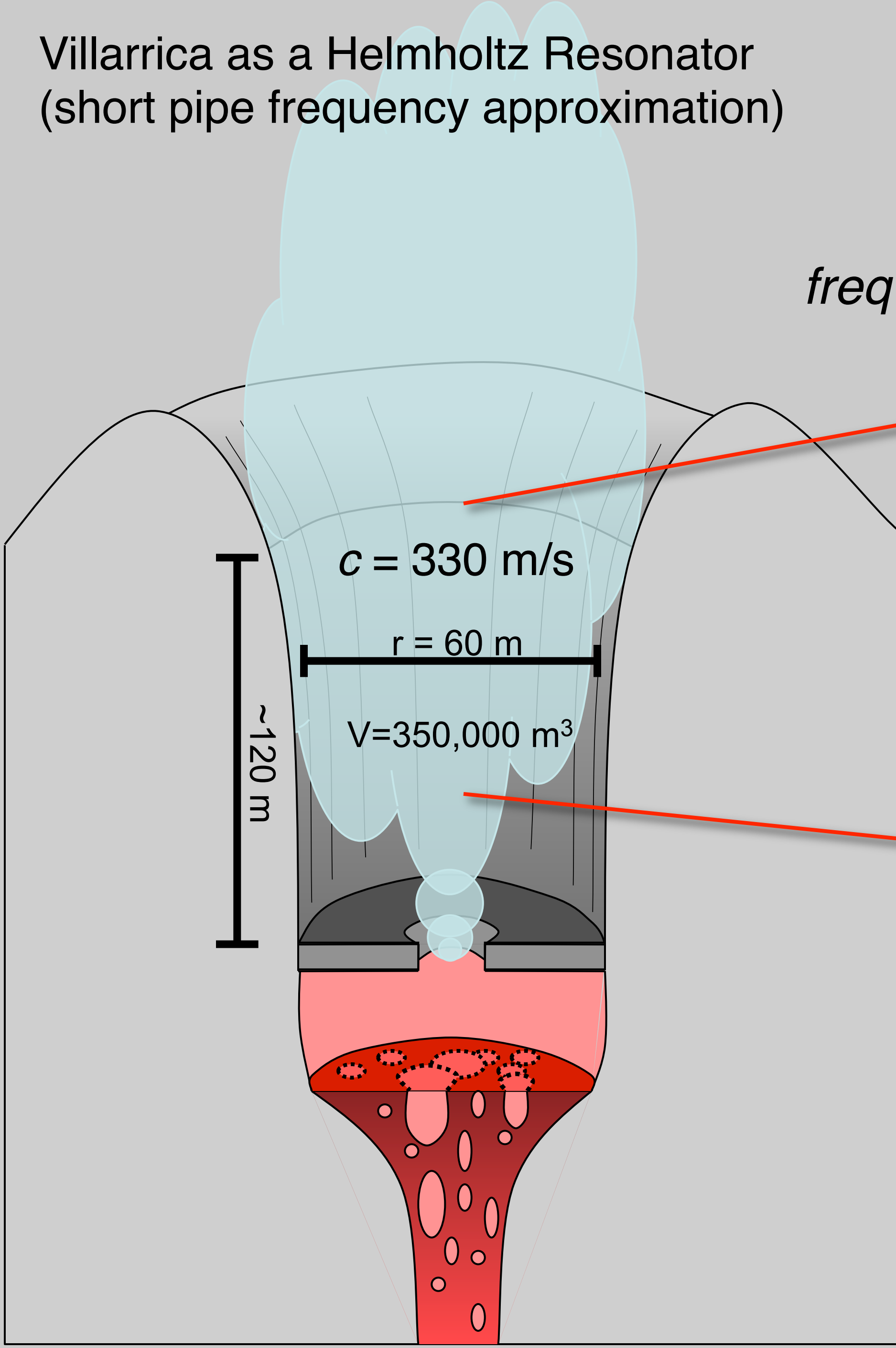

freq (f) = 0.65 Hz

=

=

Goto, A., and J. B. Johnson (2011), Monotonic infrasound and Helmholtz resonance at Volcan Villarrica (Chile), *Geophys. Res. Lett.*, *38*(L06301).


USGS

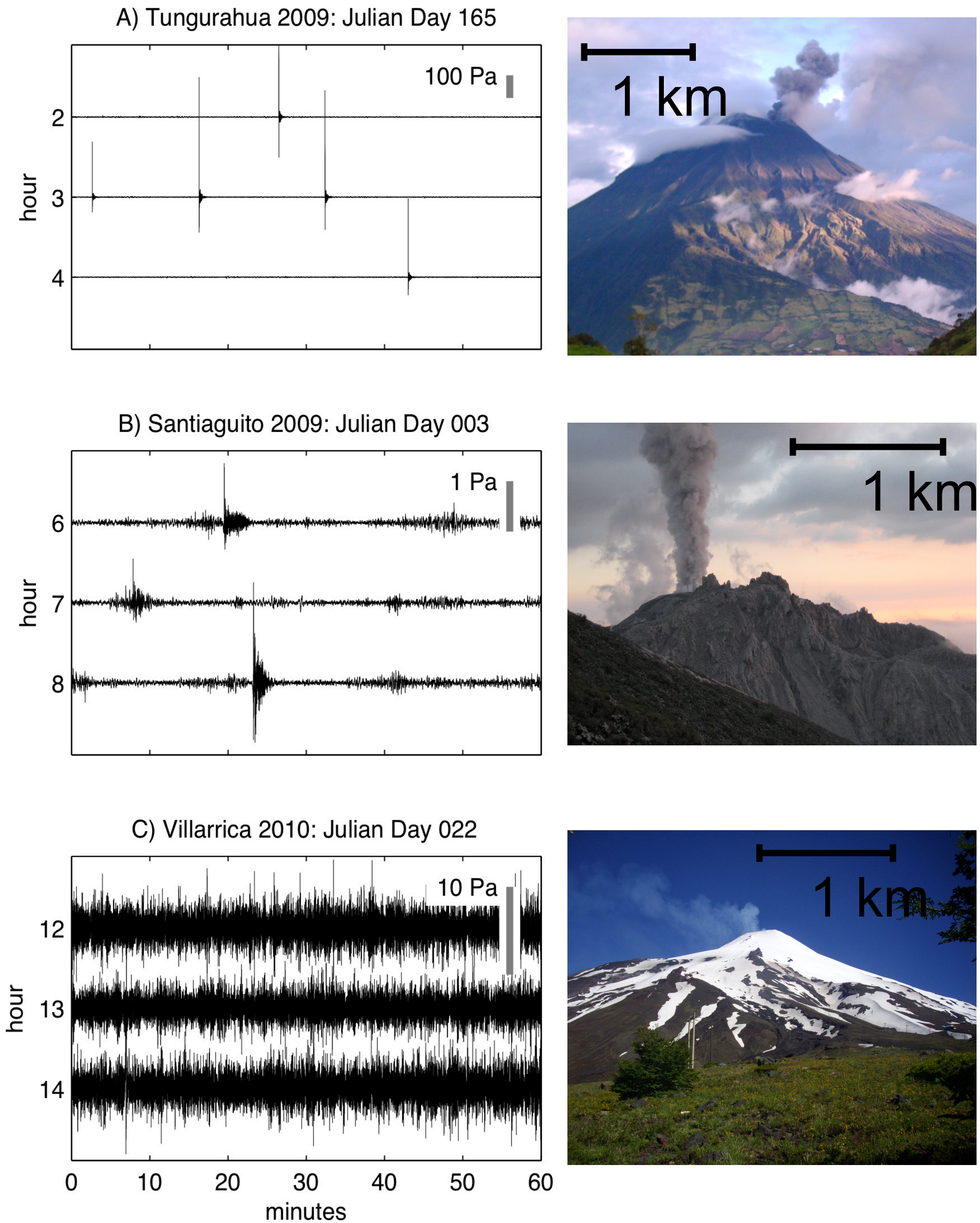

A) Tungurahua 2009: Julian Day 165
100 Pa
hour
2
3
4
1 km
B) Santiaguito 2009: Julian Day 003
1 Pa
hour
6
7
8
1 km
C) Villarrica 2010: Julian Day 022
10 Pa
hour
12
13
14
0
10
20
30
40
50
60
minutes
1 km

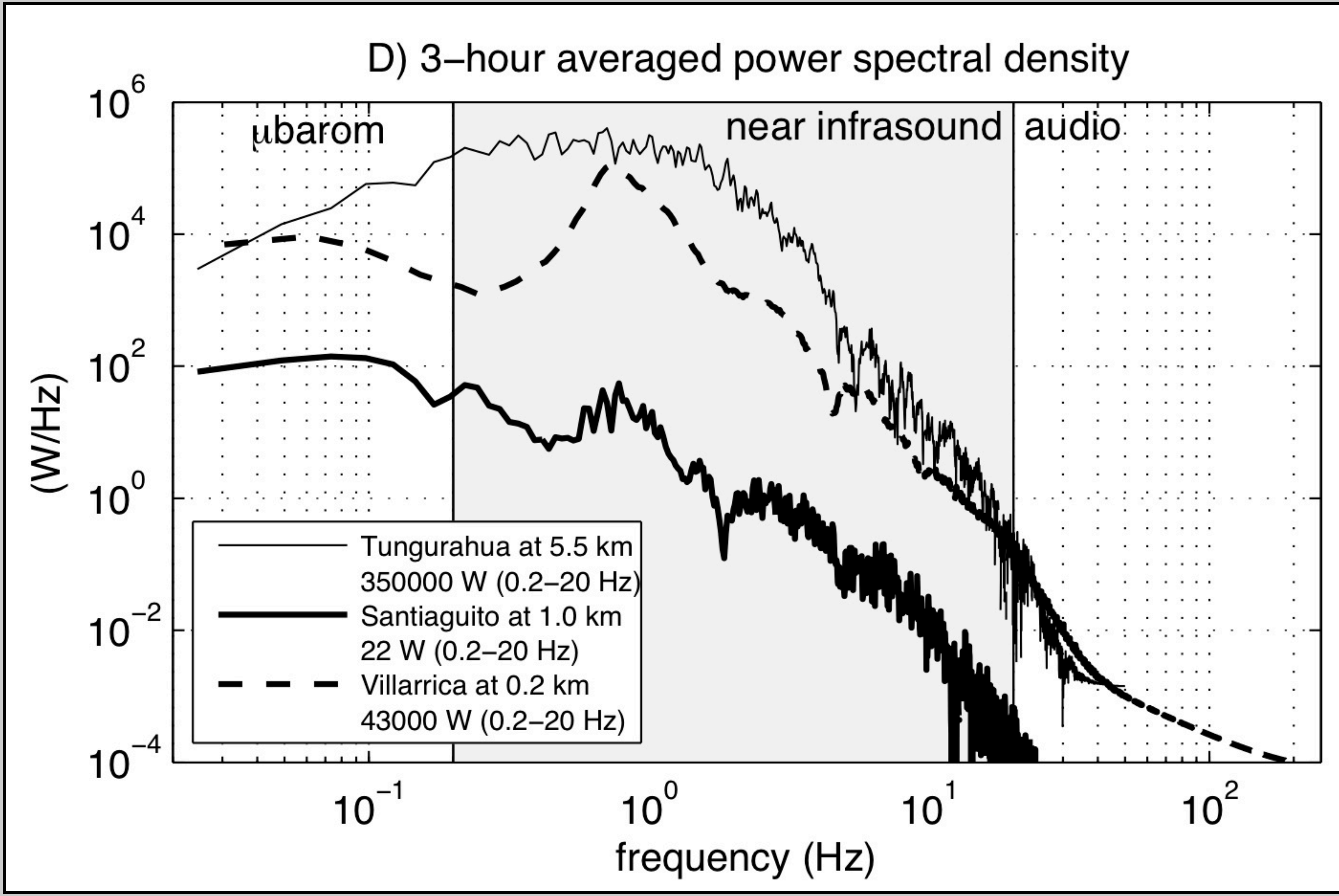

$$P(t) = \Omega \frac{\overline{p^2\left(t + r/c\right)}}{\rho c}$$

Seismo-acoustic datasets: Nick and John

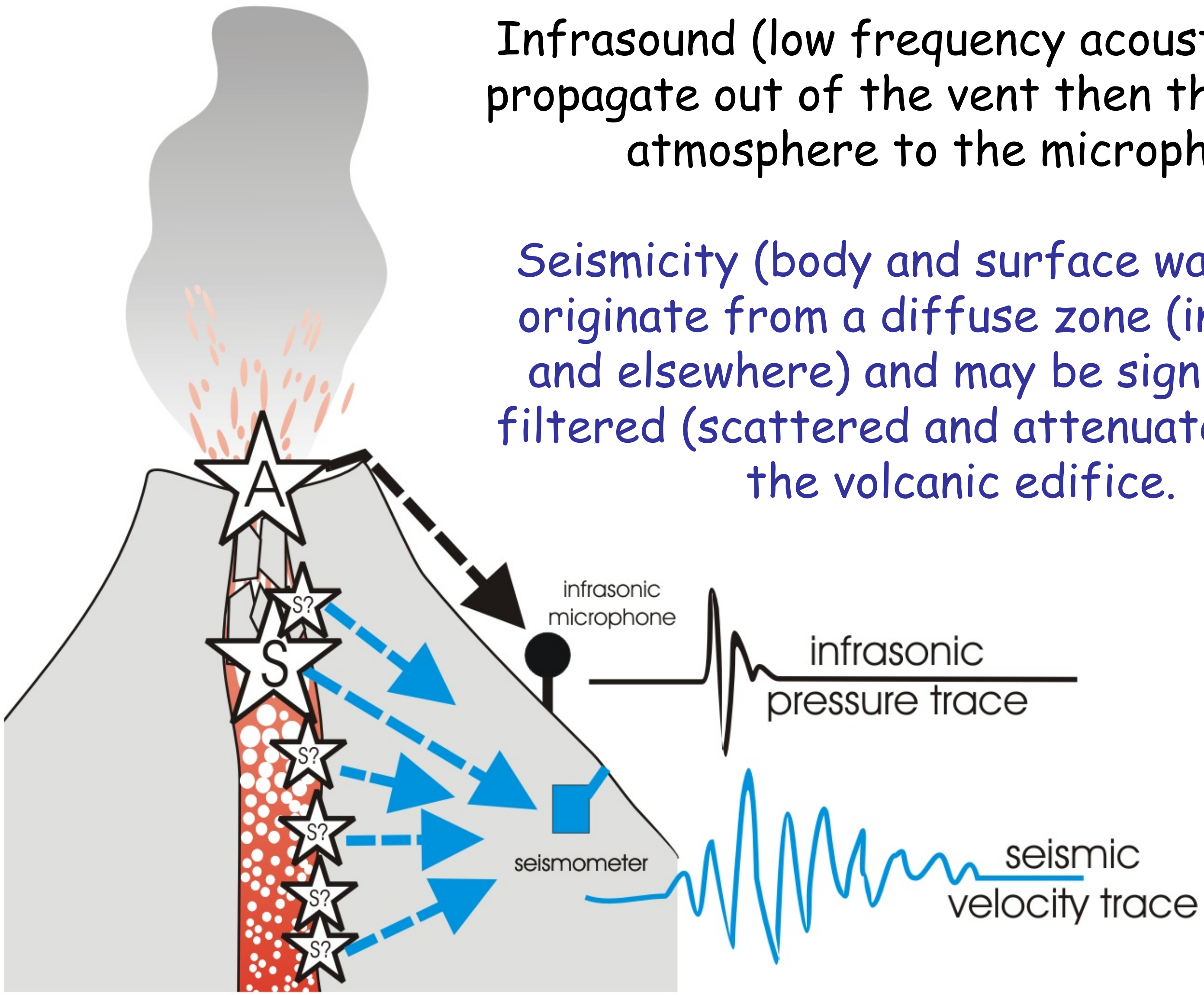

Infrasound (low frequency acoustic waves) propagate out of the vent then through the atmosphere to the microphone.

Seismicity (body and surface waves) may originate from a diffuse zone (in conduit and elsewhere) and may be significantly filtered (scattered and attenuated) within the volcanic edifice.

Acknowledgments:

- Mount Erebus - Rick Aster, Phil Kyle, Bill McIntosh, many others
- Tungurahua - Mario Ruiz, many others from IG-EPN, and GEOP572 class
- Santiaguito - John Lyons, Greg Waite, Rudiger Wolf (MTU), Richard Sanderson (NMT student), and many others.
- Villarrica - Akio Goto (Tohoku University), Richard Sanderson, Jake Anderson (students), Nick Varley (University of Colima)
- Kilauea video - Matt Patrick (Hawaii Volcanoes Observatory)

Funding

- NSF EAR
- National Geographic Expeditions Council

Some local observations of volcano infrasound in the literature

Bouche, E. et al., 2010. The role of large bubbles detected from acoustic measurments on the dynamics of **Erta 'Ale** lava lake (Ethiopia). Earth and Planetary Science Letters, 295: 37-48.

Braun, T. and Ripepe, M., 1993. Interaction of seismic and air waves as recorded at **Stromboli** Volcano. Geophys. Res. Lett., 20: 65-68.

Cannata, A., Montalto, P., Privitera, E., Russo, G. and Gresta, S., 2009. Tracking eruptive phenomena by infrasound: May 13, 2008 eruption at **Mt. Etna**. Geophys. Res. Lett., 36(L05304).

Fee, D. et al., 2010. Infrasonic harmonic tremor and degassing bursts from Halemaumau Crater, **Kilauea** Volcano, Hawaii. J. Geophys. Res.

Firstov, P.P. and Storcheus, A.V., 1987. Acoustic signals that accompanied the March-June 1983 eruption at **Klyuchevskoy** Volcano. Volcanol. Seismol., 5: 66-80.

Garces, M.A. et al., 1999. Infrasonic precursors to a Vulcanian eruption at **Sakurajima** Volcano, Japan. Geophys. Res. Lett., 26(16): 2537-2540.

Hagerty, M.T., Schwartz, S.Y., Garces, M.A. and Protti, M., 2000. Analysis of seismic and acoustic observations at **Arenal** Volcano, Costa Rica, 1995-1997. Journal of Volcanology and Geothermal Research, 101(1-2): 27-65.

Johnson, J.B., 2007. On the relation between infrasound, seismicity, and small pyroclastic explosions at **Karymsky** Volcano. Journal of Geophysical Research-Solid Earth, 112(B8).

Johnson, J.B. and Lees, J.M., 2010. Long period infrasound at **Santiaguito** produced by rapid dome inflation. Geophys. Res. Lett.

Jones, K., Johnson, J.B., Aster, R., Kyle, P. and McIntosh, W., 2008. Infrasonic tracking of large bubble bursts and ash venting at **Erebus** volcano, Antarctica. J. Volc. Geotherm. Res., 177: 661-672.

Kobayashi, T., Ida, Y. and Ohminato, T., 2005. Small inflation sources producing seismic and infrasonic pulses during the 2000 eruptions of **Miyake-jima**, Japan. Earth and Planetary Science Letters, 240(2): 291-301.

Lees, J.M., Johnson, J.B., Ruiz, M., Troncoso, L. and Welsh, M., 2008. **Reventador** Volcano 2005: Eruptive activity inferred from seismo-acoustic observation. Journal of Volcanology and Geothermal Research, 176(1): 179-190.

Lees, J.M. and Ruiz, M., 2008. Non-linear explosion tremor at **Sangay**, Volcano, Ecuador. Journal of Volcanology and Geothermal Research, 176(1): 170-178.

Lyons, J.J., Waite, G.P., Rose, W.I. and Chigna, G., 2010. Patterns in open vent, strombolian behavior at **Fuego** volcano, Guatemala, 2005-2007. Bulletin of Volcanology, 72(1): 1-15.

Petersen, T., De Angelis, S., Tytgat, G. and McNutt, S.R., 2006. Local infrasound observations of large ash explosions at **Augustine** Volcano, Alaska, during January 11-28, 2006. Geophysical Research Letters, 33(12).

Ripepe, M., De Angelis, S., Lacanna, G. and Voight, B., 2010. Observation of infrasonic and gravity waves at Soufriere Hills Volcano, **Montserrat**. Geophys. Res. Lett., 37(L00E14).

Ripepe, M. et al., 2010. Monochromatic infrasonic tremor driven by persistent degassing and convection at **Villarrica** Volcano, Chile. Geophys. Res. Lett., 37(L15303).

Ruiz, M., Lees, J.M. and Johnson, J.B., 2006. Source constraints of **Tungurahua** volcano explosion events. Bulletin of Volcanology, 68(5): 480-490.

Vergniolle, S. and Caplan-Auerbach, J., 2006. Basaltic thermals and subplinian plumes: Constraints from acoustic measurements at **Shishaldin** volcano, Alaska. Bulletin of Volcanology, 68(7-8): 611-630.

Yamasato, H., 1998. Nature of infrasonic pulse accompanying low frequency earthquake at **Unzen** Volcano, Japan. Bull. Volcanol. Soc. Japan, 43: 1-13.

Yokoo, A. and Iguchi, M., 2010. Using infrasound waves from eruption video to explain ground deformation preceding the eruption of **Suwanosejima** volcano, Japan. J. Volc. Geotherm. Res., 196(3-4): 287-294.

Types of Infrasonic Microphones

Electret condenser elements

Pro – nice signal-to-noise.

Pro – cheap.. One dollar a piece!

Con – frequency response rolls off in zone of interest

Microelectromechanical (MEMS) pressure transducer

Pro – response is linear down to DC.

Pro – relatively cheap - $100 a piece

Con – doesn't filter out barometric pressure fluctuations

Con – Inferior signal-to-noise

Microbarometer (MB2000)

Pro – Flat response

Pro – very low noise

Con – pricey (~$10,000)

Con – difficult to manage for field deployments

$$\Delta P = P_A - P_B$$

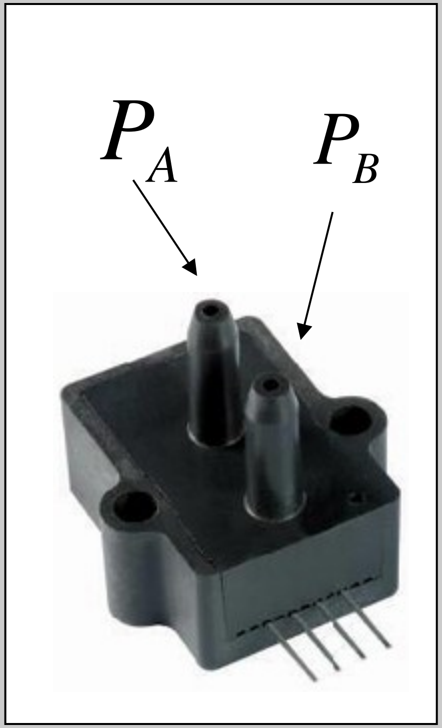

$$\Delta P \rightarrow excess\ pressure\ (measured)$$

$$\Delta P = P_A - P_V$$

$\Delta P \rightarrow excess\ pressure\ (measured)$

$P_A \rightarrow ambient\ atmospheric + sound\ pressure$

$P_V \rightarrow pressure\ in\ volume \approx atmospheric\ pressure$

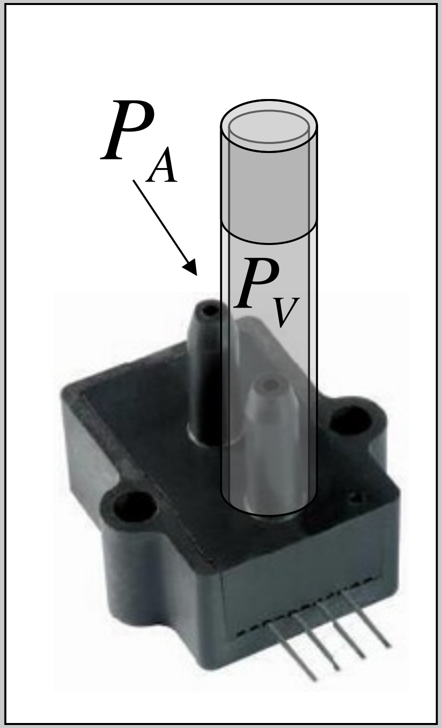

$$P_V(t) = P_0 + (P_i - P_0)\, e^{-c\left(\frac{r^4}{Vl}\right)t}$$

$$\text{where} \quad f_c = \frac{c\, r^4}{V\, l}$$

$P_V \rightarrow$ *pressure in volume ≈ atmospheric pressure*

$P_i \rightarrow$ *initial pressure at time zero*

$P_0 \rightarrow$ *ambient pressure*

$c \rightarrow$ *gas constant*

$r \rightarrow$ *radius of capillary tube* $(\sim 50 \times 10^{-6}\, m)$

$l \rightarrow$ *capillary tube length* $(\sim 1 \times 10^{-2}\, m)$

$V \rightarrow$ *reservoir volume* $(\sim 1 \times 10^{-6}\, m^3)$

$t \rightarrow$ *time*

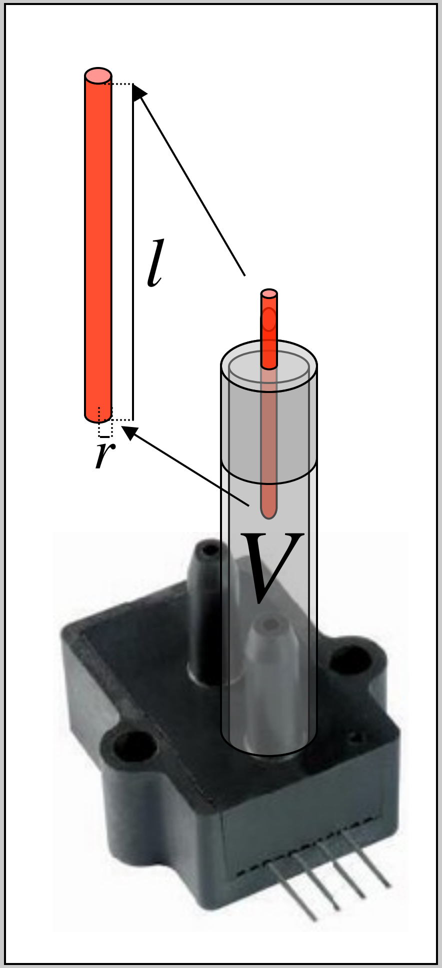

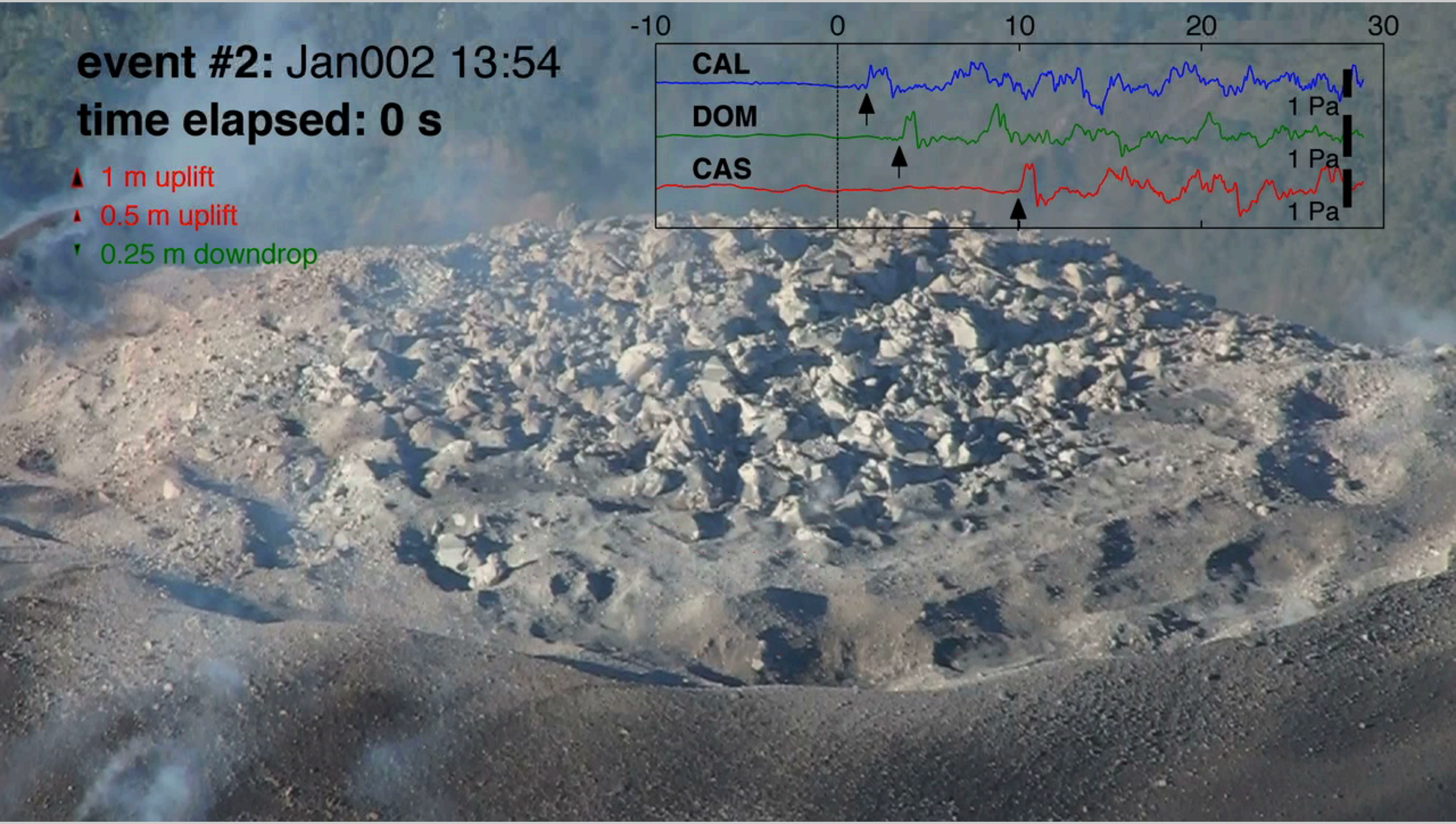

event #2: Jan002 13:54
time elapsed: 0 s
1 m uplift
0.5 m uplift
0.25 m downdrop
-10
0
10
20
30
CAL
DOM
CAS
1 Pa
1 Pa
1 Pa

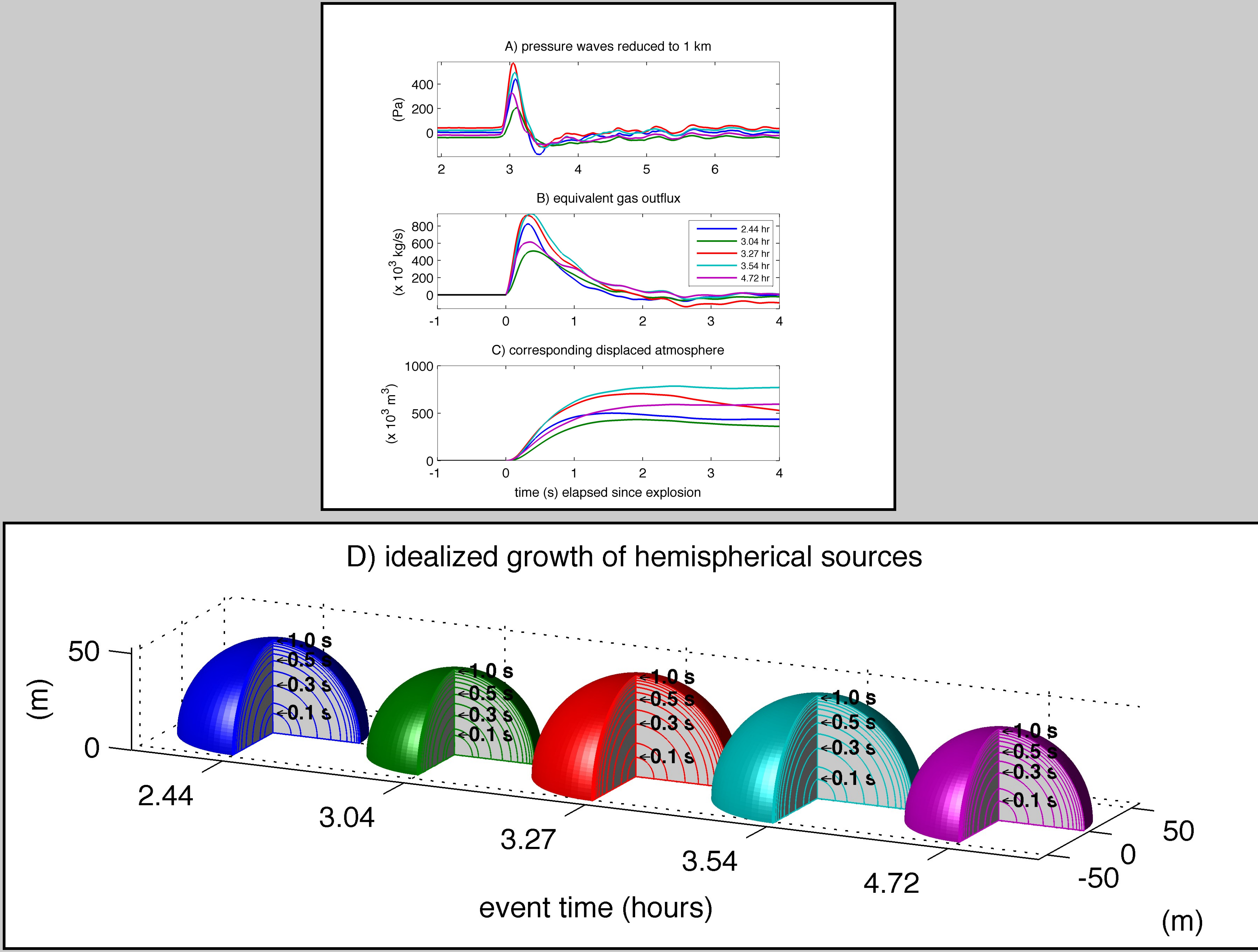

A) pressure waves reduced to 1 km
(Pa)
400
200
0
2
3
4
5
6
B) equivalent gas outflux
(x 10^3 kg/s)
800
600
400
200
0
-1
0
1
2
3
4
2.44 hr
3.04 hr
3.27 hr
3.54 hr
4.72 hr
C) corresponding displaced atmosphere
(x 10^3 m^3)
1000
500
0
time (s) elapsed since explosion
D) idealized growth of hemispherical sources
(m)
50
0
1.0 s
0.5 s
0.3 s
0.1 s
2.44
3.04
3.27
3.54
4.72
event time (hours)
50
0
-50
(m)

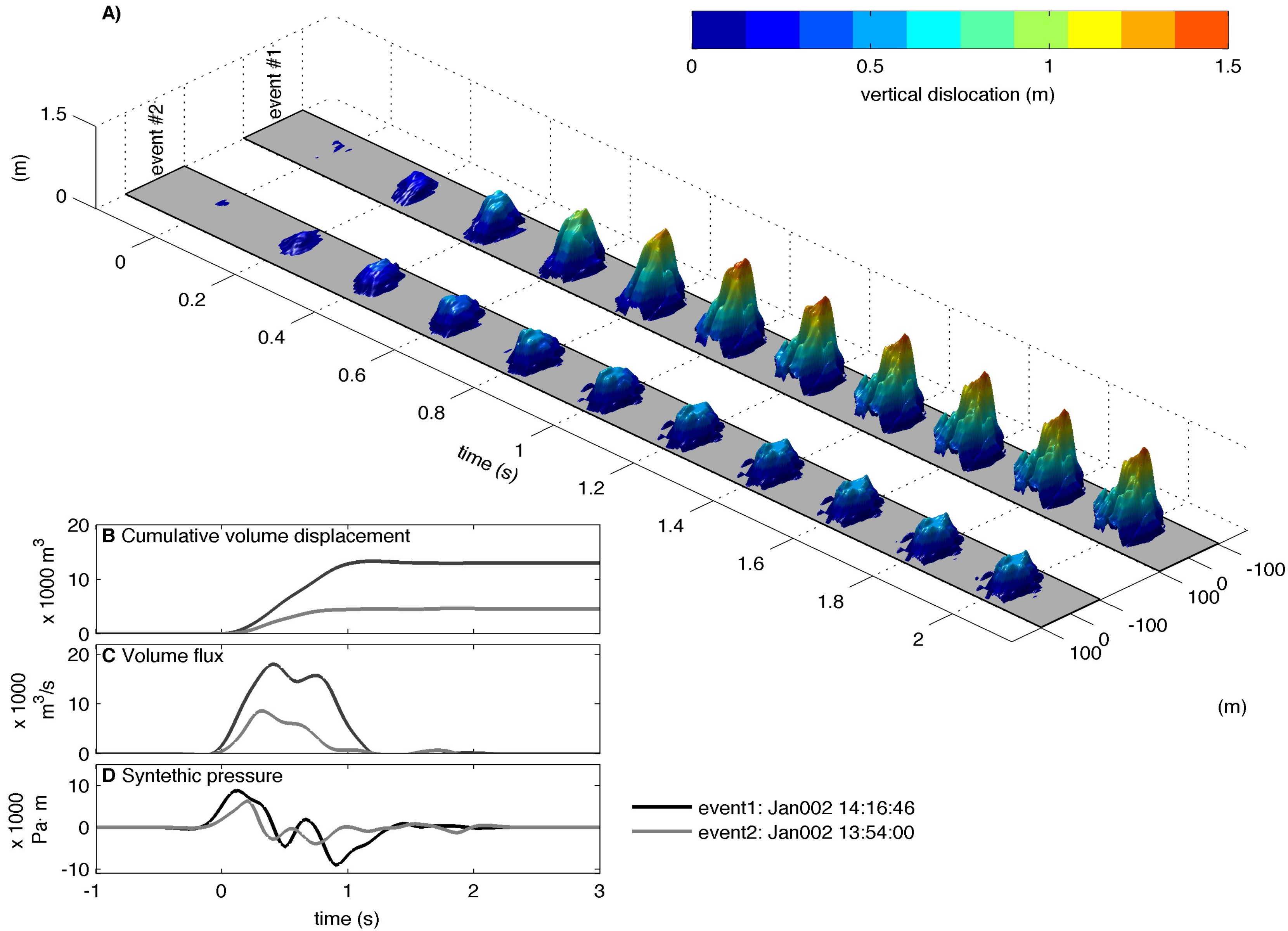

A)
vertical dislocation (m)
0
0.5
1
1.5
event #1
event #2
1.5
(m)
0
time (s)
0
0.2
0.4
0.6
0.8
1
1.2
1.4
1.6
1.8
2
-100
0
100
(m)
B Cumulative volume displacement
x 1000 m^3
20
10
0
C Volume flux
x 1000 m^3/s
D Synthethic pressure
x 1000 Pa· m
10
-10
-1
3
time (s)
event1: Jan002 14:16:46
event2: Jan002 13:54:00

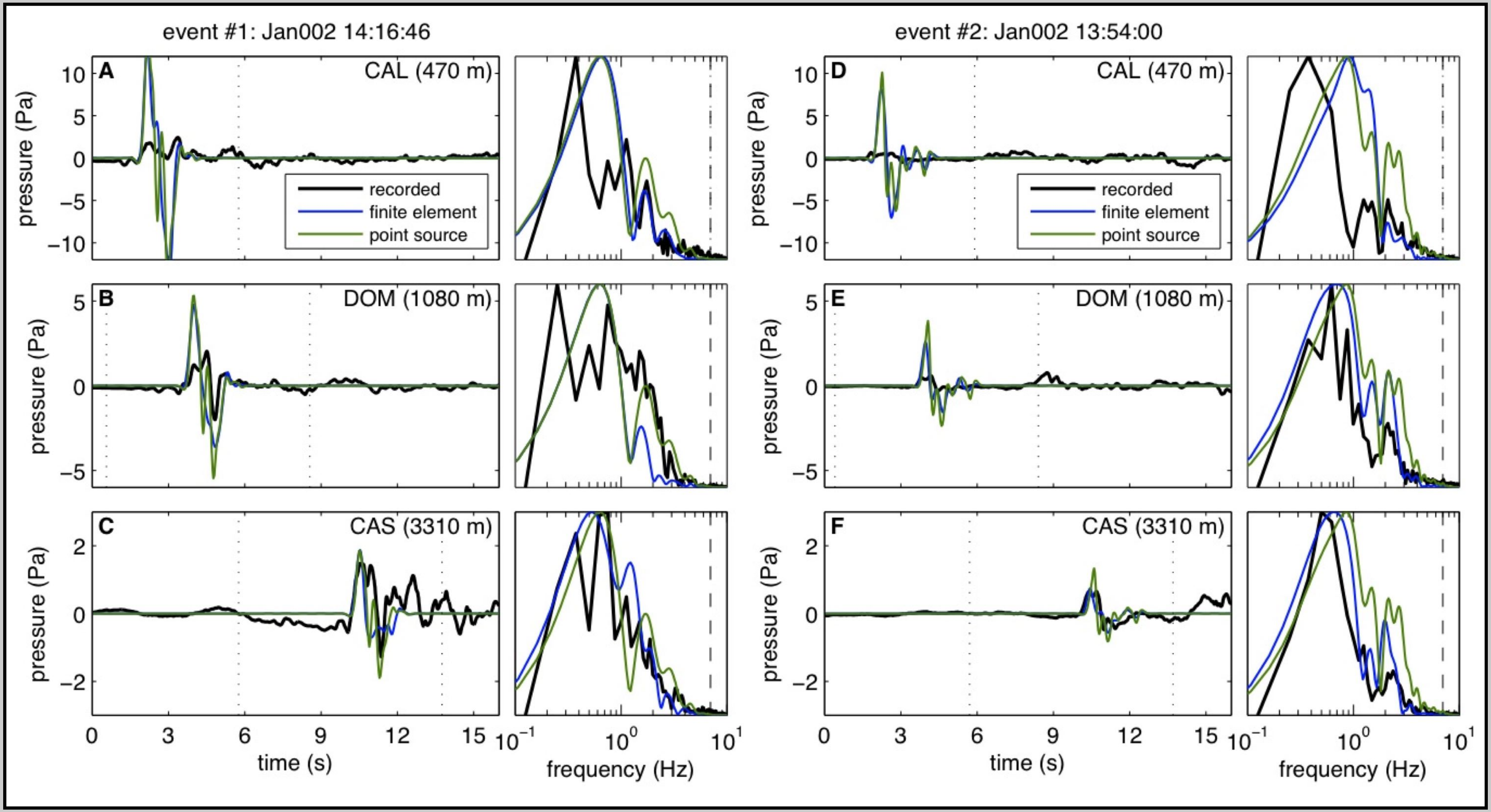

event #1: Jan002 14:16:46
event #2: Jan002 13:54:00
A
CAL (470 m)
B
DOM (1080 m)
C
CAS (3310 m)
D
CAL (470 m)
E
DOM (1080 m)
F
CAS (3310 m)
recorded
finite element
point source
pressure (Pa)
time (s)
frequency (Hz)

Modeled waveforms at DOM and CAL have excessive amplitudes

	Distance	Event #1 p_{syn}/p_{obs}	Event #2 p_{syn}/p_{obs}
CAS	3.3 km	0.88	0.93
DOM	1.0 km	2.1	3.33
CAL	0.5 km	6.3	6.8

Possible explanations:

- Topographic shadowing
- Atmospheric focusing
- Near-source anelastic propagation not considered

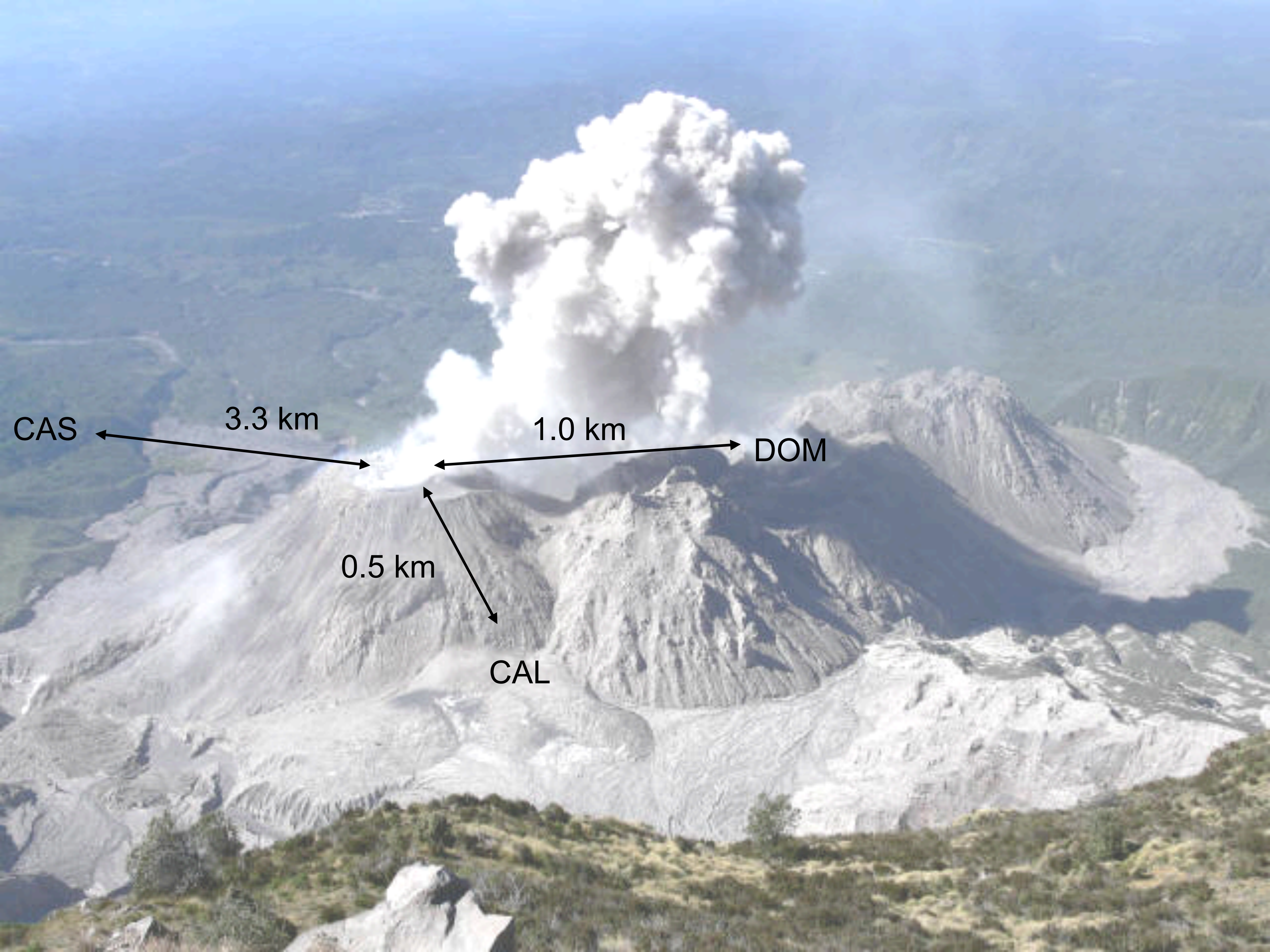
CAS
3.3 km
1.0 km
DOM
0.5 km
CAL

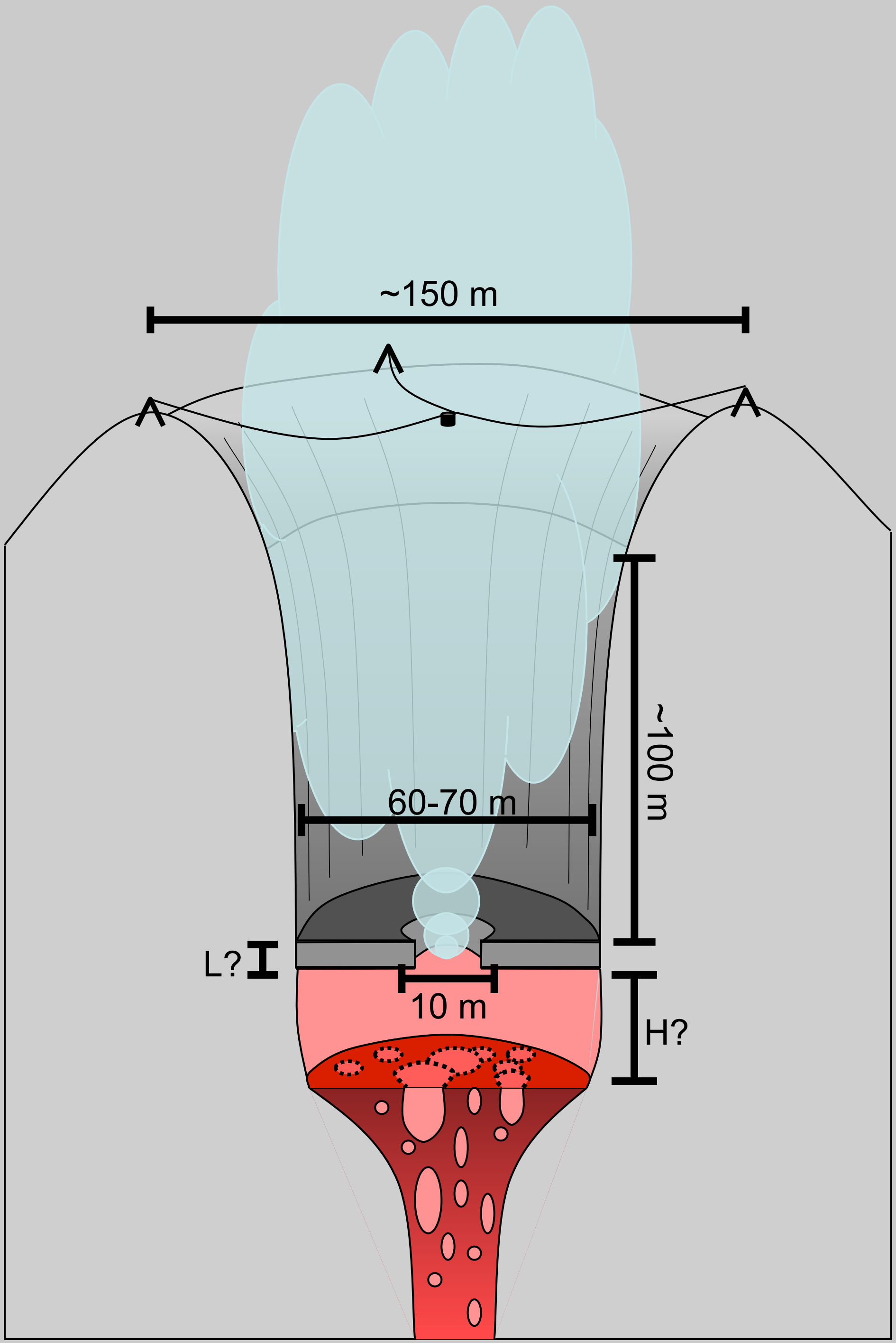

Classic Helmholtz resonance:

$$f = \frac{c}{2\pi}\sqrt{\frac{A}{V\,L}}$$

f is resonance frequency = ~0.8 Hz
c is sound velocity = 515 m/s (Fee et al., 2010)
A is pipe cross sectional area = ~75 m^2
r is skylight radius (4-5 m)
L is pipe length = 3 m (?)
V is cavity volume (unknown)
D = diameter of cavity volume = 60-70 m

Solving for volume:

$$V = \frac{A}{L}\left(\frac{c}{2\pi f}\right)^2 = \frac{\pi D^2}{4} H$$

V = 260,000 m^3 *and H = ~80 m*